

UNIMORE

UNIVERSITÀ DEGLI STUDI DI
MODENA E REGGIO EMILIA

Dipartimento di Scienze Fisiche, Informatiche e Matematiche

Corso di Laurea Magistrale in Physics - Fisica

Tesi di Laurea Magistrale

How to evade the CMB limit on Dark Matter interactions

Relatore:

Prof. Enrico Bertuzzo

Laureando:

Giovanni Sghedoni

Anno Accademico 2025/2026

Odi et amo. Quare id faciam, fortasse requiris.
Nescio, sed fieri sentio et excrucior.

— Catullo, Carme LXXXV

Abstract

One of the probes used to constrain Dark Matter (DM) is the Cosmic Microwave Background (CMB) bound, deriving from the small modifications on the CMB spectrum due to the interactions between photons and the free particles produced by DM annihilation.

After a general introduction to Dark Matter physics and the CMB, in this thesis we will analyze different scalar and fermionic operators entering the interactions between Dark Matter and Standard Model particles to determine whether the thermally-averaged cross-section $\langle \sigma v \rangle$ is s- or p-wave. In particular, we will try to bypass the computation of the total amplitude of the process, focusing directly on the structure of the DM fermionic bilinear in the non-relativistic limit.

This study is aimed at determining which DM candidates evade the CMB bound by construction. Indeed, unlike s-wave annihilation processes, where $\langle \sigma v \rangle$ is velocity-independent and can be probed by the CMB bound, p-wave annihilation processes evade it since, in that case, $\langle \sigma v \rangle$ is proportional to v^2, so it is strongly suppressed by the time of recombination.

Sommario

Una delle sonde usate per vincolare la Materia Oscura (DM) è il limite della Radiazione Cosmica di Fondo (CMB), che deriva dalle piccole modifiche allo spettro del CMB dovute alle interazioni tra i fotoni e le particelle libere prodotte dall'annichilazione di DM.

Dopo un'introduzione generale sulla fisica della Materia Oscura e sul CMB, in questa tesi analizzeremo diversi operatori scalari e fermionici che compaiono nelle interazioni tra particelle di Materia Oscura e del Modello Standard, per determinare se la sezione d'urto mediata termicamente $\langle \sigma v \rangle$ è in onda s o in onda p. In particolare, cercheremo di evitare di calcolare l'ampiezza totale del processo, concentrandoci direttamente sulla struttura del bilineare fermionico di DM nel limite non relativistico.

Questo studio ha lo scopo di determinare quali candidati di DM evadono il vincolo del CMB per costruzione. Infatti, a differenza dei processi di annichilazione in onda s, in cui $\langle \sigma v \rangle$ è indipendente dalla velocità e può essere sondata dal limite del CMB, i processi di annichilazione in onda p lo evadono dal momento che, in tal caso, $\langle \sigma v \rangle$ è proporzionale a v^2, per cui è fortemente soppressa all'epoca della ricombinazione.

Contents

Introduction **1**

1 Introduction to Dark Matter **3**
1.1 Evidences for Dark Matter existence . . . 3
1.1.1 Cosmological evidences . . . 3
1.1.2 Astrophysical evidences . . . 5
1.2 Properties of Dark Matter . . . 9
1.3 Dark Matter candidates . . . 11
1.3.1 Thermal candidates: the freeze-out mechanism . . . 12
1.3.2 Non-thermal candidates: freeze-in and misalignment . . . 14
1.4 Dark Matter detection . . . 17

2 The CMB and its limit **21**
2.1 Introduction to the Cosmic Microwave Background . . . 21
2.2 Recombination and last-scattering . . . 22
2.3 The CMB limit . . . 26

3 Partial-wave classification of Dark Matter operators **29**
3.1 Overview and preliminaries . . . 29
3.2 Scalar Dark Matter operators . . . 30
3.3 Fermionic Dark Matter operators . . . 34
3.3.1 Non-relativistic limit of Dirac spinors . . . 34
3.3.2 The scalar fermion bilinear . . . 36
3.3.3 The pseudoscalar fermion bilinear . . . 37
3.3.4 The vector fermion bilinear . . . 37
3.3.5 The axial vector fermion bilinear . . . 40
3.3.6 The tensor fermion bilinear . . . 42
3.3.7 The axial tensor fermion bilinear . . . 44
3.3.8 Summary of the bilinear analysis . . . 47
3.3.9 Majorana fermions . . . 47
3.3.10 The role of the mediator . . . 49
3.3.11 t-channel annihilation . . . 53

Conclusions **57**

Appendix **59**

Bibliography **67**

Introduction

What is the universe made of? Although the Standard Model (SM), which describes ordinary matter, is considered the most precise theory in physics, it does not account for a fundamental component of unknown nature: Dark Matter (DM), which constitutes about 85% of the matter content of the universe. Over the course of Chapter 1, after presenting the cosmological and the astrophysical evidences for its existence, we analyze the properties of Dark Matter, among which the fact that it is non-relativistic, stable, insensitive to electromagnetism and feebly interacting apart from gravity. Since no SM particle satisfies all of these requirements, we discuss the production mechanisms that could generate new particles in the early universe. Among them, freeze-out gives rise to thermal candidates, such as Weakly Interacting Massive Particles (WIMPs), while freeze-in and misalignment both produce non-thermal Dark Matter. We then turn to the strategies used to detect Dark Matter, focusing on WIMPs. In particular, we present three complementary experimental techniques: direct detection, indirect detection and collider searches, which all place bounds on DM-SM interactions, obtained under different assumptions on the velocity regime and the environment in which the interaction is probed.

In Chapter 2, after introducing the Cosmic Microwave Background (CMB) as a map of photons with slightly different temperatures, emitted around 380,000 years after the Big Bang, we turn to recombination and last-scattering. These are two phenomena that occurred in the early universe, which correspond to the formation of the first hydrogen atoms and to the moment when photons decoupled from any charged particle, respectively. Furthermore, since the universe is not neutral today, another phenomenon, known as reionization, must have taken place after recombination. This phenomenon has astrophysical origins, but DM annihilation can still give a small contribution to the fraction of free electrons after recombination, leaving an imprint on the CMB spectrum, which allows us to place the so-called CMB bounds. In particular, these bounds apply provided that DM annihilation occurs in s-wave, which means that the thermally-averaged cross-section $\langle \sigma v \rangle$ is constant and does not depend on the relative velocity v of the incoming DM particles. On the other hand, if DM annihilation proceeds through p-wave, $\langle \sigma v \rangle$ is proportional to v^2, so it is strongly suppressed by the time of recombination, implying that the corresponding processes evade the CMB bound.

Finally, in Chapter 3, we analyze different scalar and fermionic operators entering DM annihilation into SM particles to determine whether the resulting annihilation is s-wave or p-wave and, therefore, whether the corresponding DM candidates evade the CMB bound by construction. This can be determined either by computing the total amplitude of the process, since $\langle \sigma v \rangle$ depends on it, or, in the fermionic case, by studying the structure of the DM fermionic bilinear in the non-relativistic limit, which, up to the effects of the mediator, carries the whole velocity dependence of the amplitude. To complete our analysis, we then consider the case in which Dark Matter is described by Majorana fermions, in order to determine which of these structures survive. We also study the role of the mediator and consider the t-channel annihilation of DM into a pair of mediators to determine whether it is possible to separate the s-wave contributions from the p-wave ones. The detailed derivations of the results used in this chapter are reported in the Appendix.

1. Introduction to Dark Matter

1.1 Evidences for Dark Matter existence

1.1.1 Cosmological evidences

To date, the Standard Model is the most precisely tested theory in physics. Nevertheless, it only accounts for a small fraction of the matter content in the universe. Indeed, the Friedmann equations, which govern the dynamics of spacetime on cosmological scales, require that today's matter abundance Ω_{m_0}, defined as

$$\Omega_{m_0} \equiv \frac{\rho_{m_0}}{\rho_c} \ , \tag{1.1}$$

where $\rho_m(t)$ is the matter energy density and

$$\rho_c \equiv \frac{3H_0^2}{8\pi G} \tag{1.2}$$

is the so-called critical density, is approximately $\Omega_{m_0} \simeq 0.3$.

On the other hand, independent probes of baryonic matter, such as X-ray emission from hot gas in galaxies, light absorption from quasars, the CMB spectrum and Big Bang Nucleosynthesis, consistently yield a baryonic (or normal) matter abundance of $\Omega_{b_0}h^2 \simeq 0.02$, where $h \simeq 0.7$ is a parameter that contains all the errors. As a consequence, since $\Omega_{b_0} \simeq 0.04$ once we divide $\Omega_{b_0}h^2$ by h^2, baryonic matter can only account for about 15% of Ω_{m_0}. Thus, the remaining 85% cannot be attributed to normal matter, indicating the existence of an additional non-baryonic component, that is Dark Matter.

There is also another cosmological evidence for Dark Matter existence, that is based on the study of the evolution of inhomogeneities in time. Inhomogeneities have been playing an important role in the history of the universe as their self-gravitation is the cause of the formation of galaxies.

With that said, an important quantity that we need to compute when talking about inhomogeneities is the so-called comoving horizon η, which corresponds to the comoving distance

travelled by photons from very early times and is essential for determining the exchange of information between an inhomogeneity and the outside world.

Considering the one-dominant fluid approximation, today's comoving horizon is

$$\eta_0 = \int_0^t \frac{dt'}{a(t')} = \int_z^{+\infty} \frac{dz'}{(1+z')H(z')} \propto \frac{1}{aH} \ , \tag{1.3}$$

where aH corresponds to the comoving size of the visible universe. In particular, in order for a perturbation to be able to exchange information with the environment, we need to require that its typical comoving size λ is smaller than $1/(aH)$ $\Big(\lambda < 1/(aH)\Big)$, which means that the perturbation is completely inside the horizon.

At this point, by defining the density contrast $\delta(t, \mathbf{x})$ as

$$\delta(t, \mathbf{x}) = \frac{\rho(t, \mathbf{x}) - \bar{\rho}(t)}{\bar{\rho}(t)} \ , \tag{1.4}$$

it is possible to consider a Newtonian treatment to determine the approximate equation of motion for that quantity, which turns out to be

$$\frac{\ddot{a}}{a} - \frac{1}{3}\ddot{\delta} - \frac{2}{3}H\dot{\delta} = -\frac{4\pi G}{3}\bar{\rho} - \frac{4\pi G}{3}\delta\bar{\rho} \ . \tag{1.5}$$

Now, since in the early universe perturbations were very small ($|\delta| \ll 1$), we can solve Equation (1.5) perturbatively, obtaining that, at first order,

$$\ddot{\delta} + 2H\dot{\delta} = 4\pi G\bar{\rho}\delta \ . \tag{1.6}$$

At this point, by studying the previous equation under different fluid dominations, it results that

$$\delta(t) \propto \begin{cases} \log(t) & \text{during Radiation Domination} \\ t^{2/3} & \text{during Matter Domination} \\ \text{constant} & \text{during } \Lambda \text{ Domination} \ . \end{cases} \tag{1.7}$$

In particular, these solutions only apply to a pressureless fluid, which means that they cannot describe the evolution of baryons and photons since they were tightly coupled before recombination and oscillate after crossing the horizon. Indeed, as shown in Figure 1.1, the solid black and grey lines, representing the baryonic (δ_b) and photonic (δ_γ) density contrasts for a representative Fourier mode, do not have a monotonic behaviour as predicted by Equation (1.7). As we will see more precisely in Section 1.2, Dark Matter is almost pressureless, so we expect the computation for $\delta(t)$, characterized by a logarithmic behaviour during Radiation Domination, followed by a power-law growth once Matter Domination begins, to describe δ_{DM}.

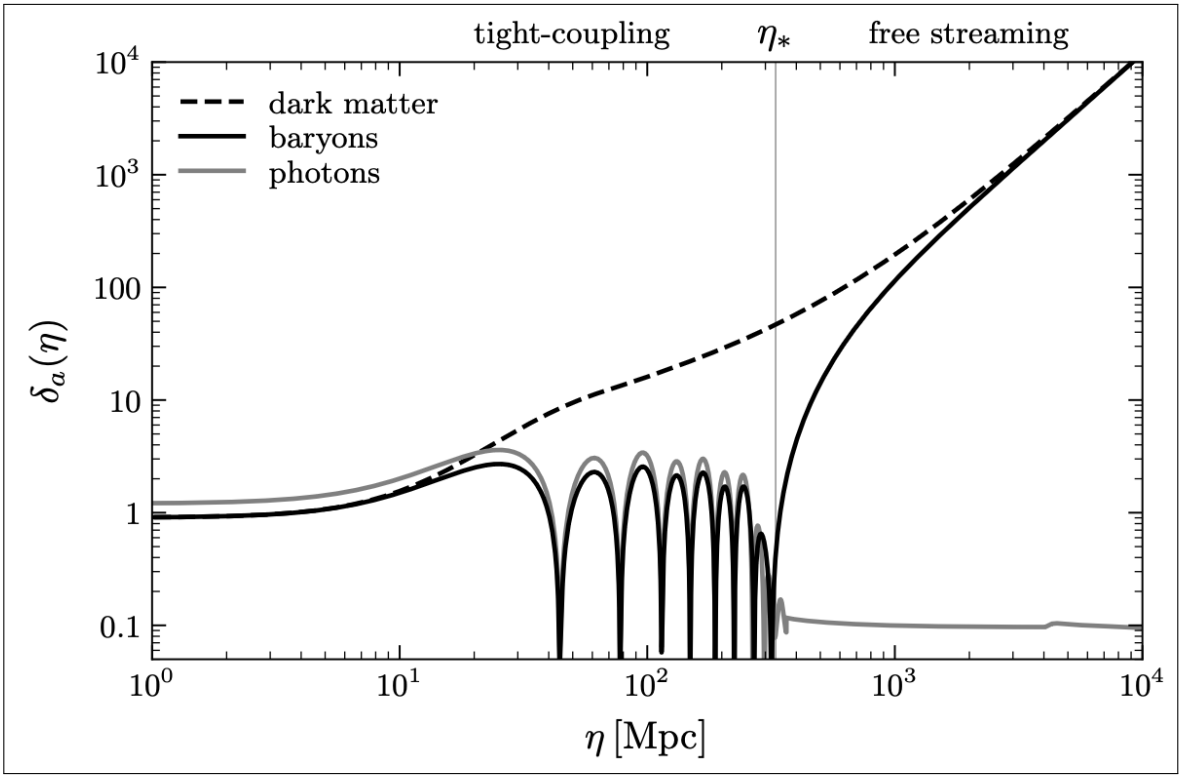


Figure 1.1: Evolution of the density contrasts of Dark Matter (black dashed line), baryons (black solid line), and photons (grey solid line) for $k = 0.25\,h$ Mpc^{-1}. Figure taken from [1].

With that said, there is also another important clue suggesting that the pressureless fluid is Dark Matter: indeed, if baryons were the only source of matter, their perturbations could only start growing after last-scattering. As a result, today's baryonic density contrast $\delta_{b,0}$ would be

$$\delta_{b,0} = \frac{a_0}{a_{LS}}\delta_{b,LS} \lesssim 0.1 \ , \tag{1.8}$$

meaning that inhomogeneities would be too small, so there would not be structures like galaxies in the universe. On the other hand, by adding a Dark Matter component, it correctly results that $\delta_{b,0} \gg 1$, which is consistent with structure formation. In particular, after decoupling, the baryons lose the pressure support of the photons and fall into the gravitational potential wells created by Dark Matter, as can be seen by inspecting the solid black line in Figure 1.1.

1.1.2 Astrophysical evidences

Besides cosmological evidences for Dark Matter existence, there are also some astrophysical ones.

First, we should mention the study of the Coma Cluster, performed in 1933 by Zwicky and based on the comparison between its luminous M_{LUM} mass and its gravitational M_{GR} mass.

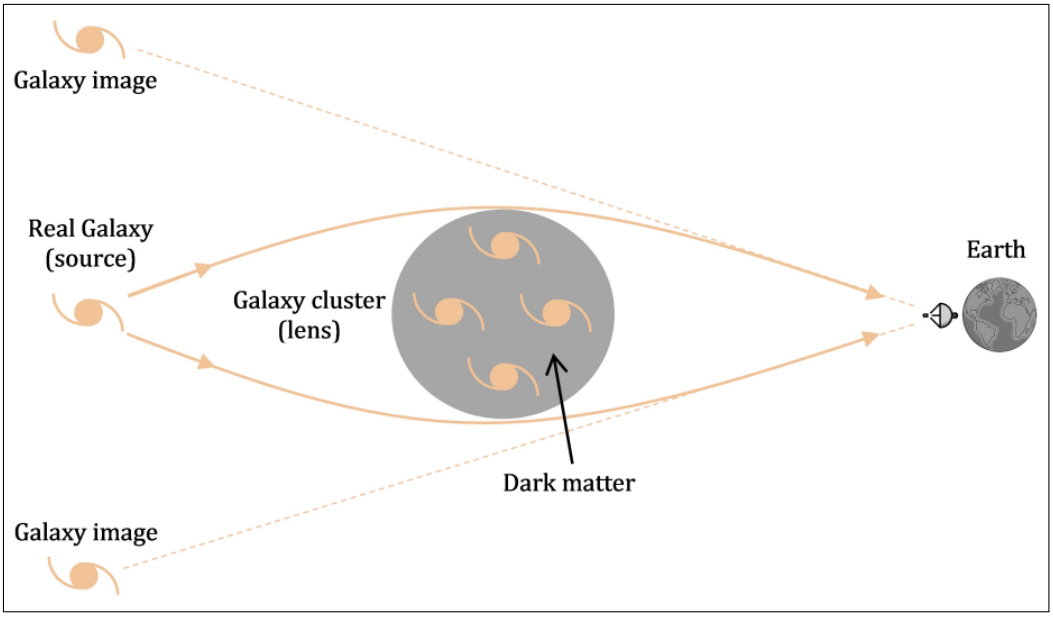


Figure 1.2: Scheme representing the weak gravitational lensing effect: light from a distant background galaxy (source) is deflected as it passes near a cluster of galaxies (lens) and then reaches the Earth. Figure taken from [2].

In particular, since Coma contains about 10^3 galaxies and since each galaxy has luminosity $\mathcal{L} \sim 8.5 \cdot 10^7 \, \mathcal{L}_\odot$ in units of the Sun's luminosity, it turns out that its luminous mass is $M_{LUM} \sim 8.5 \cdot 10^{10} \, M_\odot$.

As for its gravitational mass estimate, we can approximate Coma as a uniform sphere because stationary clusters (clusters that are neither losing nor gaining stars) can be considered as spherical objects that oscillate around some equilibrium configuration to a first approximation. Considering the potential energy of a uniform sphere and using the virial theorem, it results that

$$M_{GR} = \frac{5}{3} R_{TOT} \frac{\langle v^2 \rangle}{G} \, , \tag{1.9}$$

where the total radius of the cluster R_{TOT} and the velocity dispersion of galaxies $\langle v^2 \rangle$ are both quantities that can be estimated from observations. As a consequence, it results that $M_{GR} \gtrsim 4.5 \cdot 10^{13} \, M_\odot$.

By comparing the two values for the masses, we observe that $M_{GR} \gg M_{LUM}$. In particular, more precise estimates tell us that M_{GR} is approximately eight times larger than M_{LUM}. This result therefore tells us that there is some source of matter, that does not emit light, suggesting, once again, the existence of Dark Matter.

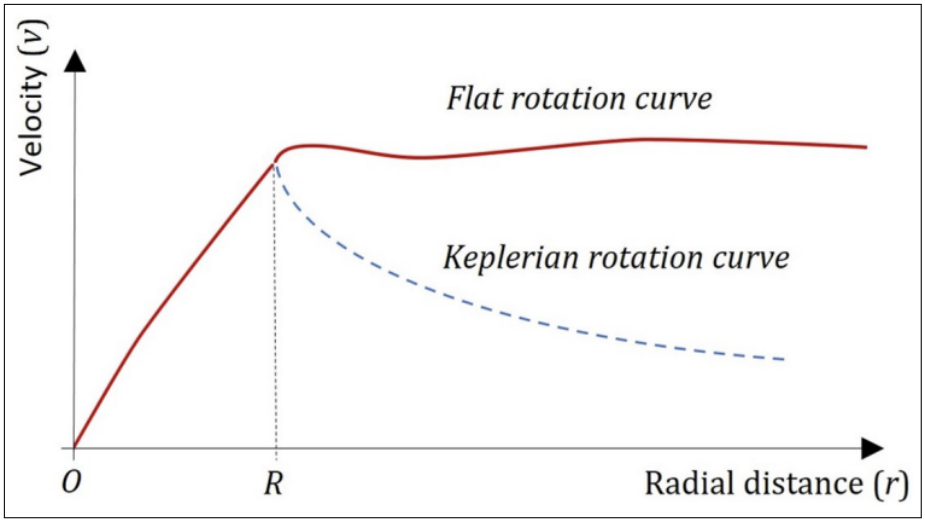


Figure 1.3: Predicted rotation curve (dashed line) and observed rotation curve (solid line) of spiral galaxies. Figure taken from [2].

Another approach that has provided some of the strongest evidence for Dark Matter existence is the weak gravitational lensing effect, a prediction of Einstein's theory of general relativity. That effect is related to the deflection of light rays from a distant source when they pass near a massive object that acts as a lens, as shown in Figure 1.2.

Once again, by comparing the values of M_{GR} with those of M_{LUM} obtained from this effect for different galaxies, we get that $M_{LUM} \simeq M_{GR}/10$.

The measurement of the rotation velocities of stars in spiral galaxies, which was first performed by Rubin and Ford in 1970, provides a further probe for Dark Matter existence.

By approximating spiral galaxies as spheres, applying Gauss's theorem and assuming that rotation is completely sustained by gravity, the two physicists expected the rotation velocity $v(r)$ to be proportional to

$$v(r) \propto \begin{cases} r & \text{if } r \leq R \\ r^{-1/2} & \text{if } r > R \ , \end{cases} \tag{1.10}$$

where R is the radius of the galaxy.

However, surprisingly, they observed a flat rotation curve for $r > R$.

The mismatch between the two curves, reported in Figure 1.3, can be explained by the fact that the mass of spiral galaxies is not only due to stars, but also due to Dark Matter. Thus, not only clusters but also galaxies are objects completely surrounded by Dark Matter.



Figure 1.4: The Bullet Cluster. The baryonic gas is coloured in pink, while DM distribution is coloured in blue. Figure taken from [3].

Finally, we can talk about the Bullet Cluster, an object composed of a pair of colliding sub-clusters.

Studying where the gravitational potential was generated, physicists were able to observe a physical separation between M_{GR} and M_{LUM}, meaning that whatever generates gravity can be in a different geometrical spot from whatever emits light. In particular, baryonic matter in the form of hot gas, traced by its X-ray emission, is located in the central region of the cluster, while DM halos, measured by gravitational lensing, are displaced from the center, as shown in Figure 1.4.

We can interpret these observations as follows: in the past the system was composed of two independent galaxy clusters, each with its own DM and baryonic contents, moving towards one another. Then, during the collision, the baryonic matter from the two clusters interacted electromagnetically, experiencing a 'drag force', that confined it to the central region. In contrast, the two DM halos, insensitive to electromagnetic interactions, did not experience this drag force and ended up on opposite sides of the system.

1.2 Properties of Dark Matter

Having established that Dark Matter must exist, we will now list its properties, that follow directly from observations, together with some theoretical constraints.

Dark Matter is cold: In order for the smallest structures to form, around $T \sim \text{keV}$, we must require that $w_{DM} \simeq 0$, where w_i is the so-called equation-of-state parameter for the species i and is defined as

$$w_i \equiv \frac{p_i}{\rho_i} \ . \tag{1.11}$$

This means that Dark Matter is cold, therefore non-relativistic, just like baryonic matter.

In order to understand why we require this property, let us first recall that a density perturbation of typical size λ can only grow gravitationally if the particles within it cannot escape the potential well before gravity pulls them back together. With that said, if Dark Matter were relativistic, therefore having an equation-of-state parameter $w \simeq 1/3$, its particles would move fast enough to escape small- and intermediate-scale perturbations almost freely, erasing them before they had time to collapse. As a consequence, in that case only the largest-scale perturbations would survive. On the other hand, if Dark Matter is non-relativistic, particles can grow at all scales, including the small ones.

In addition, as already discussed in Subsection 1.1.1, Dark Matter is pressureless. This follows directly from the requirement that $w_{DM} \simeq 0$, which implies that $p_{DM} \simeq 0$ as well.

Dark Matter is insensitive to electromagnetism: To enable structure growth, the DM fluid must not be strongly coupled (it must not have strong and frequent interactions) with the photon fluid.

Recent studies, such as [4], have shown that DM particles may have a small charge (which is why we talk about *millicharged DM candidates*). As displayed in Figure 1.5, there are two allowed regions in the (q, M) graph that escape all existing bounds. In particular, the blue region corresponds to very massive particles ($M \gtrsim 10^{10}\,\text{eV}$) with tiny charge ($q \lesssim 10^{-5}\,e$), that have never been thermally produced in the early universe; the green region, instead, corresponds to lighter particles ($10^{8}\,\text{eV} \lesssim M \lesssim 10^{10}\,\text{eV}$) with larger charge ($10^{-3}\,e \lesssim q \lesssim 10^{-1}\,e$).

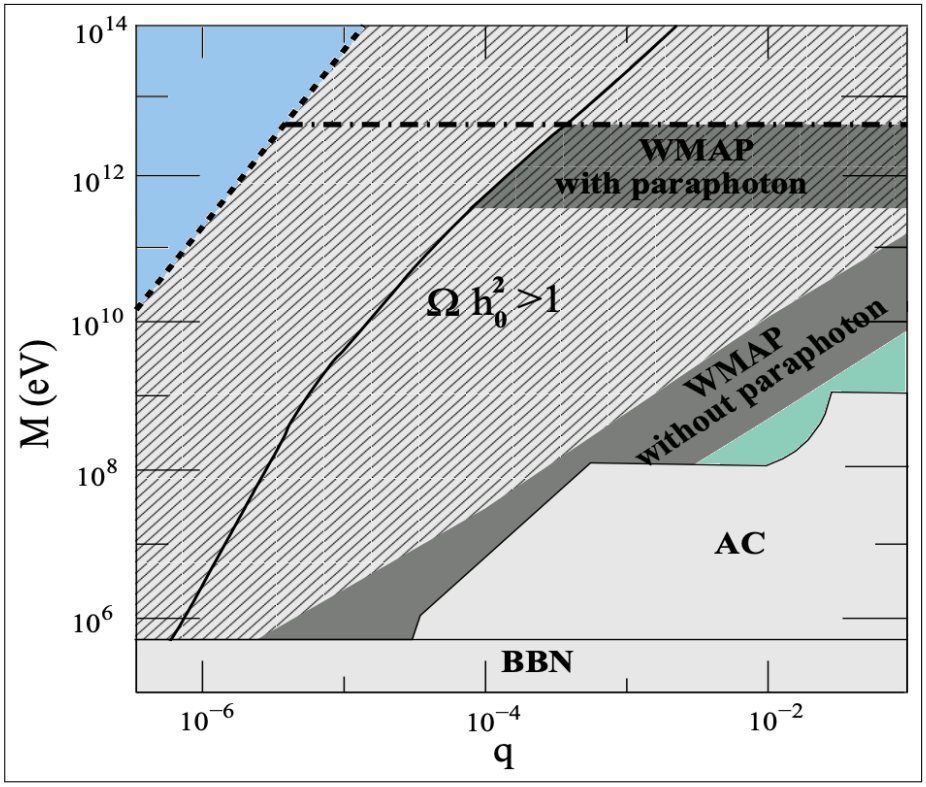


Figure 1.5: Constraints on the mass M and electric charge q of a millicharged Dark Matter candidate. Blue and green regions denote the surviving, unexcluded parameter space. Figure adapted from [4].

Dark Matter is stable: Since Dark Matter is observable, it must be present at the astrophysical level today. Nevertheless, it can still decay, but its average lifetime τ_{DM} must be larger than the age of the universe $t_{un} \simeq 13.8\,\mathrm{Gyr}$.

To be more quantitative, as reported in [5], if we denote by Γ_{DM} the DM decay width and by f_{dDM} the fraction of decaying Dark Matter, it results that

$$f_{dDM}\Gamma_{DM} < 6.3 \cdot 10^{-3}\,\mathrm{Gyr}^{-1} \lesssim \frac{0.086}{t_{un}}\ . \tag{1.12}$$

Thus, if we assume that $f_{dDM} = 1$, meaning that all of the Dark Matter decays, then it results that $\tau_{DM} \gtrsim 10\, t_{un}$.

Dark Matter is feebly interacting: As discussed in Section 1.1, Dark Matter is certainly subject to gravity. However, it is more difficult to determine whether it is also subject to SM interactions: we have already stated that the DM electric charge can be tiny, yet non-zero, implying an electromagnetic coupling. However, that coupling would be extremely suppressed.

As discussed in [6], Dark Matter may have a colour charge. In particular, in order to be compatible with data, Dark Matter must have a mass $M \gtrsim 12\,\text{TeV}$, which is only possible if it transforms as an octet of $SU(3)_c$.

As for Dark Matter self-interactions, observations of the Bullet Cluster have set an upper bound on the DM–DM scattering cross-section: $\sigma_{DM-DM}/M \lesssim 1\,\text{cm}^2/\text{g}$.

Dark Matter is classical today: DM quantum effects cannot interfere with the astronomical observations of the smallest structures, such as dwarf galaxies. This property sets two different lower-mass bounds on DM particles, according to their nature:

- if DM is composed of bosonic particles, its de Broglie wavelength λ_{dB} must be smaller than the size of dwarf galaxies $D_{dg} \sim \text{kpc}$. As a consequence, since
$$\lambda_{dB} = \frac{h}{Mv}\ , \tag{1.13}$$
taking $v \sim 10^3\,\text{km/s}$, it results that $M \gtrsim 10^{-23}\,\text{eV}$;
- if DM is made up of fermionic particles, due to the Pauli exclusion principle, its mass must satisfy $M \gtrsim (10\text{–}100)\,\text{eV}$. This is known as the Tremaine–Gunn bound.

Galaxy clusters are stable: Dark Matter must be sufficiently small for its gravitational potential not to destroy clusters. This requirement sets an upper bound on the DM mass to $M \lesssim 10^3\,M_\odot \sim 10^{69}\,\text{eV}$.

Correct cosmological abundance: From the statistical properties of the CMB, the DM abundance is $\Omega_{DM}h^2 = 0.120 \pm 0.001$.

1.3 Dark Matter candidates

Before introducing new candidates, let us try to determine whether any of the known SM particles satisfy the properties listed in Section 1.2. We will just restrict ourselves to the neutral particles of the Standard Model because, although Dark Matter does not necessarily need to have zero electric charge, there are no particles in the Standard Model with charge values as small as those allowed in Figure 1.5. In any case, none of the neutral SM particles turn out to be suitable DM candidates. Indeed:

- photons and gluons are massless, meaning that they are a source of radiation and cannot

therefore be non-relativistic;

- Z bosons and Higgs bosons are unstable and have very short average lifetimes ($\tau \ll 1\,\mathrm{s}$);
- neutrinos are neutral, stable and massive, but their mass $m_\nu \lesssim 0.1\,\mathrm{eV}$ is too small to satisfy the Tremaine–Gunn bound and implies that at $T \sim$ keV they are still relativistic.

As a result, Dark Matter must come from outside the Standard Model, so we now turn to different mechanisms for its production.

1.3.1 Thermal candidates: the freeze-out mechanism

In analogy with the Standard Model, a natural way to produce the observed DM abundance is to assume that Dark Matter was once in thermal equilibrium with the primordial plasma and that this abundance was fixed when that equilibrium was lost during the expansion of the universe. This thermal production mechanism is known as freeze-out.

Let us consider 2-to-2 interactions with DM particles χ and $\bar{\chi}$ in the initial state and SM particles SM and $\overline{SM}$ in the final state:

$$\chi\,\bar{\chi} \longrightarrow \mathrm{SM}\,\overline{\mathrm{SM}} \tag{1.14}$$

and write down the Boltzmann equations:

$$\begin{cases} x\frac{dY_\chi}{dx} = \frac{\Gamma}{H} Y_{\bar{\chi}}^{eq}\left(1 - \frac{Y_\chi Y_{\bar{\chi}}}{Y_\chi^{eq} Y_{\bar{\chi}}^{eq}}\right) \\ x\frac{dY_{\bar{\chi}}}{dx} = \frac{\Gamma}{H} Y_\chi^{eq}\left(1 - \frac{Y_\chi Y_{\bar{\chi}}}{Y_\chi^{eq} Y_{\bar{\chi}}^{eq}}\right) \end{cases} \tag{1.15}$$

in terms of the new variable

$$x = \frac{M}{T} \tag{1.16}$$

that we use instead of time, the interaction rate

$$\Gamma = n_\chi^{eq}\left\langle \sigma\left(\chi\,\bar{\chi} \longrightarrow \mathrm{SM}\,\overline{\mathrm{SM}}\right)\right\rangle \tag{1.17}$$

and the yield

$$Y_\chi \equiv \frac{n_\chi}{s}\ , \tag{1.18}$$

that corresponds to the ratio between the number and the entropy densities.

At this point, by assuming that there is no asymmetry, therefore requiring that

$$Y_\chi = Y_{\bar{\chi}} \tag{1.19}$$

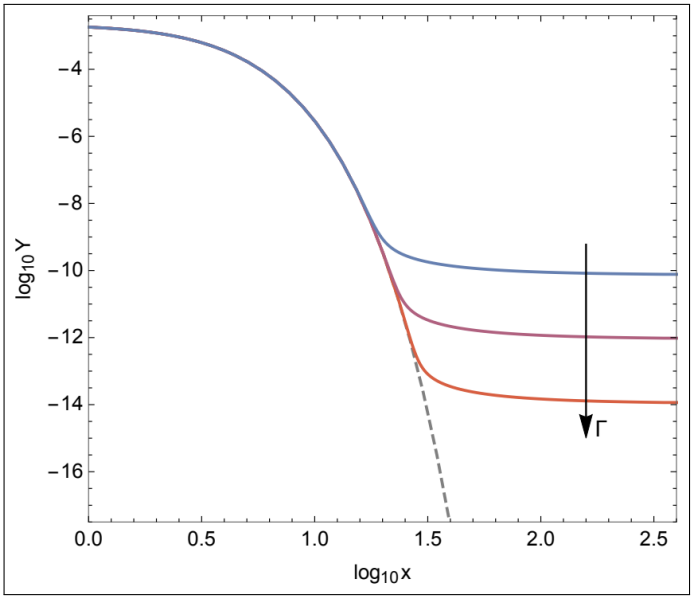


Figure 1.6: Qualitative solutions of the Riccati equation describing the yield $Y(x)$ during freeze-out for three different values of the interaction rate Γ (coloured lines). The grey dashed line represents the equilibrium yield Y_{eq}. Figure taken from [7].

and by defining

$$Y \equiv Y_{\chi} + Y_{\bar{\chi}} \ , \tag{1.20}$$

the Equations (1.15) reduce to the so-called Riccati equation:

$$x\frac{dY}{dx} = \frac{\Gamma}{H}Y^{eq}\left(1 - \frac{Y^2}{Y_{eq}^2}\right) \ , \tag{1.21}$$

which has no analytic solutions and whose qualitative behaviour is illustrated in Figure 1.6.

An approximate solution can be obtained by requiring that Dark Matter is cold and by solving the Riccati equation before decoupling, after decoupling and exactly at decoupling (or freeze-out), that is defined by the condition $\Gamma(x) = H(x)$. As a result, the residual DM abundance today is inversely proportional to the thermally-averaged annihilation cross-section, as expressed by

$$\Omega_{DM}h^2 \simeq \frac{10^{-27}\,\mathrm{cm}^3/\mathrm{s}}{\langle\sigma v\rangle_{FO}} \ . \tag{1.22}$$

At this point, since we know that $\Omega_{DM}h^2 \simeq 0.12$, we can invert Equation (1.22) and obtain that

$$\langle\sigma v\rangle_{FO} \simeq 3 \cdot 10^{-26}\,\mathrm{cm}^3/\mathrm{s} \simeq \frac{2.7 \cdot 10^{-9}}{\mathrm{GeV}^2} \tag{1.23}$$

in natural units.

To interpret this result for $\langle\sigma v\rangle_{FO}$, let us consider the interaction $\chi\,\bar{\chi} \longrightarrow \mathrm{SM}\,\overline{\mathrm{SM}}$, which can be represented by the Feynman diagram in Figure 1.7.

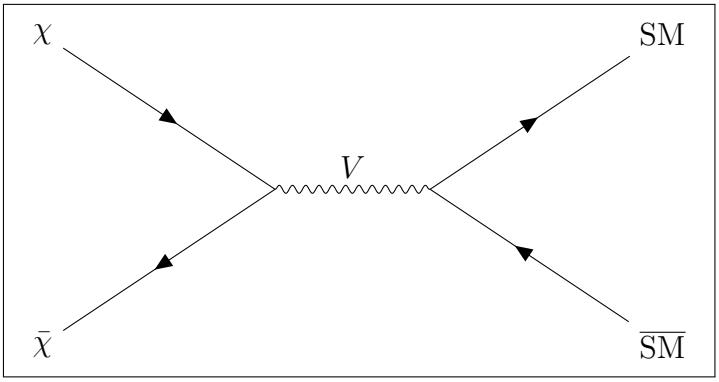


Figure 1.7: Feynman diagram for the annihilation process $\chi\bar{\chi} \to \text{SM}\,\overline{\text{SM}}$, mediated by a generic particle V (drawn as a vector for illustration only).

By assuming that $g_\chi \sim g_{SM} \equiv g$ and that $M_\chi \sim M_V \equiv M$, where g_χ and g_{SM} are the coupling constants of the $\chi\bar{\chi}V$ and $\text{SM}\overline{\text{SM}}V$ vertices, while M_χ and M_V are the masses of the DM particle and the mediator, we find that

$$\sigma \simeq \frac{|\mathcal{A}|^2}{M^2} \simeq \frac{g^4}{M^2} \simeq \frac{10^{-9}}{\text{GeV}^2} = \frac{(10^{-1})^4}{(10^2\text{GeV})^2} \ . \tag{1.24}$$

A particular combination of values of g and M that is consistent with Equation (1.24) is

$$\begin{aligned} g &\sim 0.1 \\ M &\sim 100\,\text{GeV} \ . \end{aligned} \tag{1.25}$$

Since these are the typical values for g and M that characterize the electroweak interaction $SU(2)_L \times U(1)_Y$, a DM candidate with these properties is generally referred to as a WIMP, a 'Weakly Interacting Massive Particle'. The fact that electroweak-scale parameters reproduce the observed DM abundance is known as the WIMP miracle.

In fact, the WIMP miracle is better described as a coincidence since there is a continuum of values in the (M, g) parameter space that reproduces the same DM abundance, as shown in Figure 1.8.

1.3.2 Non-thermal candidates: freeze-in and misalignment

Unlike the freeze-out mechanism, that relies on the assumption that Dark Matter was, at some point, in thermal equilibrium with the primordial plasma, there are also other mechanisms, among which freeze-in and misalignment, that do not require a thermal bath, making them non-thermal production mechanisms.

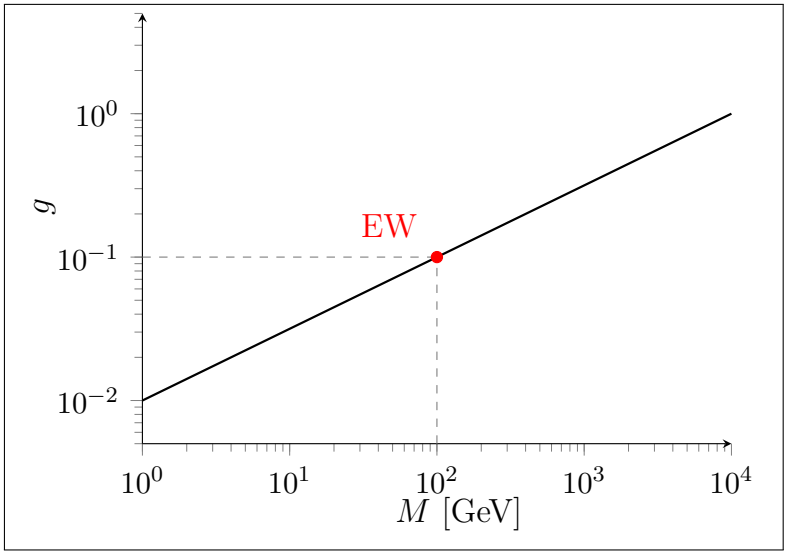


Figure 1.8: Combinations of coupling constant g and mass M reproducing $\Omega_{DM}h^2$, following $g^4/M^2 \sim$ const. The point labeled EW corresponds to $g \sim 0.1$ and $M \sim 100\,\text{GeV}$.

Let us start by discussing freeze-in, which is illustrated in Figure 1.9. In the freeze-in scenario, the yield starts at a very low value in the early universe, where $Y \ll Y_{eq}$ since thermal equilibrium is never reached, and then increases until it finally reaches a saturation value Y_∞. Its behaviour is therefore completely different from the one described by freeze-out (see Figure 1.6): indeed, in that case $Y \simeq Y_{eq}$ up to decoupling. Thus, although the DM abundance was completely different in the early universe according to the two mechanisms, they both agree with the observed value today.

With that said, since in the freeze-in scenario Dark Matter is never able to reach the equilibrium value ($Y \ll Y_{eq}$) when x is small, we assume that the coupling constant λ between DM and SM particles is very small ($\lambda \ll 1$). As a consequence, the DM candidates produced by this mechanism are called FIMPs ('Feebly Interacting Massive Particles').

There are two types of freeze-in scenarios:

- IR-dominated freeze-in, which has $\langle\sigma v\rangle \sim \lambda^4/T^2$ [8];
- UV-dominated freeze-in, which has $\langle\sigma v\rangle \sim \lambda^4 T^2/m_V^4$ for dimension-6 operators, where m_V is the mass of the mediator [9].

In any case, by solving the Riccati equation for both types of FIMPs, we obtain that

$$\lambda \ll g_{FO} \sim 0.1\ , \tag{1.26}$$

therefore confirming that these DM candidates have really feeble interactions with SM particles.

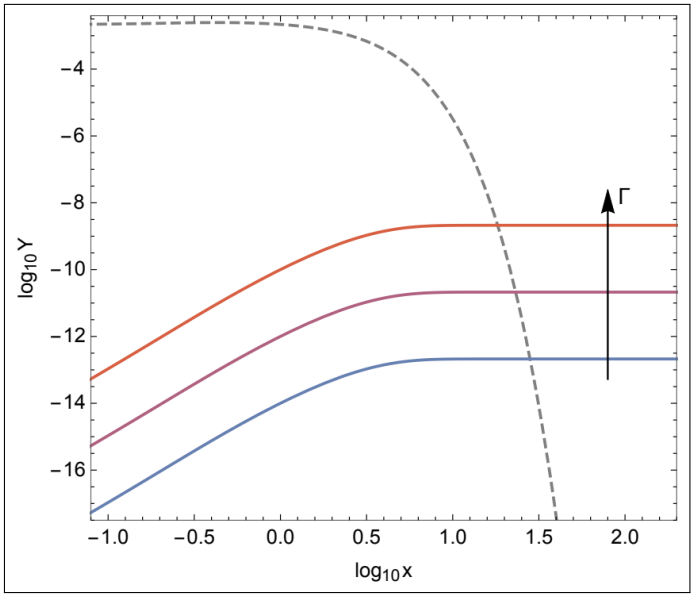


Figure 1.9: Qualitative behaviour of the yield $Y(x)$ during freeze-in for three different values of the interaction rate Γ (coloured lines). The grey dashed line represents the equilibrium yield Y_{eq}. Figure taken from [7].

Another non-thermal production mechanism is the so-called misalignment, that relies on very light scalar fields. Such fields, to a good approximation, behave as classical fields, meaning that they act on states with a very large occupation number from the point of view of Quantum Field Theory.

Following [10], in the early universe the scalar field Φ was displaced from the minimum of its potential $V(\Phi)$, where it remained throughout the early-time regime, defined by the condition $H \gg M$, where M is the mass of the DM candidate. Later, in the late-time regime, determined by the condition $H \ll M$, the field reaches the equilibrium configuration, where $V(\Phi) \simeq M^2\Phi^2/2$, and starts to oscillate around the minimum of the potential as a harmonic oscillator. By introducing the auxiliary field χ as

$$\chi(x) = a^{3/2}(t)\Phi(x) \ , \tag{1.27}$$

the equation of the harmonic oscillator is

$$\ddot{\chi} + M^2\chi \simeq 0 \ , \tag{1.28}$$

whose solution is

$$\chi(t) \simeq \chi_0 \cos(Mt + \varphi) \ . \tag{1.29}$$

As a result, it turns out that

$$\Phi(t) \simeq \frac{\chi_0}{a^{3/2}(t)} \cos(Mt + \varphi) \ . \tag{1.30}$$

At this point, by computing the average energy density ρ_Φ over one period of oscillation, we obtain that $\langle \rho_\Phi \rangle \sim a^{-3}$, exactly like baryonic matter, meaning that very light scalar fields behave as non-relativistic particles.

Having discussed several mechanisms to produce the observed DM abundance, we now turn to how such particles can be experimentally detected.

1.4 Dark Matter detection

We now introduce the experimental techniques used to detect Dark Matter. Since these techniques rely on a non-negligible coupling between DM and SM particles, we focus specifically on WIMP detection. Indeed, both FIMPs and particles produced by misalignment require completely different detection strategies.

Focusing on 2-to-2 processes involving DM and SM particles, we can identify three complementary techniques, depending on the direction in which the interaction $\chi\,\bar{\chi} \longleftrightarrow \mathrm{SM}\,\overline{\mathrm{SM}}$ is read:

- Direct Detection (DD), based on $\chi\mathrm{SM} \longrightarrow \chi\mathrm{SM}$ interactions, that can occur on Earth and that give us information on DM particles by measuring the recoil energy of the final-state SM particle;
- Indirect Detection (ID), built on $\chi\bar{\chi} \longrightarrow \mathrm{SM}\,\overline{\mathrm{SM}}$ interactions, that are frequent in the regions of the universe where there is a large concentration of Dark Matter, such as in the center of the Milky Way or in dwarf galaxies. The SM particles produced are then detected on Earth, where we expect to observe a number of events per year of the order of 10^2.
- Collider searches, based on $\mathrm{SM}\,\overline{\mathrm{SM}} \longrightarrow \chi\bar{\chi}$ interactions. In this case, since χ's have no charge (or their charge is very small) and interact very weakly with baryonic matter, meaning that they are almost invisible to detectors, we actually need to look for processes with one additional SM particle in the final state: $\mathrm{SM}\,\overline{\mathrm{SM}} \longrightarrow \chi\,\bar{\chi}\,\mathrm{SM}$. As a result, information on DM particles will be obtained considering energy and momentum conservation.

Each of these strategies determines bounds on DM–SM interactions, which are obtained under different assumptions on the velocity regime and the environment in which the interaction is probed.

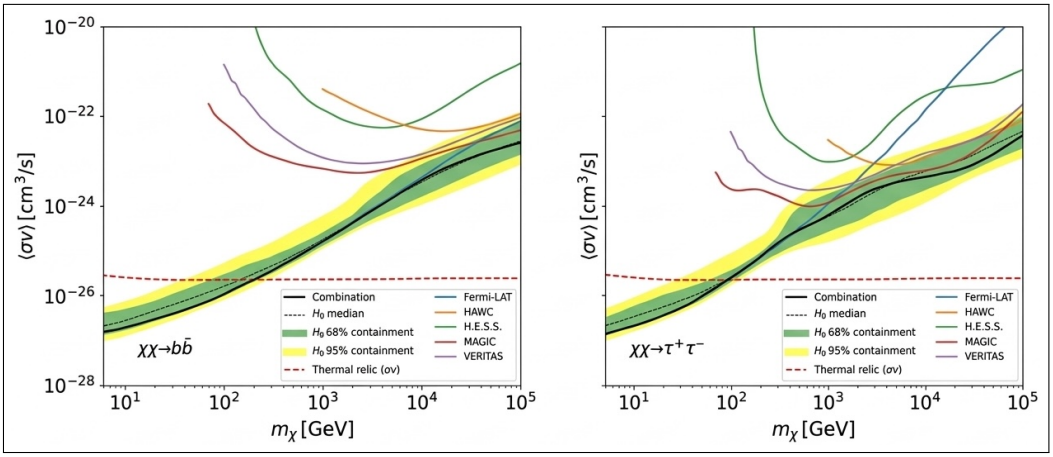


Figure 1.10: Upper limits on $\langle\sigma v\rangle$ as a function of the DM mass for the annihilation channels $b\bar{b}$ (left) and $\tau^+\tau^-$ (right). The black solid line represents the observed combined limit, while combined upper limits for each individual detector are indicated as solid coloured lines. Figure adapted from [11].

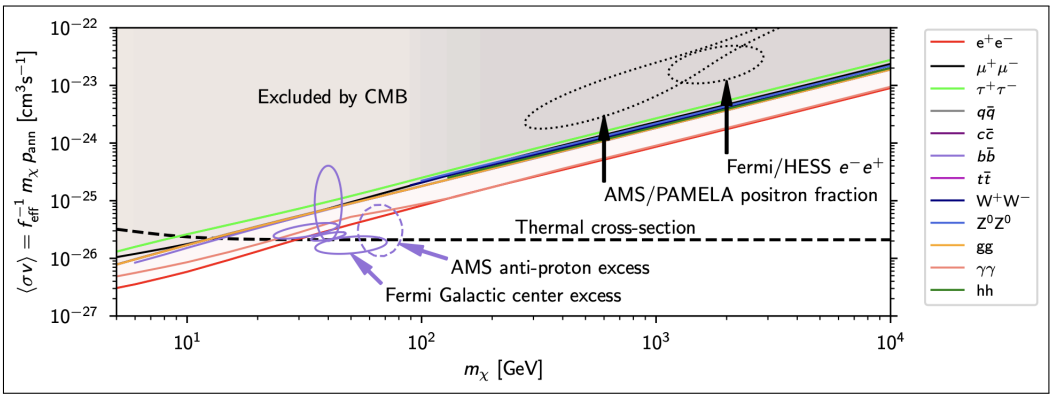


Figure 1.11: Planck 2018 constraints on the DM mass and $\langle\sigma v\rangle$. Solid coloured lines show joint CMB constraints on several annihilation channels. Figure taken from [12].

As for Indirect Detection, the $\langle\sigma v\rangle$ bounds, which differ according to the final-state particles, are illustrated in Figure 1.10.

There is also another bound for ID, known as the CMB bound, that will be discussed in detail in Chapter 2 and that is displayed in Figure 1.11.

With that said, these two bounds are related to the same quantity but have clearly different shapes. This is because the first one measures $\langle\sigma v\rangle$ today ($z = 0$), while the second one is related to $\langle\sigma v\rangle$ measured from recombination ($z \simeq 1100$) to reionization ($z \simeq 8$). We therefore need to determine when this comparison is sensible. In order to do so, let us organize σv as a Taylor expansion in powers of v:

$$\sigma v = a + bv^2 + cv^4 + \mathcal{O}(v^6)\ , \tag{1.31}$$

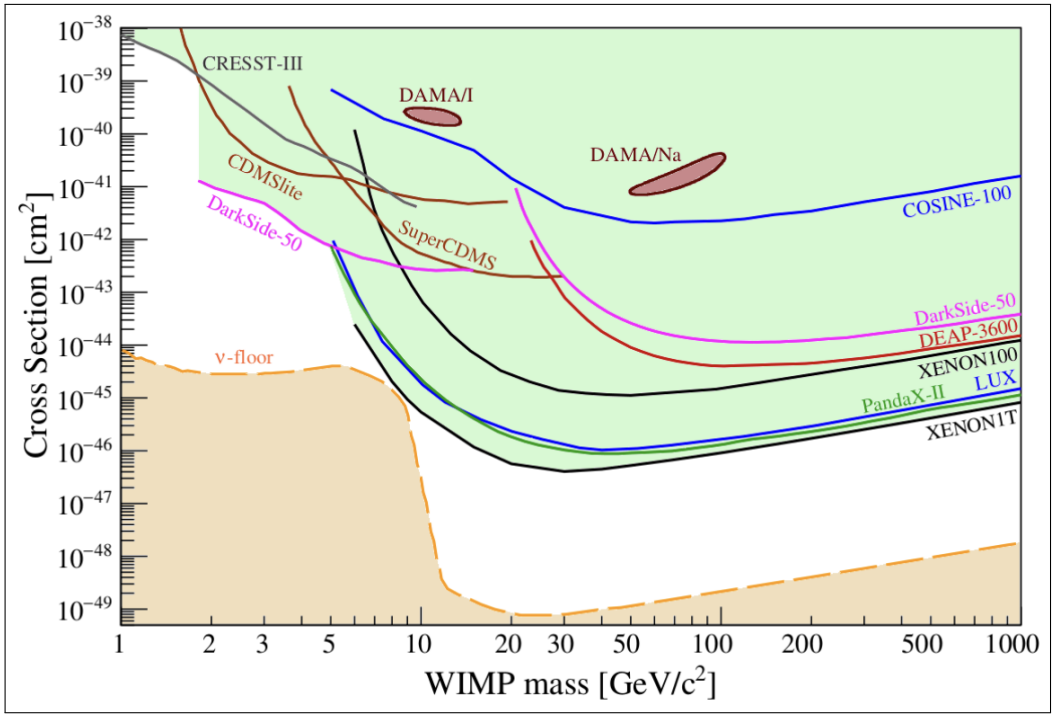


Figure 1.12: Current experimental parameter space for spin-independent WIMP-nucleon cross-section. Figure taken from [13].

where odd-order terms are not considered since $\langle \sigma v \rangle$ is a scalar quantity, while $\mathbf{v}$ is a vector, so we need to take into account only the even powers of v to correctly obtain a sum of scalar quantities. In particular, when

- $\sigma v = a$, the cross-section is s-wave;
- $\sigma v = bv^2$, the cross-section is p-wave;
- $\sigma v = cv^4$, the cross-section is d-wave.

At this point, by thermally averaging Equation (1.31), we obtain

$$\langle \sigma v \rangle \simeq a + 3b\frac{T}{m_\chi} \ . \tag{1.32}$$

As a result, back to the $\langle \sigma v \rangle$ bounds argument, it turns out that the comparison makes sense only if the cross-section is s-wave because in that case there is no dependence on T and, therefore, on z.

In the case of Direct Detection, experimental collaborations usually present bounds in the plane $(m_\chi, \sigma_{\chi n})$, where $\sigma_{\chi n}$ is the elastic-scattering cross-section between a DM particle and a nucleon. For reference, Figure 1.12 shows the current bounds on the spin-independent WIMP-nucleon cross-section.

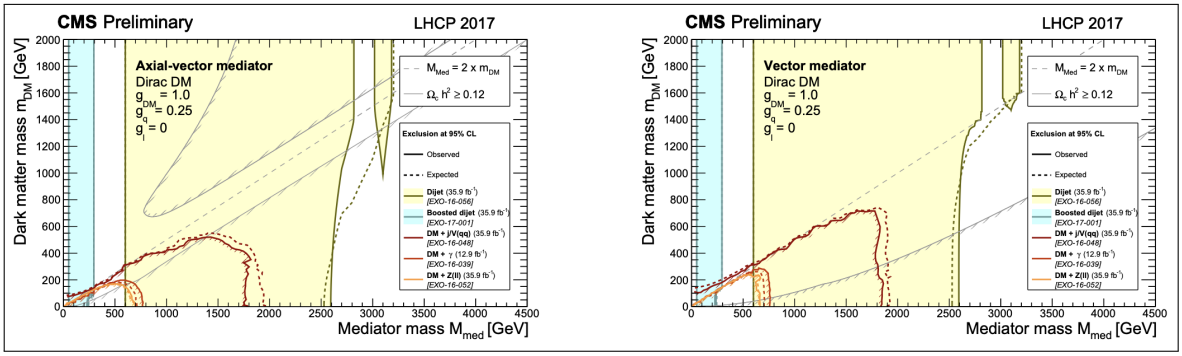


Figure 1.13: 95% CL expected and observed exclusion regions in the (M_{med}, m_χ) plane for di-jet searches from CMS in the case of an axial-vector (left) and vector (right) mediator. Both bounds are obtained considering coupling constants $g_{DM} = 1$ and $g_{SM} \equiv g_q = 0.25$. Figure taken from [14].

Finally, collider searches place bounds in the (M_{med}, m_χ) plane. For reference, Figure 1.13 shows the excluded regions obtained from di-jet searches for both an axial-vector and a vector mediator.

To conclude, we have presented several evidences for the existence of Dark Matter, listed its fundamental properties, and then discussed which particles are suitable as DM candidates and how to detect them. Specifically, DM detection strategies set different bounds on the thermally-averaged annihilation cross-section. Among these, the CMB bound is particularly important since it excludes DM candidates with s-wave thermal cross-sections and masses below a few tens of GeV. We will therefore focus on it in Chapter 2, in order to understand why it is important to determine whether an interaction is s-wave or p-wave.

2. The CMB and its limit

2.1 Introduction to the Cosmic Microwave Background

Discovered in 1964 and interpreted the following year by Penzias and Wilson [15], the Cosmic Microwave Background (CMB) is a flux of radiation with energy in the range of microwaves that was emitted at the epoch of last-scattering, around 380,000 years after the Big Bang, when photons decoupled from the primordial plasma.

As shown in Figure 2.1, the CMB is represented by a map, in which each point is coloured differently according to the energy, hence the temperature, of the photons arriving at Earth from all directions in space. In particular, regions coloured blue have a lower temperature than the average CMB temperature $\langle T \rangle \simeq 2.7\,\mathrm{K}$, while regions coloured red have a higher temperature [17]. In any case, by dividing the temperature fluctuation δT by $\langle T \rangle$, we obtain that

$$\frac{\delta T}{\langle T \rangle} \sim 10^{-5} \ , \tag{2.1}$$

implying that the universe is almost perfectly homogeneous and isotropic at large scales.

Furthermore, the CMB exhibits an almost perfect black-body spectrum [1], expressed by the following distribution:

$$f(p,T) = \frac{1}{e^{E_\gamma/T_\gamma} - 1} \ . \tag{2.2}$$

This means that, at the epoch of last-scattering, photons were in thermal equilibrium with the primordial plasma, which was maintained by frequent and quick interactions. Remarkably, the CMB retains a black-body spectrum even today, although photons have not been subject to any interaction since last-scattering. This follows from the fact that $f(p,T)$ depends only on the ratio between E_γ and T_γ, two quantities that scale with redshift z in the same way [18]:

$$\begin{aligned} E_\gamma(z) &= (1+z)E_\gamma(z=0) \ ; \\ T_\gamma(z) &= (1+z)T_\gamma(z=0) \ . \end{aligned} \tag{2.3}$$

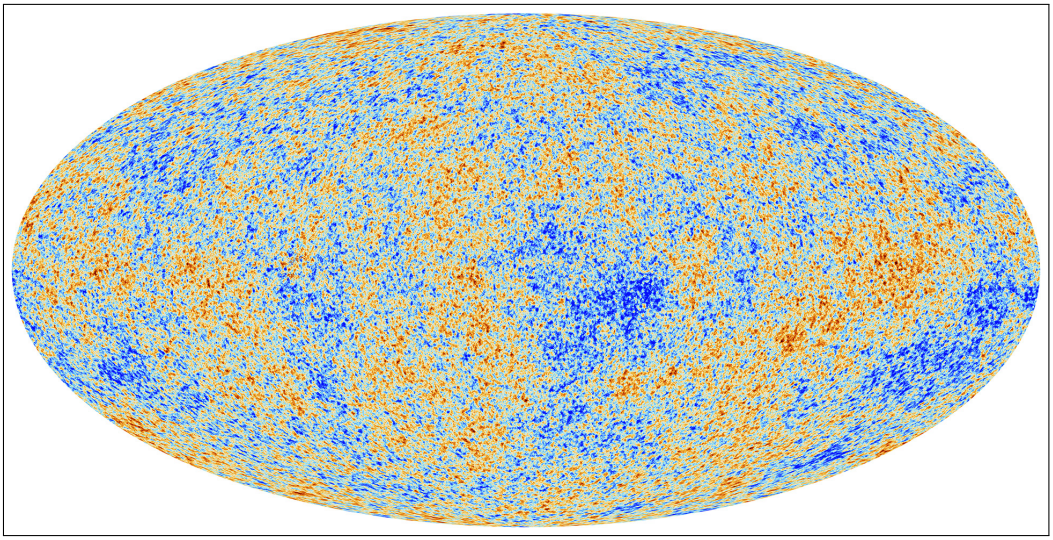


Figure 2.1: The Cosmic Microwave Background. Figure taken from [16].

2.2 Recombination and last-scattering

Recombination and last-scattering are two phenomena that appear when the energy of the early universe is of the order of eV. These processes are particularly important as they determine how the fraction of free electrons X_e evolves with T. We will describe them following [1].

Qualitatively, as shown in Figure 2.2, above $T \simeq 0.29\,\text{eV}$ the universe is opaque: indeed, since there are many charged particles around, photons have a very small mean free path. Then, at $T \simeq 0.29\,\text{eV}$, neutral hydrogen atoms start to form through

$$p + e \longrightarrow H + \gamma \tag{2.4}$$

due to recombination. As a consequence, since the number of charged particles begins to diminish, the photon mean free path increases. Finally, at $T \simeq 0.25\,\text{eV}$, last-scattering arises: having no more charged particles around, photons decouple from any particle and the universe becomes transparent. This, therefore, corresponds to the moment in which the CMB is generated.

Let us now briefly discuss these phenomena quantitatively through an equilibrium treatment, also known as the Saha treatment.

Starting from recombination, the equilibrium particle density for species i is

$$n_i^{\text{eq}} = g_i \left(\frac{m_i T}{2\pi}\right)^{3/2} \exp\left(\frac{\mu_i - m_i}{T}\right) , \tag{2.5}$$

where g_i is the number of degrees of freedom. To remove the dependence on the chemical

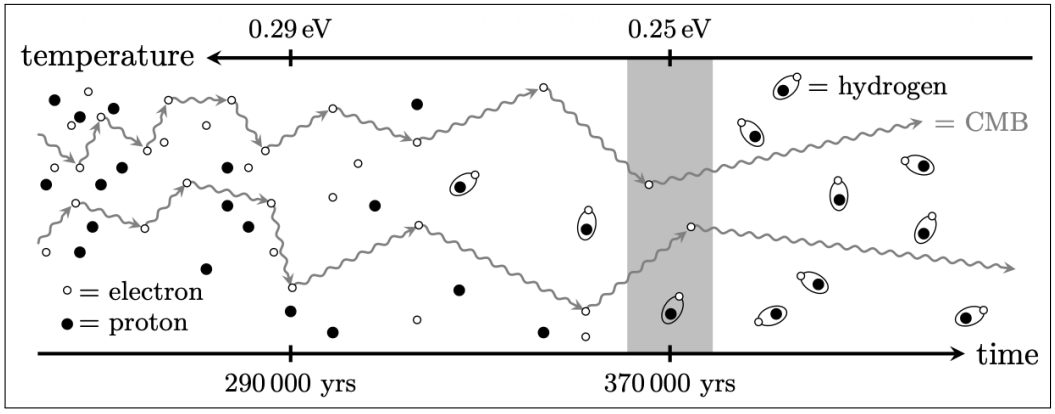


Figure 2.2: Sketch of the recombination of protons and electrons into neutral hydrogen atoms and the corresponding decoupling of photons. Figure taken from [1].

potentials, since $\mu_e + \mu_p = \mu_H$, we consider the following ratio:

$$\left(\frac{n_H}{n_e n_p}\right)_{\text{eq}} = \frac{g_H}{g_e g_p}\left(\frac{m_H}{m_e m_p}\frac{2\pi}{T}\right)^{3/2} \exp\left(\frac{m_e + m_p - m_H}{T}\right) \ . \tag{2.6}$$

Now, since $m_H \simeq m_p$ and

$$\frac{g_H}{g_e g_p} = \frac{4}{2 \cdot 2} = 1 \ , \tag{2.7}$$

if we define the hydrogen binding energy as

$$m_e + m_p - m_H \equiv E_H \simeq 13.6\,\text{eV} \ , \tag{2.8}$$

Equation (2.6) reduces to

$$\left(\frac{n_H}{n_e n_p}\right)_{\text{eq}} \simeq \left(\frac{2\pi}{m_e T}\right)^{3/2} e^{E_H/T} \ . \tag{2.9}$$

At this point, we can define the fraction of free electrons X_e as

$$X_e \equiv \frac{n_e}{n_p + n_H} = \frac{n_e}{n_e + n_H} \ , \tag{2.10}$$

a quantity that lies in the range $[0, 1]$. In particular, if $X_e = 1$, the universe is fully ionized, so there are no hydrogen atoms around. On the other hand, if $X_e = 0$, the universe is completely neutral as all electrons are bound into H.

Now, since we can approximate the denominator of X_e by the baryon density n_b, which, in terms of the photon density n_γ and the parameter $\eta \sim 10^{-10}$, is

$$n_b = \eta n_\gamma = \eta \frac{2\zeta(3)}{\pi^2} T^3 \ , \tag{2.11}$$

it turns out that

$$\left(\frac{1 - X_e}{X_e^2}\right)_{\text{eq}} = \left(\frac{n_H}{n_e n_p}\right)_{\text{eq}} n_b = \eta \frac{2\zeta(3)}{\pi^2}\left(\frac{2\pi T}{m_e}\right)^{3/2} e^{E_H/T} \ . \tag{2.12}$$

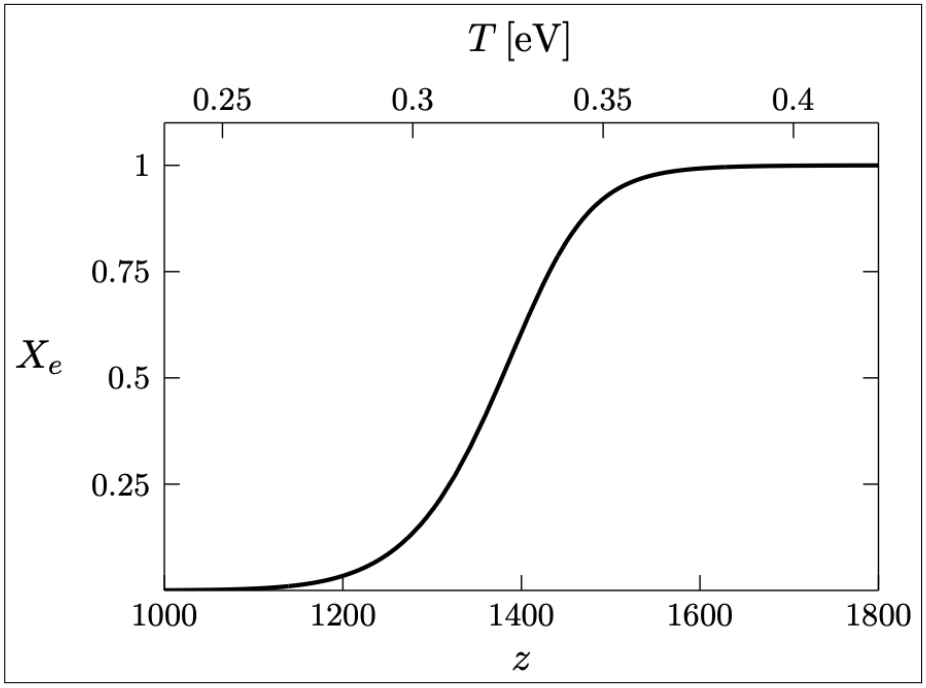


Figure 2.3: Fraction of free electrons as a function of temperature (or redshift) according to the Saha equation. Figure taken from [1].

This is known as the Saha equation and its numerical solution is plotted in Figure 2.3.

Now, since the recombination temperature T_{rec} is defined by the condition $X_e(T_{rec}) = 0.5$, using the Saha equation we obtain that $T_{rec} \simeq 0.32\,\text{eV}$, which corresponds to redshift $z_{rec} \simeq 1380$, a result that is close to $z'_{rec} \simeq 1270$, derived more rigorously by solving Boltzmann equations.

Last-scattering, or photon decoupling, is the phenomenon corresponding to the moment at which photons decouple from the surrounding plasma. As in the case of freeze-out, that moment is defined by the condition $\Gamma(T_{ls}) = H(T_{ls})$, where the Hubble parameter is expressed by

$$H(T_{ls}) \simeq H_0\sqrt{\Omega_m}\left(\frac{T_{ls}}{T_0}\right)^{3/2} \tag{2.13}$$

in the one-dominant fluid approximation. On the other hand, the interaction rate is given by

$$\Gamma_{ls} = n_b X_e(T_{ls})\sigma_T \simeq \frac{2\zeta(3)}{\pi^2}\eta\sigma_T X_e(T_{ls})T_{ls}^3\ , \tag{2.14}$$

where σ_T is the cross-section for Thomson scattering

$$e + \gamma \longrightarrow e + \gamma \tag{2.15}$$

that keeps electrons and photons in equilibrium in the early universe. With that said, by equating Equations (2.13) and (2.14), using the Saha approximation for X_e, we obtain that $T_{ls} \simeq 0.27\,\text{eV}$, while in the more precise treatment we find that decoupling occurs at $T'_{ls} \simeq 0.25\,\text{eV}$, which corresponds to $z'_{ls} \simeq 1090$.

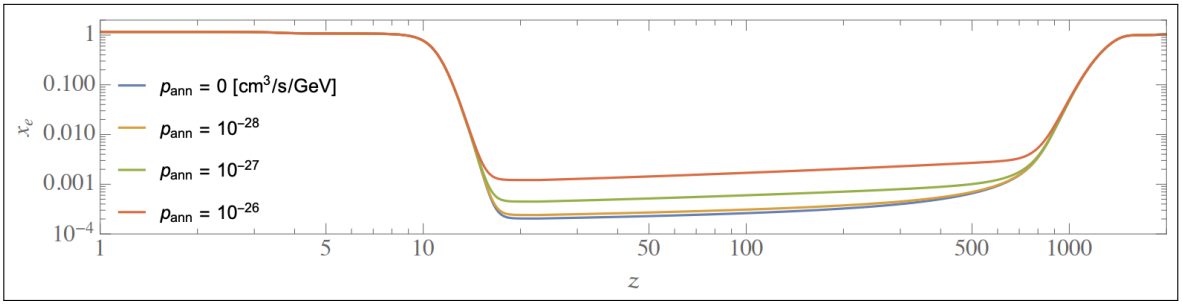


Figure 2.4: Measured fraction of free electrons as a function of redshift for different values of $p_{ann} \equiv f_{eff}\langle\sigma v\rangle/m_\chi$. Figure taken from [19].

Last-scattering can also be defined by the condition $\tau(z_{ls}) = 1$, where τ is the so-called optical depth, a quantity that counts the number of photon scattering events from some emission time to today. Formally, the optical depth is expressed by [18]

$$\tau(z) = \int_t^{t_0} dt' \Gamma(t') = \int_t^{t_0} dt' n_e(t') \sigma_T c \; = \int_0^z dz' \frac{c\sigma_T n_b(z') X_e(z')}{(1+z')H(z')} \; , \tag{2.16}$$

where in the last step we have changed variable according to

$$dt = -\frac{dz'}{(1+z')\, H(z')} \tag{2.17}$$

and used the fact that $n_e = X_e n_b$. At this point, by approximating the Hubble parameter as

$$H(z) \simeq H_0 \sqrt{\Omega_m \, (1+z)^3} \; , \tag{2.18}$$

we obtain that

$$\tau(z) \simeq \tau_0 \int_0^z dz' \frac{(1+z')^3 \, X_e(z')}{(1+z')^{5/2}} = \tau_0 \int_0^z dz' \, (1+z')^{1/2} \, X_e(z') \; , \tag{2.19}$$

where τ_0 is a factor that collects all the constants.

This computation for $\tau(z)$ assumes that X_e remains vanishingly small from recombination to today. However, this is not the case: indeed, precise Planck measurements reveal that, as illustrated in Figure 2.4, the fraction of free electrons drops to very small values after recombination before rising back to 1 around $z \simeq 8$. This process, known as *reionization*, has astrophysical origins and tells us that today the universe is not neutral, but ionized, similarly to the very early times. Nevertheless, DM annihilation can still play a minor role in reionization: indeed, since Dark Matter starts to annihilate during the formation of primordial microhalos at $z \sim 100 - 200$, well before reionization, even a percent-level contribution to X_e could still be reflected in the optical depth τ [20].

2.3 The CMB limit

Let us study in detail the CMB bound that we have briefly mentioned in Section 1.4 and represented in Figure 1.11. As discussed in Section 2.2, DM annihilation can give rise to a small contribution to the fraction of free electrons observed today, which in turn affects the optical depth. Let us therefore study this contribution, denoted as $\Delta\tau$.

Before doing so, let us first introduce a new quantity. Following [18] and [21], we can express the equation for the evolution of the free-electron density as

$$\dot{n}_e + 3Hn_e = I_{std} + Q \ , \tag{2.20}$$

where I_{std} denotes the contribution due to the standard recombination and ionization, while Q is the rate at which $\chi\bar{\chi}$ annihilations happen and, according to a formula similar to the one reported in [22], is given by

$$Q = f\frac{2n_\chi^2\langle\sigma v\rangle m_\chi}{E_H}\frac{1-X_e}{3} \ . \tag{2.21}$$

Thus, Q depends on the number of DM annihilations per unit time and volume, $2n_\chi^2\langle\sigma v\rangle$, each one releasing an energy m_χ per annihilating particle. In addition, it depends on the hydrogen binding energy E_H and on the efficiency parameter f, a number lying in $[0,1]$, representing the fraction of energy that is absorbed by the baryonic gas. Finally, since the absorbed energy contributes both to the ionization and the heating of the gas, we insert a factor $(1-X_e)/3$ to account only for the former effect.

Now, since the baryon number is conserved, meaning that the baryon density n_b satisfies

$$\dot{n}_b + 3Hn_b = 0 \ , \tag{2.22}$$

and since

$$n_e + n_H = n_b \ , \tag{2.23}$$

implying that

$$X_e = \frac{n_e}{n_e + n_H} = \frac{n_e}{n_b} \ , \tag{2.24}$$

it turns out that

$$\Delta\dot{X}_e = \frac{\dot{n}_e}{n_b} \simeq \frac{Q}{n_b} \ . \tag{2.25}$$

This therefore indicates that the time-derivative of the additional contribution ΔX_e to X_e due

to DM annihilation is linearly proportional to Q. As a result, if we consider Equation (2.16), we can determine the analytic expression for $\Delta\tau$ from recombination to today [18]:

$$\Delta\tau(z) = \int_0^{z_{rec}} dz' \frac{c\sigma_T n_b(z')\Delta X_e(z')}{(1+z')H(z')} = \int_0^{z_{rec}} dz' \frac{c\sigma_T n_b(z')}{(1+z')H(z')} \int_{z'}^{z_{rec}} d\zeta \frac{1}{(1+\zeta)H(\zeta)} \frac{Q(\zeta)}{n_b(\zeta)} \ . \quad (2.26)$$

Now, considering Equation (2.21) for Q, if we approximate X_e as a step function and, therefore, the factor $(1 - X_e)/3$ as $\vartheta(z_{rec} - z)/3$, we obtain that

$$\Delta\tau(z) \simeq \int_0^{z_{rec}} dz' \frac{c\sigma_T n_b(z')}{(1+z')H(z')} \int_{z'}^{z_{rec}} d\zeta \frac{1}{(1+\zeta)H(\zeta)} \frac{2f\rho_\chi^2\langle\sigma v\rangle}{3E_H m_\chi n_b(\zeta)} \ . \quad (2.27)$$

At this point, we can further simplify that expression if we assume that DM annihilation occurs in s-wave because in that case, according to Equations (1.31) and (1.32), $\langle\sigma v\rangle$ does not depend on temperature and, therefore, redshift, so it can be factored out of the integrals. Consequently, it turns out that

$$\Delta\tau = \frac{2}{3} \frac{\langle\sigma v\rangle f}{m_\chi} \frac{c\sigma_T \rho_\chi^2(z=0)}{E_H H_0^2 \Omega_m} \int_0^{z_{rec}} dz' \, z'^{1/2} \int_{z'}^{z_{rec}} d\zeta \, \zeta^{1/2} \ . \quad (2.28)$$

Finally, as shown in [18], by plugging the known values for the parameters into the previous equation, we end up with

$$\Delta\tau = \left[\frac{\langle\sigma v\rangle f}{3 \cdot 10^{-26}\,\mathrm{cm^3/s}}\right] \left[\frac{m_\chi}{10\,\mathrm{GeV}}\right]^{-1} \cdot 0.1 \ . \quad (2.29)$$

Now, since reionization has mostly astrophysical origins and DM annihilation can only play a minor role in it, $\Delta\tau$ must remain within the experimental uncertainty σ_τ on the optical depth. Thus, by comparing $\Delta\tau$, obtained either through Equation (2.29) or through a more rigorous numerical treatment, with the observed value for the total optical depth $\tau = 0.054 \pm 0.007$ [12], we can extract bounds on DM annihilation. Indeed, since $\Delta\tau$ depends on both $\langle\sigma v\rangle$ and m_χ, requiring that $\Delta\tau \lesssim \sigma_\tau = 0.007$ translates into an upper bound on $\langle\sigma v\rangle$ as a function of m_χ. With that said, these bounds, represented in Figure 1.11, are known as CMB bounds because they depend on small modifications of the CMB spectrum generated by the interactions between CMB photons and the additional free electrons produced after recombination.

In any case, as stated before, the approximate derivation that we have found relies on an important assumption: the fact that DM annihilation occurs in s-wave, so that $\langle\sigma v\rangle$ is constant and can be factored out of the integral. If, however, DM annihilation proceeds through a p-wave interaction, $\langle\sigma v\rangle \propto v^2$ is no longer constant but decreases with the expansion of the universe since $v \propto (1+z)$ in the non-relativistic limit. As a consequence, by the time of recombination the annihilation rate is extremely small compared to its value at freeze-out and the CMB

bound cannot be applied, which is why p-wave DM candidates evade it. This motivates us to take a closer look at the nature of DM interactions and, therefore, to determine whether the annihilation cross-section is s-wave or p-wave for different scalar and fermionic DM candidates in Chapter 3.

3. Partial-wave classification of Dark Matter operators

3.1 Overview and preliminaries

In this chapter we focus on 2-to-2 DM annihilation processes and quantitatively analyze which ones occur in s-wave and which in p-wave for different scalar and fermionic DM operators in order to determine which structures evade the CMB limit, as previously discussed in Section 2.3.

As shown in standard Quantum Field Theory textbooks, such as [23] and [24], the differential cross-section $d\sigma/d\Omega$ of the process $\chi\bar{\chi} \to \mathrm{SM}\,\overline{\mathrm{SM}}$ is related to the squared amplitude $|\mathcal{A}|^2$ as

$$\frac{d\sigma}{d\Omega} = \frac{1}{2E_\chi \cdot 2E_{\bar{\chi}}} \frac{1}{|\mathbf{v}_\chi - \mathbf{v}_{\bar{\chi}}|} \frac{|\mathbf{p}_{\mathrm{SM}}|}{16\pi^2 E_{cm}} |\mathcal{A}|^2 \ , \tag{3.1}$$

where E_χ and $E_{\bar{\chi}}$ are the energies of the incoming particles, $\mathbf{v}_\chi$ and $\mathbf{v}_{\bar{\chi}}$ their velocities, $\mathbf{p}_{\mathrm{SM}}$ the momentum of one of the outgoing particles and E_{cm} the center-of-mass energy. This equation is the starting point for another expression that relates $|\mathcal{A}|^2$ to σv and that, therefore, allows us to determine whether an interaction proceeds through s-wave or p-wave just by looking at its amplitude. To proceed, let us consider the center-of-mass reference frame, defined by the condition

$$\mathbf{p}_\chi = -\mathbf{p}_{\bar{\chi}} \ . \tag{3.2}$$

Since the two incoming particles have the same mass, they also turn out to have the same energy, implying that

$$E_{cm} = E_\chi + E_{\bar{\chi}} = 2E_\chi \ . \tag{3.3}$$

As a result, we can rewrite one of the factors that enter the differential cross-section as

$$|\mathbf{v}_\chi - \mathbf{v}_{\bar{\chi}}| = \left| \frac{\mathbf{p}_\chi}{E_\chi} - \frac{\mathbf{p}_{\bar{\chi}}}{E_{\bar{\chi}}} \right| = \frac{2}{E_{cm}} |\mathbf{p}_\chi - \mathbf{p}_{\bar{\chi}}| = \frac{4|\mathbf{p}_\chi|}{E_{cm}} \ . \tag{3.4}$$

Thus,

$$\frac{d\sigma}{d\Omega} = \frac{4}{4 \cdot E_{cm} \cdot E_{cm}} \frac{E_{cm}}{4|\mathbf{p}_\chi|} \frac{|\mathbf{p}_{\mathrm{SM}}|}{16\pi^2 E_{cm}} |\mathcal{A}|^2 = \frac{1}{64\pi^2} \frac{1}{E_{cm}^2} \frac{|\mathbf{p}_{\mathrm{SM}}|}{|\mathbf{p}_\chi|} |\mathcal{A}|^2 \ . \tag{3.5}$$

At this point, by recalling that DM particles are non-relativistic (see Section 1.2), we obtain that

$$E_{cm} = 2E_\chi \simeq 2m \tag{3.6}$$

and that

$$|\mathbf{p}_\chi| \simeq m|\mathbf{v}_\chi| = \frac{mv}{2} \ , \tag{3.7}$$

where m denotes the mass of DM particles, while

$$v \equiv |\mathbf{v}_\chi - \mathbf{v}_{\bar{\chi}}| = 2|\mathbf{v}_\chi| \tag{3.8}$$

is the modulus of their relative velocity. Furthermore, if we assume that the outgoing particles are ultra-relativistic, therefore having $|\mathbf{p}_{\rm SM}| \simeq E_{\rm SM}$, it turns out that

$$|\mathbf{p}_{\rm SM}| \simeq E_{\rm SM} = \frac{E_{cm}}{2} \simeq m \ , \tag{3.9}$$

provided that the final-state particles have the same mass. It is now possible to substitute Equations (3.6), (3.7) and (3.9) into Equation (3.5), obtaining

$$\frac{d\sigma}{d\Omega} \simeq \frac{1}{64\pi^2}\frac{1}{4m^2}\frac{2m}{mv}|\mathcal{A}|^2_{\rm NR} = \frac{1}{128\pi^2 m^2}\frac{|\mathcal{A}|^2_{\rm NR}}{v} \ , \tag{3.10}$$

where $|\mathcal{A}|^2_{\rm NR}$ represents the non-relativistic limit of the amplitude. At this point, if we multiply both sides by v and integrate over the solid angle Ω, the previous equation becomes

$$\sigma v \simeq \frac{1}{128\pi^2 m^2}\int d\Omega |\mathcal{A}|^2_{\rm NR} \ . \tag{3.11}$$

Therefore, recalling Equation (1.31), we conclude that whether an annihilation process occurs in s-wave or in p-wave can be directly determined from its amplitude in the non-relativistic limit.

In the following sections, we will compute the non-relativistic amplitude of the annihilation process for several scalar and fermionic DM operators (mainly in the s-channel), in order to classify them as s-wave or p-wave and identify those that evade the CMB bound.

3.2 Scalar Dark Matter operators

Let us start by considering two complex scalar DM particles Φ and $\Phi^\dagger$ annihilating into two SM particles:

$$\Phi^\dagger\Phi \longrightarrow {\rm SM}\,\overline{\rm SM} \tag{3.12}$$

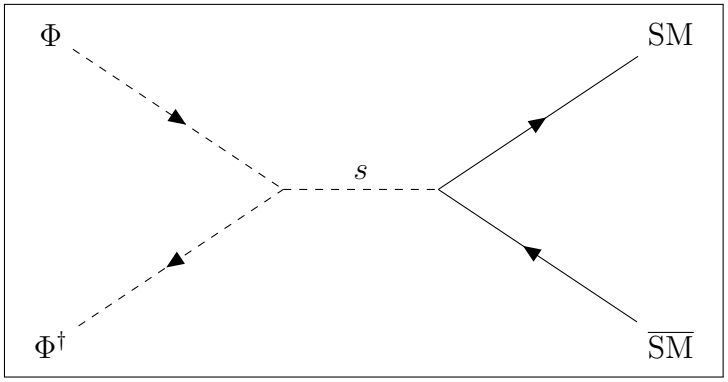


Figure 3.1: Feynman diagram for the annihilation process $\Phi^\dagger\Phi \to \mathrm{SM}\,\overline{\mathrm{SM}}$, mediated by a scalar s.

Represented in Figure 3.1, the simplest case is the one with a scalar mediator s, whose interaction Lagrangian is

$$\mathcal{L}_{int} = \mathcal{L}_{int}^{\Phi-s} + \mathcal{L}_{int}^{s-SM} = -g_\Phi^s \Phi^\dagger \Phi s + \mathcal{L}_{int}^{s-SM} \ , \tag{3.13}$$

where g_Φ^s is the coupling constant of the first vertex. In order to classify this kind of interaction, let us first consider the expression for the amplitude of a generic s-channel process:

$$i\mathcal{A} = J_{DM} D(k) J_{SM} \ , \tag{3.14}$$

where J_{DM} and J_{SM} are the DM and SM currents, respectively, and $D(k)$ is the propagator with momentum k, which depends on the momenta p and q of the incoming particles through

$$k = p + q \ . \tag{3.15}$$

Now, if we apply the Feynman rules to the interaction in Equation (3.13), we obtain that

$$i\mathcal{A} = -ig_\Phi^s \frac{i}{k^2 - m_s^2} J_{SM} \ , \tag{3.16}$$

where m_s is the mass of the mediator. In particular, we have not expanded J_{SM} because the possible v-dependence of the amplitude arises only from the relative velocity of the incoming particles. With that said, since the amplitude, and hence its square, does not depend on v, we can conclude that the $\Phi^\dagger\Phi \to \mathrm{SM}\,\overline{\mathrm{SM}}$ annihilation process mediated by a scalar particle is always s-wave.

Let us now study a more complex process, represented in Figure 3.2, in which we consider the annihilation of two scalar DM particles mediated by a vector particle V_μ.

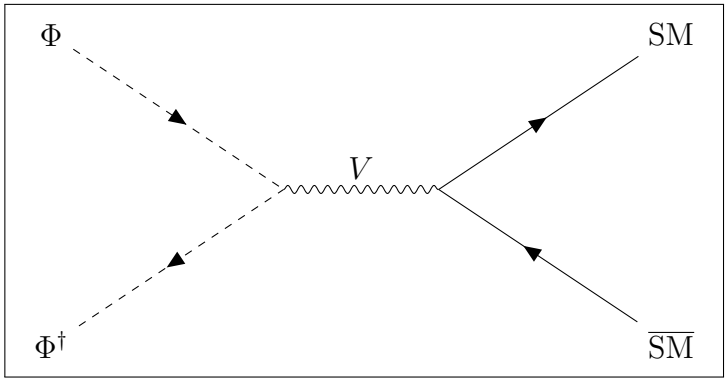


Figure 3.2: Feynman diagram for the annihilation process $\Phi^\dagger\Phi \to \mathrm{SM}\,\overline{\mathrm{SM}}$, mediated by a vector V.

In this case, we assume that the interaction Lagrangian is

$$\mathcal{L}_{int} = i g_\Phi^V \Phi^\dagger \overleftrightarrow{\partial}^\mu \Phi V_\mu + \mathcal{L}_{int}^{V-SM} \ , \tag{3.17}$$

where $\overleftrightarrow{\partial}^\mu$ acts as follows:

$$\Phi^\dagger \overleftrightarrow{\partial}^\mu \Phi = (\partial^\mu \Phi^\dagger)\Phi - \Phi^\dagger(\partial^\mu \Phi) \ . \tag{3.18}$$

Since the mediator is now a vector, the general structure of the amplitude in Equation (3.14) acquires Lorentz indices, as expressed by

$$i\mathcal{A} = J_{DM}^\mu D_{\mu\nu}(k) J_{SM}^\nu \ , \tag{3.19}$$

where

$$D_{\mu\nu}(k) = \frac{-i}{k^2 - m_V^2}\left(\eta_{\mu\nu} - \frac{k_\mu k_\nu}{m_V^2}\right) \tag{3.20}$$

is the propagator of the vector mediator and depends on its mass m_V, its momentum $k = p + q$ and the Minkowski metric $\eta_{\mu\nu}$. Consequently,

$$i\mathcal{A} = \frac{-i}{k^2 - m_V^2} J_{DM}^\mu \left(\eta_{\mu\nu} - \frac{k_\mu k_\nu}{m_V^2}\right) J_{SM}^\nu = \frac{-i}{k^2 - m_V^2}\left(J_{DM}\cdot J_{SM} - \frac{(k\cdot J_{DM})(k\cdot J_{SM})}{m_V^2}\right) . \tag{3.21}$$

At this point, from Equation (3.17) we have that

$$J_{DM}^\mu = i\left(i g_\Phi^V \Phi^\dagger \overleftrightarrow{\partial}^\mu \Phi\right) = -g_\Phi^V \Phi^\dagger \overleftrightarrow{\partial}^\mu \Phi \ . \tag{3.22}$$

Let us now rewrite it in a different form, in order to make explicit its dependence on the momenta of the incoming DM particles.

Recalling that

$$\Phi(x) = \int \frac{d^3k}{(2\pi)^3\sqrt{2\omega_{\mathbf{k}}}}\left[a_{\mathbf{k}} e^{-ik\cdot x} + b_{\mathbf{k}}^\dagger e^{ik\cdot x}\right] \tag{3.23}$$

and that

$$\Phi^\dagger(x) = \int \frac{d^3k}{(2\pi)^3\sqrt{2\omega_{\mathbf{k}}}} \left[a^\dagger_{\mathbf{k}} e^{ik\cdot x} + b_{\mathbf{k}} e^{-ik\cdot x}\right] \ , \tag{3.24}$$

since we want to destroy a scalar particle–antiparticle pair, we will consider the following substitutions for Φ and $\Phi^\dagger$:

$$\begin{aligned} \Phi &\supset a_{\mathbf{p}} e^{-ip\cdot x} \to e^{-ip\cdot x} \ ; \\ \Phi^\dagger &\supset b_{\mathbf{q}} e^{-iq\cdot x} \to e^{-iq\cdot x} \ . \end{aligned} \tag{3.25}$$

Indeed, from a practical point of view, $a_{\mathbf{p}}$ and $b_{\mathbf{q}}$ act on the initial state and destroy the particle–antiparticle pair, leaving only the two exponentials (and the normalization constants that we will not include in the computation). As a consequence, we have that

$$\begin{aligned} \partial^\mu \Phi &\to (-ip^\mu) e^{-ip\cdot x} \ ; \\ \partial^\mu \Phi^\dagger &\to (-iq^\mu) e^{-iq\cdot x} \ . \end{aligned} \tag{3.26}$$

This explains why we can generally substitute ∂^μ with $-ip_i^\mu$, where p_i is the momentum of the incoming particle considered. In addition, we can omit the exponentials as they disappear once we integrate over spacetime.

With that said, the action of the derivative becomes

$$\Phi^\dagger \overleftrightarrow{\partial}^\mu \Phi \to (-iq^\mu) - (-ip^\mu) = i(p^\mu - q^\mu) \ . \tag{3.27}$$

As a result, the DM current is

$$J^\mu_{DM} = -g^V_\Phi \cdot i(p^\mu - q^\mu) = -ig^V_\Phi (p^\mu - q^\mu) \ . \tag{3.28}$$

Let us now determine its temporal and spatial components. In order to do so, we consider the center-of-mass reference frame, where, as a reminder, $\mathbf{p} + \mathbf{q} = 0$. This implies that the two incoming particles have the same energy ($E_p = E_q \equiv E$) since they have the same mass and their momenta are opposite. As a result,

$$\begin{aligned} J^0_{DM} &= -ig^V_\Phi (p^0 - q^0) = -ig^V_\Phi (E - E) = 0 \ ; \\ \mathbf{J}_{DM} &= -ig^V_\Phi (\mathbf{p} - \mathbf{q}) = -2ig^V_\Phi \mathbf{p} \ . \end{aligned} \tag{3.29}$$

Having determined the explicit expression of J_{DM}, we can now insert it into Equation (3.21) to determine the nature of this interaction. In particular, since

$$k \cdot J_{DM} = (p+q)[-ig^V_\Phi (p-q)] = -ig^V_\Phi (p^2 + p\cdot q - q\cdot p - q^2) = 0 \ , \tag{3.30}$$

the amplitude becomes

$$i\mathcal{A} = \frac{-i}{k^2 - m_V^2}(J_{DM} \cdot J_{SM}) = \frac{-i}{k^2 - m_V^2}(J^0_{DM} J^0_{SM} - \mathbf{J}_{DM} \cdot \mathbf{J}_{SM}) \ . \tag{3.31}$$

Finally, considering Equations (3.29), we obtain that

$$i\mathcal{A} = \frac{i}{k^2 - m_V^2}\mathbf{J}_{DM} \cdot \mathbf{J}_{SM} = \frac{i}{k^2 - m_V^2}[-2ig^V_\Phi \mathbf{p} \cdot \mathbf{J}_{SM}] = \frac{2g^V_\Phi}{k^2 - m_V^2}\mathbf{p} \cdot \mathbf{J}_{SM} \ . \tag{3.32}$$

This final result shows that the annihilation process described by Equation (3.17) is p-wave since its amplitude is proportional to the relative velocity v in the non-relativistic limit (see Equation (3.7)), implying that $|\mathcal{A}|^2$, and therefore $\langle \sigma v \rangle$, are proportional to v^2.

3.3 Fermionic Dark Matter operators

3.3.1 Non-relativistic limit of Dirac spinors

Before focusing on specific fermionic operators, let us first recall the general expression of a spinor field $\chi(x)$ in terms of creation and destruction operators:

$$\chi(x) = \int \frac{d^3k}{(2\pi)^3\sqrt{2\omega_{\mathbf{k}}}} \sum_{\lambda=1}^{2} \left[u^\lambda(k) a_{\mathbf{k}\lambda} e^{-ik\cdot x} + v^\lambda(k) b^\dagger_{\mathbf{k}\lambda} e^{ik\cdot x} \right] \ , \tag{3.33}$$

where λ represents the spin index, k the momentum, while the spinors $u^\lambda(k)$ and $v^\lambda(k)$ can be written in terms of Pauli matrices as

$$u^\lambda(k) = \begin{pmatrix} \sqrt{\sigma \cdot k}\, \xi^\lambda \\ \sqrt{\bar{\sigma} \cdot k}\, \xi^\lambda \end{pmatrix} \quad , \quad v^\lambda(k) = \begin{pmatrix} \sqrt{\sigma \cdot k}\, \eta^\lambda \\ -\sqrt{\bar{\sigma} \cdot k}\, \eta^\lambda \end{pmatrix} \ . \tag{3.34}$$

In particular, as shown in [25], the square roots of the matrices $\sigma \cdot k$ and $\bar{\sigma} \cdot k$ can be written in an alternative way as

$$\begin{aligned} \sqrt{\sigma \cdot k} &= \frac{1}{\sqrt{2(k^0 + m)}}(\sigma \cdot k + m) \ ; \\ \sqrt{\bar{\sigma} \cdot k} &= \frac{1}{\sqrt{2(k^0 + m)}}(\bar{\sigma} \cdot k + m) \ , \end{aligned} \tag{3.35}$$

where m is the mass of the fermionic particle.

We can now use these results to derive the non-relativistic limit of the spinors $u^r(p)$ and $v^s(q)$, as shown in [26].

As for $u^r(p)$, we have that

$$u^r(p) = \begin{pmatrix} \sqrt{\sigma \cdot p}\,\xi^r \\ \sqrt{\bar{\sigma} \cdot p}\,\xi^r \end{pmatrix} = \frac{1}{\sqrt{2(p^0+m)}} \begin{pmatrix} (\sigma \cdot p + m)\,\xi^r \\ (\bar{\sigma} \cdot p + m)\,\xi^r \end{pmatrix} \overset{\text{NR}}{\simeq} \frac{1}{\sqrt{4m}} \begin{pmatrix} (2m - \boldsymbol{\sigma} \cdot \mathbf{p})\,\xi^r \\ (2m + \boldsymbol{\sigma} \cdot \mathbf{p})\,\xi^r \end{pmatrix} . \tag{3.36}$$

In particular, in the last step we have considered that

$$\begin{aligned} \sigma^\mu = (\mathbb{1}\,,\,\boldsymbol{\sigma}) \quad &\Rightarrow \quad \sigma_\mu = (\mathbb{1}\,,\,-\boldsymbol{\sigma}) \ ; \\ \bar{\sigma}^\mu = (\mathbb{1}\,,\,-\boldsymbol{\sigma}) \quad &\Rightarrow \quad \bar{\sigma}_\mu = (\mathbb{1}\,,\,\boldsymbol{\sigma}) \end{aligned} \tag{3.37}$$

in the Weyl representation and that

$$p^\mu = (m\,,\,\mathbf{p}) \tag{3.38}$$

in the non-relativistic limit. As a consequence,

$$\begin{aligned} \sigma \cdot p + m = p^\mu \sigma_\mu + m = \left(p^0 \sigma_0 + p^i \sigma_i + m\right) = (m\mathbb{1} - \boldsymbol{\sigma} \cdot \mathbf{p} + m) = 2m - \boldsymbol{\sigma} \cdot \mathbf{p} \ ; \\ \bar{\sigma}_\mu \cdot p + m = p^\mu \bar{\sigma}_\mu + m = \left(p^0 \bar{\sigma}_0 + p^i \bar{\sigma}_i + m\right) = (m\mathbb{1} + \boldsymbol{\sigma} \cdot \mathbf{p} + m) = 2m + \boldsymbol{\sigma} \cdot \mathbf{p} \ . \end{aligned} \tag{3.39}$$

Similarly, as for $v^s(q)$, we obtain that

$$v^s(q) = \begin{pmatrix} \sqrt{\sigma \cdot q}\,\eta^s \\ -\sqrt{\bar{\sigma} \cdot q}\,\eta^s \end{pmatrix} = \frac{1}{\sqrt{2(q^0+m)}} \begin{pmatrix} (\sigma \cdot q + m)\,\eta^s \\ -\,(\bar{\sigma} \cdot q + m)\,\eta^s \end{pmatrix} \overset{\text{NR}}{\simeq} \frac{1}{\sqrt{4m}} \begin{pmatrix} (2m - \boldsymbol{\sigma} \cdot \mathbf{q})\,\eta^s \\ -\,(2m + \boldsymbol{\sigma} \cdot \mathbf{q})\,\eta^s \end{pmatrix} . \tag{3.40}$$

Having derived the non-relativistic limit of the spinors $u^r(p)$ and $v^s(q)$, we can now study the velocity dependence of some fermion bilinears built from them: the scalar, the pseudoscalar, the vector, the axial vector, the tensor and the axial tensor bilinears. This analysis follows the approach of [26], which considers the bilinears $\bar{u}^{r'}(p')\Gamma u^r(p)$, relevant for DM scattering in Direct Detection. However, since we want to determine which processes evade the CMB bound, we focus on the bilinears $\bar{v}^s(q)\Gamma u^r(p)$, relevant for DM annihilation, described by

$$\chi\bar{\chi} \longrightarrow \mathrm{SM}\,\overline{\mathrm{SM}} \ , \tag{3.41}$$

where χ and $\bar{\chi}$ are the annihilating DM fermion and antifermion. In the following, we only report the main steps of the computation, while the complete derivations are presented in the Appendix.

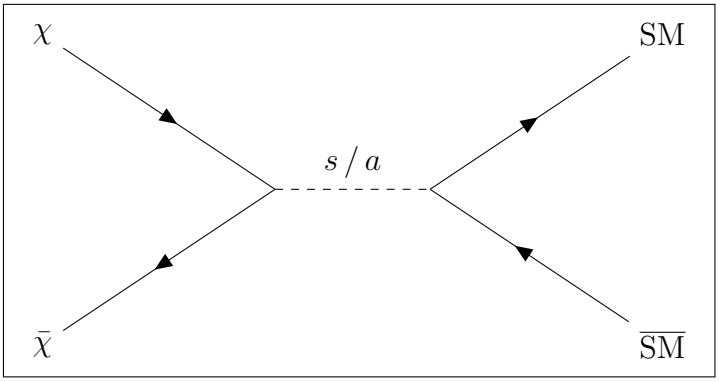


Figure 3.3: Feynman diagram for the annihilation process $\chi\bar{\chi} \to \text{SM}\,\overline{\text{SM}}$, mediated by either a scalar s or a pseudoscalar a.

3.3.2 The scalar fermion bilinear

Let us start our analysis by considering the simplest fermion bilinear, that is the scalar one $\bar{v}^s(q)u^r(p)$. This structure appears when we consider the process represented in Figure 3.3, in which the annihilation of the DM fermion–antifermion pair is mediated by a scalar s. The interaction Lagrangian of the process is

$$\mathcal{L}_{int} = -g_\chi^s \bar{\chi}\chi s + \mathcal{L}_{int}^{s-SM} \ , \tag{3.42}$$

from which the amplitude reads

$$i\mathcal{A} = \bar{v}^s(q)(-ig_\chi^s)u^r(p)\frac{i}{k^2 - m_s^2}J_{SM} \ . \tag{3.43}$$

Since we are interested in computing the non-relativistic limit of the bilinear $\bar{v}^s(q)u^r(p)$, let us first determine the Weyl representation for $\bar{v}^s(q)$:

$$\bar{v}^s(q) = v^s(q)^\dagger\gamma^0 = \begin{pmatrix} \eta^{s\dagger}\sqrt{\sigma\cdot q} & -\eta^{s\dagger}\sqrt{\bar{\sigma}\cdot q} \end{pmatrix}\begin{pmatrix} 0 & \mathbb{1} \\ \mathbb{1} & 0 \end{pmatrix} = \begin{pmatrix} -\eta^{s\dagger}\sqrt{\bar{\sigma}\cdot q} & \eta^{s\dagger}\sqrt{\sigma\cdot q} \end{pmatrix} \ . \tag{3.44}$$

Similarly to Equations (3.36) and (3.40), we therefore obtain that

$$\bar{v}^s(q) \overset{\text{NR}}{\simeq} \frac{1}{\sqrt{4m}}\begin{pmatrix} -\eta^{s\dagger}\,(2m + \boldsymbol{\sigma}\cdot\mathbf{q}) & \eta^{s\dagger}\,(2m - \boldsymbol{\sigma}\cdot\mathbf{q}) \end{pmatrix} \ , \tag{3.45}$$

from which (see Appendix A.1 for the details)

$$\begin{aligned} \bar{v}^s(q)u^r(p) &\overset{\text{NR}}{\simeq} \frac{1}{4m}\begin{pmatrix} -\eta^{s\dagger}\,(2m + \boldsymbol{\sigma}\cdot\mathbf{q}) & \eta^{s\dagger}\,(2m - \boldsymbol{\sigma}\cdot\mathbf{q}) \end{pmatrix}\begin{pmatrix} (2m - \boldsymbol{\sigma}\cdot\mathbf{p})\,\xi^r \\ (2m + \boldsymbol{\sigma}\cdot\mathbf{p})\,\xi^r \end{pmatrix} \\ &= \eta^{s\dagger}\boldsymbol{\sigma}\cdot(\mathbf{p} - \mathbf{q})\,\xi^r \\ &= 2\eta^{s\dagger}\boldsymbol{\sigma}\cdot\mathbf{p}\,\xi^r \ , \end{aligned} \tag{3.46}$$

where in the last step we have moved to the center-of-mass frame. As a result, due to its dependence on $\mathbf{p}$, the scalar fermionic bilinear gives rise to a p-wave interaction in the non-relativistic limit.

3.3.3 The pseudoscalar fermion bilinear

We now want to determine the non-relativistic limit of the pseudoscalar fermion bilinear $\bar{v}^s(q)\,(i\gamma^5)\,u^r(p)$, which arises in the process of Figure 3.3 when the mediator is a pseudoscalar a with mass m_a. The interaction Lagrangian in this case is expressed by

$$\mathcal{L}_{int} = -ig_\chi^a \bar{\chi}\gamma^5\chi a + \mathcal{L}_{int}^{a-SM} \ , \tag{3.47}$$

while the amplitude to study is

$$i\mathcal{A} = \bar{v}^s(q)[-ig_\chi^a(i\gamma^5)]u^r(p)\frac{i}{k^2-m_a^2}J_{SM} \ . \tag{3.48}$$

At this point, by recalling that

$$\gamma^5 = i\gamma^0\gamma^1\gamma^2\gamma^3 = \begin{pmatrix} -\mathbb{1} & 0 \\ 0 & \mathbb{1} \end{pmatrix} \tag{3.49}$$

and by omitting i in the computation since it is just a constant, it turns out that

$$\begin{aligned} \bar{v}^s(q)\gamma^5 u^r(p) &\overset{\text{NR}}{\simeq} \frac{1}{4m}\begin{pmatrix} -\eta^{s\dagger}\,(2m+\boldsymbol{\sigma}\cdot\mathbf{q}) & \eta^{s\dagger}\,(2m-\boldsymbol{\sigma}\cdot\mathbf{q}) \end{pmatrix}\begin{pmatrix} -\,(2m-\boldsymbol{\sigma}\cdot\mathbf{p})\,\xi^r \\ (2m+\boldsymbol{\sigma}\cdot\mathbf{p})\,\xi^r \end{pmatrix} \\ &= \frac{1}{4m}\eta^{s\dagger}\cdot 2\left(4m^2-(\boldsymbol{\sigma}\cdot\mathbf{q})(\boldsymbol{\sigma}\cdot\mathbf{p})\right)\xi^r \ . \end{aligned} \tag{3.50}$$

Now, since $(\boldsymbol{\sigma}\cdot\mathbf{q})(\boldsymbol{\sigma}\cdot\mathbf{p})$ is a second-order term in the momentum, we can neglect it, obtaining

$$\bar{v}^s(q)\gamma^5 u^r(p) \simeq \frac{1}{4m}\cdot 2\cdot 4m^2\eta^{s\dagger}\xi^r = 2m\eta^{s\dagger}\xi^r \ . \tag{3.51}$$

For reference, the full computation for this bilinear can be found in Appendix A.2.

Therefore, this final result shows that the DM annihilation described by the pseudoscalar bilinear $\bar{v}^s(q)\,(i\gamma^5)\,u^r(p)$ is s-wave since the corresponding amplitude does not depend on v.

3.3.4 The vector fermion bilinear

Let us study the vector fermion bilinear $\bar{v}^s(q)\gamma^\mu u^r(p)$, which follows from the interaction Lagrangian

$$\mathcal{L}_{int} = -g_\chi^V \bar{\chi}\gamma^\mu\chi V_\mu + \mathcal{L}_{int}^{V-SM} \ , \tag{3.52}$$

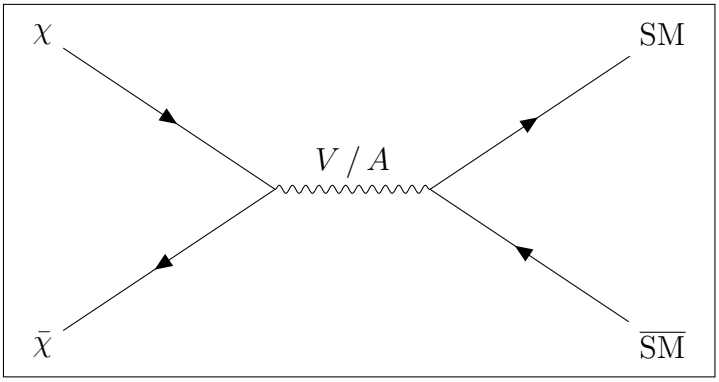


Figure 3.4: Feynman diagram for the annihilation process $\chi\bar{\chi} \to \mathrm{SM}\,\overline{\mathrm{SM}}$, mediated by either a vector V or an axial vector A.

describing the DM annihilation mediated by a vector V, as shown in Figure 3.4. In this case, the amplitude is

$$i\mathcal{A} = \bar{v}^s(q)(-ig_\chi^V \gamma^\mu)u^r(p)\frac{-i}{k^2 - m_V^2}\left(\eta_{\mu\nu} - \frac{k_\mu k_\nu}{m_V^2}\right)J_{SM}^\nu \ . \tag{3.53}$$

Once again, we focus only on the non-relativistic limit of the fermion bilinear to classify this process. Thus, recalling that

$$\gamma^\mu = \begin{pmatrix} 0 & \sigma^\mu \\ \bar{\sigma}^\mu & 0 \end{pmatrix} \ , \tag{3.54}$$

in the Weyl representation, we can write (see Appendix A.3 for the full computation) that

$$\begin{aligned} \bar{v}^s(q)\gamma^\mu u^r(p) &\overset{\mathrm{NR}}{\simeq} \frac{1}{4m}\begin{pmatrix} -\eta^{s\dagger}\left(2m + \boldsymbol{\sigma}\cdot\mathbf{q}\right) & \eta^{s\dagger}\left(2m - \boldsymbol{\sigma}\cdot\mathbf{q}\right)\end{pmatrix}\begin{pmatrix} \sigma^\mu\left(2m + \boldsymbol{\sigma}\cdot\mathbf{p}\right)\xi^r \\ \bar{\sigma}^\mu\left(2m - \boldsymbol{\sigma}\cdot\mathbf{p}\right)\xi^r \end{pmatrix} \\ &= \frac{1}{4m}\eta^{s\dagger}\Big(-\left(2m + \boldsymbol{\sigma}\cdot\mathbf{q}\right)\sigma^\mu\left(2m + \boldsymbol{\sigma}\cdot\mathbf{p}\right) \\ &\qquad + \left(2m - \boldsymbol{\sigma}\cdot\mathbf{q}\right)\bar{\sigma}^\mu\left(2m - \boldsymbol{\sigma}\cdot\mathbf{p}\right)\Big)\xi^r \ . \end{aligned} \tag{3.55}$$

Since the bilinear carries a Lorentz index, we study its temporal ($\mu = 0$) and spatial ($\mu = i$) components separately, as they may have a different velocity dependence. In order to proceed, let us consider Equations (3.37), which imply that

$$\begin{aligned} \sigma^0 = \bar{\sigma}^0 = \mathbb{1} \ ; \\ \sigma^i = -\bar{\sigma}^i \ . \end{aligned} \tag{3.56}$$

As a consequence, the temporal component of the bilinear is

$$\begin{aligned} \bar{v}^s(q)\gamma^0 u^r(p) &\simeq \frac{1}{4m}\eta^{s\dagger}\Big(-\left(2m + \boldsymbol{\sigma}\cdot\mathbf{q}\right)\left(2m + \boldsymbol{\sigma}\cdot\mathbf{p}\right) + \left(2m - \boldsymbol{\sigma}\cdot\mathbf{q}\right)\left(2m - \boldsymbol{\sigma}\cdot\mathbf{p}\right)\Big)\xi^r \\ &= -\eta^{s\dagger}\boldsymbol{\sigma}\cdot\left(\mathbf{p} + \mathbf{q}\right)\xi^r \ . \end{aligned} \tag{3.57}$$

Thus, in the center-of-mass reference frame, where $\mathbf{p} + \mathbf{q} = 0$, we have that

$$\bar{v}^s(q)\gamma^0 u^r(p) = 0 \ , \tag{3.58}$$

so the temporal component always vanishes.

As for the spatial component, we have that

$$\begin{aligned} \bar{v}^s(q)\gamma^i u^r(p) &\simeq \frac{1}{4m}\eta^{s\dagger}\Big(-(2m + \boldsymbol{\sigma}\cdot\mathbf{q})\,\sigma^i\,(2m + \boldsymbol{\sigma}\cdot\mathbf{p}) \\ &\qquad -(2m - \boldsymbol{\sigma}\cdot\mathbf{q})\,\sigma^i\,(2m - \boldsymbol{\sigma}\cdot\mathbf{p})\Big)\xi^r \\ &\simeq -2m\eta^{s\dagger}\sigma^i\xi^r \ . \end{aligned} \tag{3.59}$$

As a result, the 4-vector bilinear can be written as

$$\bar{v}^s(q)\gamma^\mu u^r(p) \simeq \eta^{s\dagger}\begin{pmatrix} 0 \\ -2m\sigma^i \end{pmatrix}\xi^r \ , \tag{3.60}$$

where the upper and lower entries of the column matrix correspond to the $\mu = 0$ and $\mu = i$ components, respectively. This shows that the vector fermion bilinear is s-wave as it does not depend on the relative velocity.

Unlike the scalar and the pseudoscalar cases, where the propagator depends only on k^2, which, in the non-relativistic limit, is equal to $4m^2$ in the center-of-mass reference frame, as we can infer from Equation (3.6), here the propagator also contains a term proportional to $k_\mu k_\nu$. Let us therefore verify that the partial-wave nature of the annihilation is still determined by the bilinear alone, by computing the amplitude explicitly.

If we denote the momenta of the outgoing SM particles by p' and q', their spins by r' and s' and the coupling constant of the second vertex by g^V_{SM}, it turns out that

$$J^\nu_{SM} = \bar{u}^{r'}(p')(-ig^V_{SM}\gamma^\nu)v^{s'}(q') \ . \tag{3.61}$$

Thus, Equation (3.53) becomes

$$i\mathcal{A} = \bar{v}^s(q)(-ig^V_\chi\gamma^\mu)u^r(p)\frac{-i}{k^2 - m_V^2}\left(\eta_{\mu\nu} - \frac{k_\mu k_\nu}{m_V^2}\right)\bar{u}^{r'}(p')(-ig^V_{SM}\gamma^\nu)v^{s'}(q') \ . \tag{3.62}$$

At this point, if we ignore constant factors and focus only on operators, we obtain that

$$\begin{aligned} \bar{v}^s(q)\gamma^\mu u^r(p)\left(\eta_{\mu\nu} - \frac{k_\mu k_\nu}{m_V^2}\right)\bar{u}^{r'}(p')\gamma^\nu v^{s'}(q') &= \Big(\bar{v}^s(q)\gamma^\mu u^r(p)\Big)\Big(\bar{u}^{r'}(p')\gamma_\mu v^{s'}(q')\Big) \\ &\quad - \frac{1}{m_V^2}\Big(\bar{v}^s(q)\gamma^\mu k_\mu u^r(p)\Big)\Big(\bar{u}^{r'}(p')\gamma^\nu k_\nu v^{s'}(q')\Big) \ , \end{aligned} \tag{3.63}$$

where we have used $\eta_{\mu\nu}\gamma^\nu = \gamma_\mu$.

Now, by applying the Dirac equations

$$\begin{aligned} \gamma^\mu p_\mu u^r(p) &= m u^r(p) \ ; \\ \bar{v}^s(q)\gamma^\mu q_\mu &= -m\bar{v}^s(q) \ , \end{aligned} \tag{3.64}$$

we obtain that

$$\begin{aligned} \bar{v}^s(q)\gamma^\mu k_\mu u^r(p) &= \bar{v}^s(q)\gamma^\mu(p_\mu + q_\mu)u^r(p) \\ &= \bar{v}^s(q)\gamma^\mu p_\mu u^r(p) + \bar{v}^s(q)\gamma^\mu q_\mu u^r(p) \\ &= m\bar{v}^s(q)u^r(p) - m\bar{v}^s(q)u^r(p) = 0 \ , \end{aligned} \tag{3.65}$$

since the two incoming DM particles have the same mass. This implies that the term proportional to $k_\mu k_\nu$ in the amplitude is zero, regardless of the contraction $\left(\bar{u}^{r'}(p')\gamma^\nu k_\nu v^{s'}(q')\right)$ on the SM side. As a result, the amplitude reduces to

$$i\mathcal{A} = (-ig_\chi^V)(-ig_{SM}^V)\frac{-i}{k^2 - m_V^2}\left(\bar{v}^s(q)\gamma^\mu u^r(p)\right)\left(\bar{u}^{r'}(p')\gamma_\mu v^{s'}(q')\right) \ . \tag{3.66}$$

The cancellation of the term proportional to $k_\mu k_\nu$ is a direct consequence of the conservation of the vector current ($k \cdot J_{\mathrm{DM}} = 0$). Therefore, apart from a constant factor, the amplitude depends only on the scalar product of J_{DM} and J_{SM}, as in the case of scalar DM annihilation mediated by a vector. As a consequence, considering Equation (3.31), since the SM bilinear does not depend on v, the whole velocity dependence of the amplitude is carried by the DM bilinear. This therefore proves that the propagator does not modify the partial-wave classification and that the annihilation is s-wave.

3.3.5 The axial vector fermion bilinear

Let us determine the non-relativistic limit of the axial vector fermion bilinear $\bar{v}^s(q)\gamma^\mu\gamma^5 u^r(p)$, which arises in the process of Figure 3.4 when the mediator is an axial vector A with mass m_A. The interaction Lagrangian in this case is expressed by

$$\mathcal{L}_{int} = -g_\chi^A \bar{\chi}\gamma^\mu\gamma^5\chi A_\mu + \mathcal{L}_{int}^{A-SM} \ , \tag{3.67}$$

while the amplitude to study is

$$i\mathcal{A} = \bar{v}^s(q)(-ig_\chi^A\gamma^\mu\gamma^5)u^r(p)\frac{-i}{k^2 - m_A^2}\left(\eta_{\mu\nu} - \frac{k_\mu k_\nu}{m_A^2}\right)J_{SM}^\nu \ . \tag{3.68}$$

We can now compute the non-relativistic limit of the bilinear (the full computation is in Appendix A.4):

$$\begin{aligned}\bar{v}^s(q)\gamma^\mu\gamma^5 u^r(p) &\overset{\text{NR}}{\simeq} \frac{1}{4m}\begin{pmatrix}-\eta^{s\dagger}\left(2m+\boldsymbol{\sigma}\cdot\mathbf{q}\right) & \eta^{s\dagger}\left(2m-\boldsymbol{\sigma}\cdot\mathbf{q}\right)\end{pmatrix}\begin{pmatrix}\sigma^\mu\left(2m+\boldsymbol{\sigma}\cdot\mathbf{p}\right)\xi^r\\ -\bar{\sigma}^\mu\left(2m-\boldsymbol{\sigma}\cdot\mathbf{p}\right)\xi^r\end{pmatrix}\\ &= -\frac{1}{4m}\eta^{s\dagger}\Big(\left(2m+\boldsymbol{\sigma}\cdot\mathbf{q}\right)\sigma^\mu\left(2m+\boldsymbol{\sigma}\cdot\mathbf{p}\right)\\ &\qquad + \left(2m-\boldsymbol{\sigma}\cdot\mathbf{q}\right)\bar{\sigma}^\mu\left(2m-\boldsymbol{\sigma}\cdot\mathbf{p}\right)\Big)\xi^r\ .\end{aligned} \tag{3.69}$$

As for the vector bilinear, we can study the temporal and the spatial components separately.

The temporal component is

$$\begin{aligned}\bar{v}^s(q)\gamma^0\gamma^5 u^r(p) &\simeq -\frac{1}{4m}\eta^{s\dagger}\Big(\left(2m+\boldsymbol{\sigma}\cdot\mathbf{q}\right)\left(2m+\boldsymbol{\sigma}\cdot\mathbf{p}\right)+\left(2m-\boldsymbol{\sigma}\cdot\mathbf{q}\right)\left(2m-\boldsymbol{\sigma}\cdot\mathbf{p}\right)\Big)\xi^r\\ &\simeq -2m\eta^{s\dagger}\xi^r\ ,\end{aligned} \tag{3.70}$$

so it is s-wave.

On the other hand, the spatial component is expressed by

$$\begin{aligned}\bar{v}^s(q)\gamma^i\gamma^5 u^r(p) &\simeq -\frac{1}{4m}\eta^{s\dagger}\Big(\left(2m+\boldsymbol{\sigma}\cdot\mathbf{q}\right)\sigma^i\left(2m+\boldsymbol{\sigma}\cdot\mathbf{p}\right)\\ &\qquad - \left(2m-\boldsymbol{\sigma}\cdot\mathbf{q}\right)\sigma^i\left(2m-\boldsymbol{\sigma}\cdot\mathbf{p}\right)\Big)\xi^r\\ &= -\eta^{s\dagger}\left(\sigma^i\left(\boldsymbol{\sigma}\cdot\mathbf{p}\right)+\left(\boldsymbol{\sigma}\cdot\mathbf{q}\right)\sigma^i\right)\xi^r\ .\end{aligned} \tag{3.71}$$

In order to determine the nature of this component, let us rewrite $\sigma^i\left(\boldsymbol{\sigma}\cdot\mathbf{p}\right)+\left(\boldsymbol{\sigma}\cdot\mathbf{q}\right)\sigma^i$ after applying some algebra. In particular, since

$$\sigma^i\sigma^j = \delta^{ij}+i\varepsilon^{ijk}\sigma^k\ , \tag{3.72}$$

we obtain that

$$\begin{aligned}\sigma^i\left(\boldsymbol{\sigma}\cdot\mathbf{p}\right)+\left(\boldsymbol{\sigma}\cdot\mathbf{q}\right)\sigma^i &= \sigma^i\sigma^j p_j + q_j\sigma^j\sigma^i\\ &= \left(\delta^{ij}+i\varepsilon^{ijk}\sigma^k\right)p_j + q_j\left(\delta^{ji}+i\varepsilon^{jik}\sigma^k\right)\\ &= \delta^{ij}p_j + i\varepsilon^{ijk}p_j\sigma^k + \delta^{ji}q_j - i\varepsilon^{ijk}q_j\sigma^k\\ &= \left(p^i+q^i\right)+i\left(\left(\mathbf{p}-\mathbf{q}\right)\times\boldsymbol{\sigma}\right)^i\ .\end{aligned} \tag{3.73}$$

Consequently, since in the center-of-mass reference frame $\mathbf{p}+\mathbf{q}=0$, the spatial component of the bilinear turns out to be

$$\bar{v}^s(q)\gamma^i\gamma^5 u^r(p) = -\eta^{s\dagger}\left[2i\left(\mathbf{p}\times\boldsymbol{\sigma}\right)^i\right]\xi^r\ , \tag{3.74}$$

so it is p-wave.

Thus, unlike the vector bilinear, the axial vector one has two non-zero components of different nature: the temporal component is s-wave, while the spatial component is p-wave. Indeed,

$$\bar{v}^s(q)\gamma^\mu\gamma^5 u^r(p) \simeq \eta^{s\dagger} \begin{pmatrix} -2m \\ -2i\,(\mathbf{p}\times\boldsymbol{\sigma})^i \end{pmatrix} \xi^r \ . \tag{3.75}$$

We will analyze the role of the mediator in selecting just one of the components in Subsection 3.3.10.

3.3.6 The tensor fermion bilinear

Let us study the tensor fermion bilinear $\bar{v}^s(q)S^{\mu\nu}u^r(p)$, which, carrying two antisymmetric Lorentz indices, cannot be coupled to a scalar or a vector mediator as in the diagrams discussed so far, but must be contracted with an antisymmetric tensor $V_{\mu\nu}$, giving rise to a dipole-type interaction.

With that said, since

$$S^{\mu\nu} = \frac{i}{4}[\gamma^\mu,\gamma^\nu] \ , \tag{3.76}$$

where $[\gamma^\mu,\gamma^\nu]$ is the commutator of two gamma matrices, the DM contribution to the amplitude is

$$J^{\mu\nu}_{DM} = \bar{v}^s(q)(-ig^T_\chi S^{\mu\nu})u^r(p) = \bar{v}^s(q)\left(-ig^T_\chi\cdot\frac{i}{4}[\gamma^\mu,\gamma^\nu]\right)u^r(p) = \frac{g^T_\chi}{4}\bar{v}^s(q)[\gamma^\mu,\gamma^\nu]u^r(p) \ . \tag{3.77}$$

Let us therefore focus on $\bar{v}^s(q)[\gamma^\mu,\gamma^\nu]u^r(p) = \bar{v}^s(q)\Big(\gamma^\mu\gamma^\nu-\gamma^\nu\gamma^\mu\Big)u^r(p)$. As reported in detail in Appendix A.5, we have that

$$\begin{aligned}\bar{v}^s(q)\gamma^\mu\gamma^\nu u^r(p) &\overset{\text{NR}}{\simeq} \frac{1}{4m}\begin{pmatrix}-\eta^{s\dagger}\,(2m+\boldsymbol{\sigma}\cdot\mathbf{q}) & \eta^{s\dagger}\,(2m-\boldsymbol{\sigma}\cdot\mathbf{q})\end{pmatrix}\begin{pmatrix}\sigma^\mu\bar{\sigma}^\nu\,(2m-\boldsymbol{\sigma}\cdot\mathbf{p})\,\xi^r \\ \bar{\sigma}^\mu\sigma^\nu\,(2m+\boldsymbol{\sigma}\cdot\mathbf{p})\,\xi^r\end{pmatrix} \\ &= \frac{1}{4m}\eta^{s\dagger}\Big(-(2m+\boldsymbol{\sigma}\cdot\mathbf{q})\,\sigma^\mu\bar{\sigma}^\nu\,(2m-\boldsymbol{\sigma}\cdot\mathbf{p}) \\ &\qquad +(2m-\boldsymbol{\sigma}\cdot\mathbf{q})\,\bar{\sigma}^\mu\sigma^\nu\,(2m+\boldsymbol{\sigma}\cdot\mathbf{p})\Big)\xi^r \ .\end{aligned} \tag{3.78}$$

We can now distinguish four cases since we can consider the temporal and the spatial components for both μ and ν.

If $\mu=0$ and $\nu=0$, we find that

$$\begin{aligned}\bar{v}^s(q)\gamma^0\gamma^0 u^r(p) &\simeq \frac{1}{4m}\eta^{s\dagger}\Big(-(2m+\boldsymbol{\sigma}\cdot\mathbf{q})\,(2m-\boldsymbol{\sigma}\cdot\mathbf{p})+(2m-\boldsymbol{\sigma}\cdot\mathbf{q})\,(2m+\boldsymbol{\sigma}\cdot\mathbf{p})\Big)\xi^r \\ &= \eta^{s\dagger}\boldsymbol{\sigma}\cdot(\mathbf{p}-\mathbf{q})\,\xi^r \ .\end{aligned} \tag{3.79}$$

If $\mu = 0$ and $\nu = j$, we obtain that

$$\begin{aligned}\bar{v}^s(q)\gamma^0\gamma^j u^r(p) &\simeq \frac{1}{4m}\eta^{s\dagger}\Big((2m + \boldsymbol{\sigma}\cdot\mathbf{q})\,\sigma^j\,(2m - \boldsymbol{\sigma}\cdot\mathbf{p}) \\ &\qquad + (2m - \boldsymbol{\sigma}\cdot\mathbf{q})\,\sigma^j\,(2m + \boldsymbol{\sigma}\cdot\mathbf{p})\Big)\xi^r \\ &\simeq 2m\eta^{s\dagger}\sigma^j\xi^r \ .\end{aligned} \tag{3.80}$$

Similarly, if $\mu = i$ and $\nu = 0$, then

$$\begin{aligned}\bar{v}^s(q)\gamma^i\gamma^0 u^r(p) &\simeq \frac{1}{4m}\eta^{s\dagger}\Big(-(2m + \boldsymbol{\sigma}\cdot\mathbf{q})\,\sigma^i\,(2m - \boldsymbol{\sigma}\cdot\mathbf{p}) \\ &\qquad - (2m - \boldsymbol{\sigma}\cdot\mathbf{q})\,\sigma^i\,(2m + \boldsymbol{\sigma}\cdot\mathbf{p})\Big)\xi^r \\ &\simeq -2m\eta^{s\dagger}\sigma^i\xi^r \ .\end{aligned} \tag{3.81}$$

Finally, if $\mu = i$ and $\nu = j$, it turns out that

$$\begin{aligned}\bar{v}^s(q)\gamma^i\gamma^j u^r(p) &\simeq \frac{1}{4m}\eta^{s\dagger}\Big((2m + \boldsymbol{\sigma}\cdot\mathbf{q})\,\sigma^i\sigma^j\,(2m - \boldsymbol{\sigma}\cdot\mathbf{p}) \\ &\qquad - (2m - \boldsymbol{\sigma}\cdot\mathbf{q})\,\sigma^i\sigma^j\,(2m + \boldsymbol{\sigma}\cdot\mathbf{p})\Big)\xi^r \\ &= \eta^{s\dagger}\Big((\boldsymbol{\sigma}\cdot\mathbf{q})\,\sigma^i\sigma^j - \sigma^i\sigma^j\,(\boldsymbol{\sigma}\cdot\mathbf{p})\Big)\,\xi^r \ .\end{aligned} \tag{3.82}$$

Thus, by implementing the following notation for a matrix $\mathcal{M}^{\mu\nu}$ with two Lorentz indices:

$$\mathcal{M}^{\mu\nu} = \begin{pmatrix} \mu = 0, \nu = 0 & \mu = 0, \nu = j \\ \mu = i, \nu = 0 & \mu = i, \nu = j \end{pmatrix} \ , \tag{3.83}$$

we have that

$$\bar{v}^s(q)\gamma^\mu\gamma^\nu u^r(p) \simeq \eta^{s\dagger}\begin{pmatrix} \boldsymbol{\sigma}\cdot(\mathbf{p}-\mathbf{q}) & 2m\sigma^j \\ -2m\sigma^i & (\boldsymbol{\sigma}\cdot\mathbf{q})\,\sigma^i\sigma^j - \sigma^i\sigma^j\,(\boldsymbol{\sigma}\cdot\mathbf{p}) \end{pmatrix}\xi^r \ . \tag{3.84}$$

At this point, by switching the two indices, we obtain that

$$\bar{v}^s(q)\gamma^\nu\gamma^\mu u^r(p) \simeq \eta^{s\dagger}\begin{pmatrix} \boldsymbol{\sigma}\cdot(\mathbf{p}-\mathbf{q}) & -2m\sigma^j \\ 2m\sigma^i & (\boldsymbol{\sigma}\cdot\mathbf{q})\,\sigma^j\sigma^i - \sigma^j\sigma^i\,(\boldsymbol{\sigma}\cdot\mathbf{p}) \end{pmatrix}\xi^r \ . \tag{3.85}$$

As a consequence,

$$\bar{v}^s(q)[\gamma^\mu,\gamma^\nu]u^r(p) \simeq \eta^{s\dagger}\begin{pmatrix} 0 & 4m\sigma^j \\ -4m\sigma^i & C \end{pmatrix}\xi^r \ . \tag{3.86}$$

In particular,

$$\begin{aligned}C &= (\boldsymbol{\sigma}\cdot\mathbf{q})\,[\sigma^i,\sigma^j] + [\sigma^j,\sigma^i]\,(\boldsymbol{\sigma}\cdot\mathbf{p}) \\ &= (\boldsymbol{\sigma}\cdot\mathbf{q})\left(2i\varepsilon^{ijk}\sigma^k\right) - \left(2i\varepsilon^{ijk}\sigma^k\right)(\boldsymbol{\sigma}\cdot\mathbf{p}) \ ,\end{aligned} \tag{3.87}$$

where we have used

$$[\sigma^i, \sigma^j] = 2i\varepsilon^{ijk}\sigma^k \ . \tag{3.88}$$

At this point, considering Equation (3.72), C can be rewritten as

$$\begin{aligned} C &= 2i\varepsilon^{ijk}\left[(\boldsymbol{\sigma}\cdot\mathbf{q})\,\sigma^k - \sigma^k\,(\boldsymbol{\sigma}\cdot\mathbf{p})\right] \\ &= 2i\varepsilon^{ijk}\left[q_a\sigma^a\sigma^k - \sigma^k\sigma^b p_b\right] \\ &= 2i\varepsilon^{ijk}\left[q_a\left(\delta^{ak} + i\varepsilon^{akc}\sigma^c\right) - \left(\delta^{bk} + i\varepsilon^{kbc}\sigma^c\right)p_b\right] \\ &= 2i\varepsilon^{ijk}\left[q^k - i\varepsilon^{kac}q_a\sigma^c - p^k - i\varepsilon^{kbc}p_b\sigma^c\right] \\ &= 2i\varepsilon^{ijk}\left[(q^k - p^k) - i\Big((\mathbf{p}+\mathbf{q})\times\boldsymbol{\sigma}\Big)^k\right] \ . \end{aligned} \tag{3.89}$$

As a consequence, we find that

$$\bar{v}^s(q)[\gamma^\mu,\gamma^\nu]u^r(p) \simeq \eta^{s\dagger}\begin{pmatrix} 0 & 4m\sigma^j \\ -4m\sigma^i & 2i\varepsilon^{ijk}\left[(q^k - p^k) - i\Big((\mathbf{p}+\mathbf{q})\times\boldsymbol{\sigma}\Big)^k\right] \end{pmatrix}\xi^r \ . \tag{3.90}$$

Once again, going to the center-of-mass reference frame, we can simplify the expression for the element with $\mu = i$ and $\nu = j$, obtaining

$$\bar{v}^s(q)[\gamma^\mu,\gamma^\nu]u^r(p) \simeq \eta^{s\dagger}\begin{pmatrix} 0 & 4m\sigma^j \\ -4m\sigma^i & -4i\varepsilon^{ijk}p^k \end{pmatrix}\xi^r \ . \tag{3.91}$$

Thus, similarly to the axial vector bilinear, the tensor one also has components of different nature: indeed, the component with both temporal indices is zero, the components with one temporal and one spatial indices are s-wave, while the component with both spatial indices is p-wave.

3.3.7 The axial tensor fermion bilinear

The final fermion bilinear that we analyze is the axial tensor $\bar{v}^s(q)\,(iS^{\mu\nu}\gamma^5)\,u^r(p)$. Since in this case the DM current that enters the amplitude is

$$J^{\mu\nu}_{DM} = \bar{v}^s(q)[-ig^{AT}_\chi(iS^{\mu\nu}\gamma^5)]u^r(p) = i\frac{g^{AT}_\chi}{4}\bar{v}^s(q)\left([\gamma^\mu,\gamma^\nu]\gamma^5\right)u^r(p) \ , \tag{3.92}$$

let us compute $\bar{v}^s(q)\,([\gamma^\mu,\gamma^\nu]\gamma^5)\,u^r(p) = \bar{v}^s(q)\,[(\gamma^\mu\gamma^\nu - \gamma^\nu\gamma^\mu)\gamma^5]\,u^r(p)$.

As shown in Appendix A.6, we have that

$$\begin{aligned}\bar{v}^s(q)\gamma^\mu\gamma^\nu\gamma^5 u^r(p) &\overset{\text{NR}}{\simeq} \frac{1}{4m}\begin{pmatrix}\eta^{s\dagger}\left(2m+\boldsymbol{\sigma}\cdot\mathbf{q}\right) & \eta^{s\dagger}\left(2m-\boldsymbol{\sigma}\cdot\mathbf{q}\right)\end{pmatrix}\begin{pmatrix}\sigma^\mu\bar{\sigma}^\nu\left(2m-\boldsymbol{\sigma}\cdot\mathbf{p}\right)\xi^r\\ \bar{\sigma}^\mu\sigma^\nu\left(2m+\boldsymbol{\sigma}\cdot\mathbf{p}\right)\xi^r\end{pmatrix}\\ &= \frac{1}{4m}\eta^{s\dagger}\Big(\left(2m+\boldsymbol{\sigma}\cdot\mathbf{q}\right)\sigma^\mu\bar{\sigma}^\nu\left(2m-\boldsymbol{\sigma}\cdot\mathbf{p}\right)\\ &\qquad + \left(2m-\boldsymbol{\sigma}\cdot\mathbf{q}\right)\bar{\sigma}^\mu\sigma^\nu\left(2m+\boldsymbol{\sigma}\cdot\mathbf{p}\right)\Big)\xi^r\ .\end{aligned} \tag{3.93}$$

As for the tensor bilinear, we need to study four different cases because both μ and ν can be either equal to 0 or to i.

If $\mu = 0$ and $\nu = 0$, we find that

$$\begin{aligned}\bar{v}^s(q)\gamma^0\gamma^0\gamma^5 u^r(p) &\simeq \frac{1}{4m}\eta^{s\dagger}\Big(\left(2m+\boldsymbol{\sigma}\cdot\mathbf{q}\right)\left(2m-\boldsymbol{\sigma}\cdot\mathbf{p}\right)+\left(2m-\boldsymbol{\sigma}\cdot\mathbf{q}\right)\left(2m+\boldsymbol{\sigma}\cdot\mathbf{p}\right)\Big)\xi^r\\ &\simeq 2m\eta^{s\dagger}\xi^r\ .\end{aligned} \tag{3.94}$$

If $\mu = 0$ and $\nu = j$, we obtain that

$$\begin{aligned}\bar{v}^s(q)\gamma^0\gamma^j\gamma^5 u^r(p) &\simeq \frac{1}{4m}\eta^{s\dagger}\Big(-\left(2m+\boldsymbol{\sigma}\cdot\mathbf{q}\right)\sigma^j\left(2m-\boldsymbol{\sigma}\cdot\mathbf{p}\right)\\ &\qquad + \left(2m-\boldsymbol{\sigma}\cdot\mathbf{q}\right)\sigma^j\left(2m+\boldsymbol{\sigma}\cdot\mathbf{p}\right)\Big)\xi^r\\ &= \eta^{s\dagger}\left(\sigma^j\left(\boldsymbol{\sigma}\cdot\mathbf{p}\right)-\left(\boldsymbol{\sigma}\cdot\mathbf{q}\right)\sigma^j\right)\xi^r\ .\end{aligned} \tag{3.95}$$

Similarly, if $\mu = i$ and $\nu = 0$, then

$$\begin{aligned}\bar{v}^s(q)\gamma^i\gamma^0\gamma^5 u^r(p) &\simeq \frac{1}{4m}\eta^{s\dagger}\Big(\left(2m+\boldsymbol{\sigma}\cdot\mathbf{q}\right)\sigma^i\left(2m-\boldsymbol{\sigma}\cdot\mathbf{p}\right)\\ &\qquad - \left(2m-\boldsymbol{\sigma}\cdot\mathbf{q}\right)\sigma^i\left(2m+\boldsymbol{\sigma}\cdot\mathbf{p}\right)\Big)\xi^r\\ &= -\eta^{s\dagger}\left(\sigma^i\left(\boldsymbol{\sigma}\cdot\mathbf{p}\right)-\left(\boldsymbol{\sigma}\cdot\mathbf{q}\right)\sigma^i\right)\xi^r\ .\end{aligned} \tag{3.96}$$

Finally, if $\mu = i$ and $\nu = j$, it turns out that

$$\begin{aligned}\bar{v}^s(q)\gamma^i\gamma^j\gamma^5 u^r(p) &\simeq \frac{1}{4m}\eta^{s\dagger}\Big(-\left(2m+\boldsymbol{\sigma}\cdot\mathbf{q}\right)\sigma^i\sigma^j\left(2m-\boldsymbol{\sigma}\cdot\mathbf{p}\right)\\ &\qquad - \left(2m-\boldsymbol{\sigma}\cdot\mathbf{q}\right)\sigma^i\sigma^j\left(2m+\boldsymbol{\sigma}\cdot\mathbf{p}\right)\Big)\xi^r\\ &\simeq -2m\eta^{s\dagger}\sigma^i\sigma^j\xi^r\ .\end{aligned} \tag{3.97}$$

Thus, by combining these results, the corresponding matrix reads

$$\bar{v}^s(q)\gamma^\mu\gamma^\nu\gamma^5 u^r(p) \simeq \eta^{s\dagger}\begin{pmatrix}2m & \sigma^j\left(\boldsymbol{\sigma}\cdot\mathbf{p}\right)-\left(\boldsymbol{\sigma}\cdot\mathbf{q}\right)\sigma^j\\ \left(\boldsymbol{\sigma}\cdot\mathbf{q}\right)\sigma^i-\sigma^i\left(\boldsymbol{\sigma}\cdot\mathbf{p}\right) & -2m\sigma^i\sigma^j\end{pmatrix}\xi^r\ , \tag{3.98}$$

while the one obtained by switching the two indices is

$$\bar{v}^s(q)\gamma^\nu\gamma^\mu\gamma^5 u^r(p) \simeq \eta^{s\dagger}\begin{pmatrix} 2m & (\boldsymbol{\sigma}\cdot\mathbf{q})\,\sigma^j - \sigma^j\,(\boldsymbol{\sigma}\cdot\mathbf{p}) \\ \sigma^i\,(\boldsymbol{\sigma}\cdot\mathbf{p}) - (\boldsymbol{\sigma}\cdot\mathbf{q})\,\sigma^i & -2m\sigma^j\sigma^i \end{pmatrix}\xi^r \ . \tag{3.99}$$

As a consequence, the $(\mu,\nu)=(0,0)$ component of $\bar{v}^s(q)\,([\gamma^\mu,\gamma^\nu]\gamma^5)\,u^r(p)$ is simply zero.

On the other hand, its $(0,j)$ component is

$$\begin{aligned} 2\left[\sigma^j\,(\boldsymbol{\sigma}\cdot\mathbf{p}) - (\boldsymbol{\sigma}\cdot\mathbf{q})\,\sigma^j\right] &= 2\left[\sigma^j\sigma^a p_a - q_b\sigma^b\sigma^j\right] \\ &= 2\left[(\delta^{ja} + i\varepsilon^{jac}\sigma^c)p_a - q_b(\delta^{bj} + i\varepsilon^{bjc}\sigma^c)\right] \\ &= 2\left[\delta^{ja}p_a + i\varepsilon^{jac}p_a\sigma^c - \delta^{bj}q_b - i\varepsilon^{bjc}q_b\sigma^c\right] \\ &= 2\left[(p^j - q^j) + i\Big((\mathbf{p}+\mathbf{q})\times\boldsymbol{\sigma}\Big)^j\right] \ . \end{aligned} \tag{3.100}$$

Similarly, the $(i,0)$ component is

$$\begin{aligned} 2\left[(\boldsymbol{\sigma}\cdot\mathbf{q})\,\sigma^i - \sigma^i\,(\boldsymbol{\sigma}\cdot\mathbf{p})\right] &= -2\left[\sigma^i\,(\boldsymbol{\sigma}\cdot\mathbf{p}) - (\boldsymbol{\sigma}\cdot\mathbf{q})\,\sigma^i\right] \\ &= -2\left[(p^i - q^i) + i\Big((\mathbf{p}+\mathbf{q})\times\boldsymbol{\sigma}\Big)^i\right] \ . \end{aligned} \tag{3.101}$$

Finally, the (i,j) component turns out to be

$$-2m\sigma^i\sigma^j + 2m\sigma^j\sigma^i = -2m[\sigma^i,\sigma^j] = -2m\cdot 2i\varepsilon^{ijk}\sigma^k = -4im\varepsilon^{ijk}\sigma^k \ . \tag{3.102}$$

We can therefore write the matrix representing $\bar{v}^s(q)\,([\gamma^\mu,\gamma^\nu]\gamma^5)\,u^r(p)$ as

$$\bar{v}^s(q)\left([\gamma^\mu,\gamma^\nu]\gamma^5\right)u^r(p) \simeq \eta^{s\dagger}\begin{pmatrix} 0 & 2\left[(p^j-q^j)+i\Big(\mathbf{P}\times\boldsymbol{\sigma}\Big)^j\right] \\ -2\left[(p^i-q^i)+i\Big(\mathbf{P}\times\boldsymbol{\sigma}\Big)^i\right] & -4im\varepsilon^{ijk}\sigma^k \end{pmatrix}\xi^r \ , \tag{3.103}$$

where $\mathbf{P}\equiv\mathbf{p}+\mathbf{q}=0$ in the center-of-mass frame. As a consequence, in that reference frame

$$\bar{v}^s(q)\left([\gamma^\mu,\gamma^\nu]\gamma^5\right)u^r(p) \simeq \eta^{s\dagger}\begin{pmatrix} 0 & 4p^j \\ -4p^i & -4im\varepsilon^{ijk}\sigma^k \end{pmatrix}\xi^r \ . \tag{3.104}$$

Thus, by reading the previous matrix, it turns out that the component with both temporal indices is zero, the components with one temporal and one spatial indices are p-wave, while the component with both spatial indices is s-wave.

Table 3.1: Non-relativistic limit of the fermion bilinears in the center-of-mass frame. Spin indices and spinor momenta are omitted for brevity.

Bilinear	Non-relativistic limit	Component	Partial-wave
Scalar	$\bar{v}\, u \simeq \eta^\dagger\, (2\boldsymbol{\sigma}\cdot\mathbf{p})\, \xi$	–	p
Pseudoscalar	$\bar{v}\, (i\gamma^5)\, u \simeq \eta^\dagger\, (2im)\, \xi$	–	s
Vector	$\bar{v}\, \gamma^\mu u \simeq \eta^\dagger \begin{pmatrix} 0 \\ -2m\sigma^i \end{pmatrix} \xi$	$\mu = 0$ $\mu = i$	– s
Axial vector	$\bar{v}\, \gamma^\mu\gamma^5 u \simeq \eta^\dagger \begin{pmatrix} -2m \\ -2i(\mathbf{p}\times\boldsymbol{\sigma})^i \end{pmatrix} \xi$	$\mu = 0$ $\mu = i$	s p
Tensor	$\bar{v}\, S^{\mu\nu} u \simeq \eta^\dagger \begin{pmatrix} 0 & im\sigma^j \\ -im\sigma^i & \varepsilon^{ijk}p^k \end{pmatrix} \xi$	$(0,0)$ $(0,j)$ $(i,0)$ (i,j)	– s s p
Axial tensor	$\bar{v}\, (iS^{\mu\nu}\gamma^5)\, u \simeq \eta^\dagger \begin{pmatrix} 0 & -p^j \\ p^i & im\varepsilon^{ijk}\sigma^k \end{pmatrix} \xi$	$(0,0)$ $(0,j)$ $(i,0)$ (i,j)	– p p s

3.3.8 Summary of the bilinear analysis

In the previous subsections, we have computed the non-relativistic limit of each fermion bilinear $\bar{v}^s(q)\Gamma\, u^r(p)$ in the center-of-mass frame. The results are reported in Table 3.1, which indicates whether each bilinear (or each of its components) is s-wave or p-wave. Note that the bilinears are written in their Hermitian form in the table, so some entries may differ by a constant factor from the expressions derived above. As we can see, the scalar bilinear is purely p-wave, while the pseudoscalar and the vector bilinears are purely s-wave. On the other hand, the remaining bilinears have components of different nature, so their behaviour depends on which components actually contribute to the annihilation amplitude. In particular, this is determined by the nature of the DM particle and by the structure of the mediator, as we discuss in the following subsections.

3.3.9 Majorana fermions

So far, we have implicitly assumed Dark Matter to be a Dirac fermion since we have considered DM antiparticles to be distinct from the corresponding DM particles. Here, however, we assume that Dark Matter is described by Majorana fermions, which, as a reminder, are spin-1/2 particles that coincide with their own antiparticles.

A Majorana field Ψ_M satisfies the condition

$$\Psi_M = \Psi_M^C \ , \tag{3.105}$$

so it coincides with its charge-conjugate field, defined as

$$\Psi_M^C = -i\gamma^2\Psi_M^* = C\bar{\Psi}_M^T \ , \tag{3.106}$$

where $C = -i\gamma^2\gamma^0$ is the charge conjugation operator. As a result, a Majorana field satisfies the condition

$$\Psi_M = C\bar{\Psi}_M^T \ . \tag{3.107}$$

It turns out that not all the fermion bilinears that we have analyzed are allowed for a Majorana field. Indeed, as shown in [24], since a Majorana field coincides with its charge conjugate, every Majorana bilinear must be even under charge conjugation. As a consequence, since

$$\begin{aligned} C^{-1}\left(\mathbb{1}\right)^T C &= +\mathbb{1} \ ; \\ C^{-1}\left(i\gamma^5\right)^T C &= +i\gamma^5 \ ; \\ C^{-1}\left(\gamma^\mu\right)^T C &= -\gamma^\mu \ ; \\ C^{-1}\left(\gamma^\mu\gamma^5\right)^T C &= +\gamma^\mu\gamma^5 \ , \end{aligned} \tag{3.108}$$

the scalar, the pseudoscalar and the axial vector bilinears are allowed, while the vector one is not.

Let us therefore study the tensor and the axial tensor bilinears in detail to determine whether they are allowed for DM Majorana fermions. Thus, using Equations (3.108), let us compute

$$\begin{aligned} C^{-1}\left([\gamma^\mu,\gamma^\nu]\right)^T C &= C^{-1}\left(\gamma^\mu\gamma^\nu\right)^T C - C^{-1}\left(\gamma^\nu\gamma^\mu\right)^T C \\ &= \left[C^{-1}\left(\gamma^\nu\right)^T C\right]\left[C^{-1}\left(\gamma^\mu\right)^T C\right] \\ &- \left[C^{-1}\left(\gamma^\mu\right)^T C\right]\left[C^{-1}\left(\gamma^\nu\right)^T C\right] \\ &= \left(-\gamma^\nu\right)\left(-\gamma^\mu\right) - \left(-\gamma^\mu\right)\left(-\gamma^\nu\right) \\ &= \gamma^\nu\gamma^\mu - \gamma^\mu\gamma^\nu \\ &= -\left[\gamma^\mu,\gamma^\nu\right] \end{aligned} \tag{3.109}$$

and

$$\begin{aligned} C^{-1}\left(i[\gamma^\mu,\gamma^\nu]\gamma^5\right)^T C &= C^{-1}\left(i\gamma^\mu\gamma^\nu\gamma^5\right)^T C - C^{-1}\left(i\gamma^\nu\gamma^\mu\gamma^5\right)^T C \\ &= \left[C^{-1}(i\gamma^5)^T C\right]\left[C^{-1}(\gamma^\nu)^T C\right]\left[C^{-1}(\gamma^\mu)^T C\right] \\ &- \left[C^{-1}(i\gamma^5)^T C\right]\left[C^{-1}(\gamma^\mu)^T C\right]\left[C^{-1}(\gamma^\nu)^T C\right] \\ &= \left(i\gamma^5\right)\left(-\gamma^\nu\right)\left(-\gamma^\mu\right) - \left(i\gamma^5\right)\left(-\gamma^\mu\right)\left(-\gamma^\nu\right) \\ &= i\gamma^5\left(\gamma^\nu\gamma^\mu\right) - i\gamma^5\left(\gamma^\mu\gamma^\nu\right) \\ &= -i\gamma^5[\gamma^\mu,\gamma^\nu] \\ &= -i[\gamma^\mu,\gamma^\nu]\gamma^5 \ , \end{aligned} \tag{3.110}$$

Table 3.2: Non-relativistic limit of the fermion bilinears allowed for Majorana fermions in the center-of-mass frame. Spin indices and spinor momenta are omitted for brevity.

Bilinear	Non-relativistic limit	Component	Partial-wave
Scalar	$\bar{v}\, u \simeq \eta^\dagger \left(2\boldsymbol{\sigma}\cdot\mathbf{p}\right)\xi$	–	p
Pseudoscalar	$\bar{v}\left(i\gamma^5\right) u \simeq \eta^\dagger \left(2im\right)\xi$	–	s
Axial vector	$\bar{v}\,\gamma^\mu\gamma^5 u \simeq \eta^\dagger \begin{pmatrix} -2m \\ -2i(\mathbf{p}\times\boldsymbol{\sigma})^i \end{pmatrix}\xi$	$\mu = 0$ $\mu = i$	s p

where in the last step we have used $[\gamma^5, [\gamma^\mu, \gamma^\nu]] = 0$. Because of the minus signs in the results, both the tensor and the axial tensor bilinears are odd under charge conjugation and, therefore, not allowed for Majorana fermions.

The bilinears allowed for Majorana DM are summarized in Table 3.2. Among them, the scalar bilinear is purely p-wave, the pseudoscalar one is purely s-wave, while the axial vector one has both an s-wave and a p-wave component.

3.3.10 The role of the mediator

As shown by Equation (3.14), the amplitude of an annihilation process depends on the product of the DM current J_{DM}, the SM current J_{SM} and the propagator $D(k)$. In particular, since $D(k)$ is a function of the exchanged momentum k, it may affect the partial-wave nature of the process. As discussed in Subsection 3.3.4, a scalar propagator depends only on $k^2 \simeq 4m^2$ in the center-of-mass reference frame, so it cannot play a role in the partial-wave classification, which is therefore determined by the DM bilinear alone. The same holds for a vector mediator coupled to the vector bilinear: indeed, although its propagator contains a term proportional to $k_\mu k_\nu$, that term vanishes due to the conservation of the vector current. Let us therefore focus on the axial vector bilinear, whose current is not conserved, and study whether the structure of the mediator can select just one of its components and, therefore, fix its partial-wave nature.

Let us first consider an annihilation process described by the amplitude

$$i\mathcal{A} = \bar{v}^s(q)(-ig_\chi^A\gamma^\mu\gamma^5)u^r(p)\frac{-i}{k^2-m_A^2}\left(\eta_{\mu\nu}-\frac{k_\mu k_\nu}{m_A^2}\right)\bar{u}^{r'}(p')\left[-i\gamma^\nu(g_{SM}^V+g_{SM}^A\gamma^5)\right]v^{s'}(q')\ , \quad (3.111)$$

in which, therefore, the DM current is described by an axial vector bilinear, while the SM current is given by a combination of a vector and an axial vector bilinear.

Now, using Equation (3.21), which allows us to rewrite $i\mathcal{A}$ as the sum of two terms, let us compute the different parts that compose the amplitude separately. We have that

$$\begin{aligned} k \cdot J_{DM} &= k_\mu \left[\bar{v}^s(q)(-ig_\chi^A \gamma^\mu \gamma^5) u^r(p)\right] \\ &= -ig_\chi^A \bar{v}^s(q)(k_\mu \gamma^\mu)\gamma^5 u^r(p) \\ &= -ig_\chi^A \bar{v}^s(q)(p_\mu \gamma^\mu + q_\mu \gamma^\mu)\gamma^5 u^r(p) \\ &= -ig_\chi^A \bar{v}^s(q) p_\mu \gamma^\mu \gamma^5 u^r(p) - ig_\chi^A \bar{v}^s(q) q_\mu \gamma^\mu \gamma^5 u^r(p) \\ &= +ig_\chi^A \bar{v}^s(q)\gamma^5 \gamma^\mu p_\mu u^r(p) - ig_\chi^A \bar{v}^s(q)\gamma^\mu q_\mu \gamma^5 u^r(p) \ , \end{aligned} \tag{3.112}$$

where in the last step we have swapped $p_\mu \gamma^\mu$ and γ^5 by using $\{\gamma^\mu, \gamma^5\} = 0$ to be able to apply the Dirac equations (3.64). As a result,

$$k \cdot J_{DM} = +ig_\chi^A m \bar{v}^s(q)\gamma^5 u^r(p) + ig_\chi^A m \bar{v}^s(q)\gamma^5 u^r(p) = 2ig_\chi^A m \bar{v}^s(q)\gamma^5 u^r(p) \ . \tag{3.113}$$

Let us now compute $k \cdot J_{SM}$:

$$\begin{aligned} k \cdot J_{SM} &= k_\nu \left(-ig_{SM}^V \bar{u}^{r'}(p')\gamma^\nu v^{s'}(q') - ig_{SM}^A \bar{u}^{r'}(p')\gamma^\nu \gamma^5 v^{s'}(q')\right) \\ &= -ig_{SM}^V \bar{u}^{r'}(p')(p'_\nu \gamma^\nu + q'_\nu \gamma^\nu) v^{s'}(q') - ig_{SM}^A \bar{u}^{r'}(p')(p'_\nu \gamma^\nu + q'_\nu \gamma^\nu)\gamma^5 v^{s'}(q') \ . \end{aligned} \tag{3.114}$$

Similarly to Equations (3.65) and (3.112), we obtain that

$$\begin{aligned} \bar{u}^{r'}(p')(p'_\nu \gamma^\nu + q'_\nu \gamma^\nu) v^{s'}(q') &= 0 \ ; \\ \bar{u}^{r'}(p')(p'_\nu \gamma^\nu + q'_\nu \gamma^\nu)\gamma^5 v^{s'}(q') &= 2m' \bar{u}^{r'}(p')\gamma^5 v^{s'}(q') \ , \end{aligned} \tag{3.115}$$

where m' is the mass of the SM particle. Thus, it turns out that

$$k \cdot J_{SM} = -2ig_{SM}^A m' \bar{u}^{r'}(p')\gamma^5 v^{s'}(q') \ . \tag{3.116}$$

We therefore find that the second term of the amplitude can be written as

$$\begin{aligned} \frac{(k \cdot J_{DM})(k \cdot J_{SM})}{m_A^2} &= \frac{1}{m_A^2}\left(2ig_\chi^A m \bar{v}^s(q)\gamma^5 u^r(p)\right)\left(-2ig_{SM}^A m' \bar{u}^{r'}(p')\gamma^5 v^{s'}(q')\right) \\ &= \frac{4g_\chi^A g_{SM}^A m m'}{m_A^2}\left(\bar{v}^s(q)\gamma^5 u^r(p)\right)\left(\bar{u}^{r'}(p')\gamma^5 v^{s'}(q')\right) \\ &\simeq \frac{8g_\chi^A g_{SM}^A m^2 m'}{m_A^2}\eta^{s\dagger}\xi^r\left(\bar{u}^{r'}(p')\gamma^5 v^{s'}(q')\right) \ , \end{aligned} \tag{3.117}$$

where in the last step we have taken the non-relativistic limit of the DM pseudoscalar bilinear, according to Table 3.1. This term is purely s-wave since it is independent of v.

Let us now consider $J_{DM} \cdot J_{SM} = J_{DM}^0 J_{SM}^0 - J_{DM}^i J_{SM}^i$. Since

$$J_{DM} = -ig_\chi^A \bar{v}^s(q)\gamma^\mu \gamma^5 u^r(p) \ , \tag{3.118}$$

we find that

$$J_{DM} \cdot J_{SM} \simeq \left(2ig_\chi^A m\eta^{s\dagger}\xi^r\right) J_{SM}^0 - \left(-2g_\chi^A \eta^{s\dagger} \left(\mathbf{p} \times \boldsymbol{\sigma}\right)^i \xi^r\right) J_{SM}^i \ . \tag{3.119}$$

The scalar product of the two currents is therefore given by a mixture of an s-wave term and a p-wave term.

At this point, since we have found two s-wave contributions in the amplitude, let us explicitly determine whether their sum is equal to zero because in that case the annihilation process would be purely p-wave. In order to do so, let us compute

$$J_{SM}^0 = -i\bar{u}^{r'}(p')\gamma^0 \left(g_{SM}^V + g_{SM}^A\gamma^5\right) v^{s'}(q') \ . \tag{3.120}$$

To simplify the picture, we recall that in an s-channel the exchanged momentum has components $k^\mu = (2E, \mathbf{0})$, implying that

$$\gamma^\mu k_\mu = \gamma^0 k_0 = 2E\gamma^0 \tag{3.121}$$

and, therefore, that

$$\gamma^0 = \frac{\gamma^\mu k_\mu}{2E} \ . \tag{3.122}$$

As a consequence, considering Equations (3.115), it turns out that

$$\begin{aligned} \bar{u}^{r'}(p')\gamma^0 v^{s'}(q') &= \frac{1}{2E}\bar{u}^{r'}(p') \left(p_\mu\gamma^\mu + q_\mu\gamma^\mu\right) v^{s'}(q') = 0 \ ; \\ \bar{u}^{r'}(p')\gamma^0\gamma^5 v^{s'}(q') &= \frac{1}{2E}\bar{u}^{r'}(p') \left(p_\mu\gamma^\mu + q_\mu\gamma^\mu\right) \gamma^5 v^{s'}(q') = \frac{m'}{E}\bar{u}^{r'}(p')\gamma^5 v^{s'}(q') \ . \end{aligned} \tag{3.123}$$

Thus, we obtain that

$$J_{SM}^0 = -ig_{SM}^A \frac{m'}{E}\bar{u}^{r'}(p')\gamma^5 v^{s'}(q') \ , \tag{3.124}$$

so the first of the two s-wave contributions reduces to

$$\begin{aligned} J_{DM}^0 J_{SM}^0 &\simeq \left(2ig_\chi^A m\eta^{s\dagger}\xi^r\right) \left(-ig_{SM}^A \frac{m'}{E}\bar{u}^{r'}(p')\gamma^5 v^{s'}(q')\right) \\ &= \frac{2g_\chi^A g_{SM}^A mm'}{E}\eta^{s\dagger}\xi^r \left(\bar{u}^{r'}(p')\gamma^5 v^{s'}(q')\right) \ . \end{aligned} \tag{3.125}$$

If we now require this term to cancel the other s-wave contribution, given by Equation (3.117), we obtain that

$$\frac{2g_\chi^A g_{SM}^A mm'}{E}\eta^{s\dagger}\xi^r \left(\bar{u}^{r'}(p')\gamma^5 v^{s'}(q')\right) = \frac{8g_\chi^A g_{SM}^A m^2 m'}{m_A^2}\eta^{s\dagger}\xi^r \left(\bar{u}^{r'}(p')\gamma^5 v^{s'}(q')\right) \ , \tag{3.126}$$

from which

$$m_A^2 = 4mE \ . \tag{3.127}$$

This condition, however, is completely accidental, meaning that in general the two s-wave contributions do not cancel each other out. As a result, the only way to switch the s-wave contribution off and obtain a purely p-wave annihilation is to set $g^A_{SM} = 0$.

Another interaction that we can analyze to determine whether the mediator selects just one of the components of the axial vector DM bilinear is the one described by the interaction Lagrangian

$$\mathcal{L}_{int} = \frac{g_0}{\Lambda^2} J^\nu_{DM} \partial^\mu A_{\mu\nu} \ , \tag{3.128}$$

where $J^\nu_{DM} = \bar{\chi}\gamma^\nu\gamma^5\chi$ is the axial vector DM current, $A_{\mu\nu} = \partial_\mu A_\nu - \partial_\nu A_\mu$ is the field strength, g_0 is a dimensionless coupling constant and Λ is the energy scale of the new physics responsible for this effective interaction.

The amplitude of the process is

$$i\mathcal{A} = J^\mu_{DM,eff} D_{\mu\nu}(k) J^\nu_{SM} = \frac{-i}{k^2 - m_A^2} \left(J_{DM,eff} \cdot J_{SM} - \frac{(k \cdot J_{DM,eff})(k \cdot J_{SM})}{m_A^2} \right) \ , \tag{3.129}$$

so it has the same form as Equation (3.21). The only difference is that here the DM current is replaced by an effective current $J_{DM,eff}$, which depends on J_{DM}. In order to build the effective current, let us first observe that

$$\partial^\mu A_{\mu\nu} = \partial^\mu \partial_\mu A_\nu - \partial^\mu \partial_\nu A_\mu = \partial^\mu \partial_\mu A_\nu - \partial_\nu \partial^\mu A_\mu \ , \tag{3.130}$$

from which, recalling that we can substitute ∂_μ with $-ik_\mu$, we obtain that

$$\partial^\mu A_{\mu\nu} \to (-ik^\mu)(-ik_\mu) A_\nu - (-ik_\nu)(-ik^\mu) A_\mu = -k^2 A_\nu + k_\nu k \cdot A = \left(-k^2 \delta^\rho_\nu + k_\nu k^\rho \right) A_\rho \ . \tag{3.131}$$

At this point, by rewriting the interaction Lagrangian as

$$\mathcal{L}_{int} = \frac{g_0}{\Lambda^2} J^\nu_{DM} \left(-k^2 \delta^\rho_\nu + k_\nu k^\rho \right) A_\rho = J^\rho_{DM,eff} A_\rho \ , \tag{3.132}$$

we obtain that

$$J^\rho_{DM,eff} = \frac{g_0}{\Lambda^2} J^\nu_{DM} \left(-k^2 \delta^\rho_\nu + k_\nu k^\rho \right) = \frac{g_0}{\Lambda^2} \left(-k^2 J^\rho_{DM} + k^\rho k \cdot J_{DM} \right) \ . \tag{3.133}$$

Interestingly, if we now compute the scalar product $k \cdot J_{DM,eff}$, we get zero identically:

$$k \cdot J_{DM,eff} = \frac{g_0}{\Lambda^2} k_\rho \left(-k^2 J^\rho_{DM} + k^\rho k \cdot J_{DM} \right) = \frac{g_0}{\Lambda^2} \left(-k^2 k \cdot J_{DM} + k^2 k \cdot J_{DM} \right) = 0 \ . \tag{3.134}$$

As a consequence, the second term in the amplitude is zero regardless of the nature of J_{SM}. We therefore obtain that

$$i\mathcal{A} = \frac{-i}{k^2 - m_A^2} J_{DM,eff} \cdot J_{SM} = \frac{i}{k^2 - m_A^2} \frac{g_0}{\Lambda^2} \left[k^2 \left(J_{DM} \cdot J_{SM} \right) - \left(k \cdot J_{DM} \right) \left(k \cdot J_{SM} \right) \right] \ . \quad (3.135)$$

At this point, if we consider the center-of-mass reference frame, where $k^\mu = (2E, \mathbf{0})$, we have that

$$\begin{aligned} k \cdot J_{DM} &= (2E)\, J^0_{DM} \ ; \\ k \cdot J_{SM} &= (2E)\, J^0_{SM} \ , \end{aligned} \quad (3.136)$$

from which the second term in the amplitude becomes

$$\left(k \cdot J_{DM} \right) \left(k \cdot J_{SM} \right) = 4E^2 J^0_{DM} J^0_{SM} = k^2 J^0_{DM} J^0_{SM} \ . \quad (3.137)$$

As a result, we find that

$$\begin{aligned} k^2 \left(J_{DM} \cdot J_{SM} \right) - \left(k \cdot J_{DM} \right) \left(k \cdot J_{SM} \right) &= k^2 \left(J^0_{DM} \cdot J^0_{SM} - \mathbf{J}_{DM} \cdot \mathbf{J}_{SM} \right) - k^2 J^0_{DM} J^0_{SM} \\ &= -k^2 \mathbf{J}_{DM} \cdot \mathbf{J}_{SM} \ . \end{aligned} \quad (3.138)$$

Thus, since only the spatial contributions of the currents enter the amplitude, which reads

$$i\mathcal{A} = \frac{-i}{k^2 - m_A^2} \frac{g_0}{\Lambda^2} k^2 \left(\mathbf{J}_{DM} \cdot \mathbf{J}_{SM} \right) \ , \quad (3.139)$$

the resulting DM annihilation will be purely s-wave or p-wave according to the spatial component of the DM bilinear, regardless of the structure of the SM current. In particular, if the DM current is described by a vector bilinear, the annihilation will be purely s-wave, while if it is described by an axial vector bilinear, the annihilation will be purely p-wave.

3.3.11 t-channel annihilation

Up to now, we have studied the DM annihilation into SM fermions through the s-channel exchange of a mediator. However, if the mediator is relativistic and much lighter than DM particles, so that its mass m_A satisfies the relation $m_A \ll m$, the annihilation process may also occur through the t-channel. Let us therefore study the process

$$\chi \bar{\chi} \longrightarrow AA \ , \quad (3.140)$$

in which two DM particles annihilate directly into a pair of observable mediators through the exchange of a virtual DM particle with momentum k, as represented in Figure 3.5.

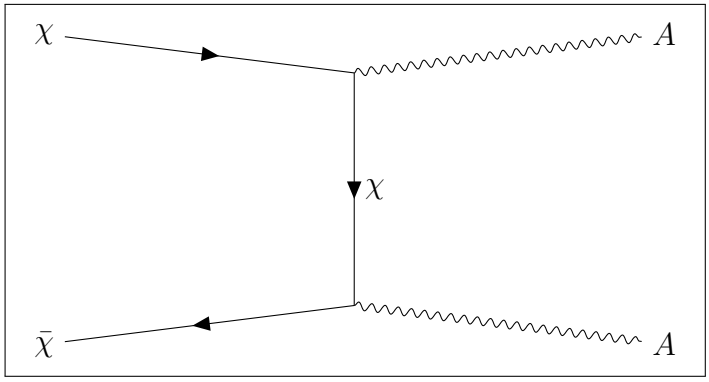


Figure 3.5: Feynman diagram for the annihilation process $\chi\bar{\chi} \to AA$ in the t-channel, mediated by the exchange of a virtual DM particle.

Let us consider the Lagrangian

$$\mathcal{L}_{int} = -g_\chi^A \bar{\chi}\gamma^\mu\gamma^5\chi A_\mu \ , \tag{3.141}$$

which, once again, contains an axial vector DM current. Since the two vertices in the diagram are given by $-ig_\chi^A\gamma^\mu\gamma^5$ and $-ig_\chi^A\gamma^\nu\gamma^5$ and the DM propagator with mass m and momentum $k \equiv p - p' = q' - q$ is

$$S_F(k) = \frac{i\left(\gamma^\alpha k_\alpha + m\right)}{k^2 - m^2} \ , \tag{3.142}$$

the amplitude of the process is

$$i\mathcal{A} = \bar{v}^s(q)\left(-ig_\chi^A\gamma^\nu\gamma^5\right)\frac{i\left(\gamma^\alpha k_\alpha + m\right)}{k^2 - m^2}\left(-ig_\chi^A\gamma^\mu\gamma^5\right)u^r(p)\varepsilon_\mu(p')\varepsilon_\nu(q') \ , \tag{3.143}$$

where $\varepsilon_\mu(p')$ and $\varepsilon_\nu(q')$ are the polarization vectors of the mediators in the final state. To simplify this expression, let us ignore constants and the polarization vectors and focus only on the spinor structure of the amplitude:

$$\bar{v}^s(q)\gamma^\nu\gamma^5\left(\gamma^\alpha k_\alpha + m\right)\gamma^\mu\gamma^5 u^r(p) = \bar{v}^s(q)\left(\gamma^\nu\gamma^5\gamma^\alpha k_\alpha\gamma^\mu\gamma^5 + \gamma^\nu\gamma^5 m\gamma^\mu\gamma^5\right)u^r(p) \ . \tag{3.144}$$

Using $\{\gamma^\mu, \gamma^5\} = 0$ and $\left(\gamma^5\right)^2 = \mathbb{1}$, we obtain that

$$\begin{aligned} \gamma^\nu\gamma^5\gamma^\alpha k_\alpha\gamma^\mu\gamma^5 &= \gamma^\nu\gamma^\alpha k_\alpha\gamma^\mu \ ; \\ \gamma^\nu\gamma^5 m\gamma^\mu\gamma^5 &= -\gamma^\nu m\gamma^\mu \ . \end{aligned} \tag{3.145}$$

As a consequence, the spinor structure of the amplitude becomes $\bar{v}^s(q)\gamma^\nu\left(\gamma^\alpha k_\alpha - m\right)\gamma^\mu u^r(p)$. At this point, since

$$\begin{aligned} \gamma^\nu\gamma^\mu &= \eta^{\nu\mu} + \frac{1}{2}[\gamma^\nu, \gamma^\mu] \ ; \\ \gamma^\nu\gamma^\alpha\gamma^\mu &= \eta^{\nu\alpha}\gamma^\mu - \eta^{\nu\mu}\gamma^\alpha + \eta^{\alpha\mu}\gamma^\nu + i\varepsilon^{\beta\nu\alpha\mu}\gamma_\beta\gamma^5 \ , \end{aligned} \tag{3.146}$$

the term proportional to m reads

$$m\bar{v}^s(q)\gamma^\nu\gamma^\mu u^r(p) = m\left(\eta^{\nu\mu}\bar{v}^s(q)u^r(p) + \frac{1}{2}\bar{v}^s(q)[\gamma^\nu,\gamma^\mu]u^r(p)\right) \ . \tag{3.147}$$

This term is therefore expressed as the sum of two DM bilinears: a scalar and a tensor one. On the other hand, the first term

$$\begin{aligned}\bar{v}^s(q)\gamma^\nu\gamma^\alpha k_\alpha\gamma^\mu u^r(p) &= \bar{v}^s(q)\left(\eta^{\nu\alpha}\gamma^\mu - \eta^{\nu\mu}\gamma^\alpha + \eta^{\alpha\mu}\gamma^\nu + i\varepsilon^{\beta\nu\alpha\mu}\gamma_\beta\gamma^5\right)k_\alpha u^r(p)\\ &= \bar{v}^s(q)\left(k^\nu\gamma^\mu - \eta^{\nu\mu}\gamma^\alpha k_\alpha + k^\mu\gamma^\nu + i\varepsilon^{\beta\nu\alpha\mu}k_\alpha\gamma_\beta\gamma^5\right)u^r(p)\\ &= k^\nu\bar{v}^s(q)\gamma^\mu u^r(p) - \eta^{\nu\mu}\bar{v}^s(q)\gamma^\alpha u^r(p)k_\alpha\\ &\quad + k^\mu\bar{v}^s(q)\gamma^\nu u^r(p) + i\varepsilon^{\beta\nu\alpha\mu}k_\alpha\bar{v}^s(q)\gamma_\beta\gamma^5 u^r(p)\end{aligned} \tag{3.148}$$

contains four bilinears: two vectors, a vector with a contraction and an axial vector. As a consequence, since the spinor structure of the amplitude is given by a combination of six bilinears with components of different nature, as reported in Table 3.1, the amplitude contains both s-wave and p-wave contributions. Therefore, unlike the s-channel annihilation described by $\mathcal{L}_{int} = (g_0/\Lambda^2)J^\nu_{DM}\,\partial^\mu A_{\mu\nu}$, the t-channel annihilation into a pair of mediators does not allow us to separate the s-wave contributions from the p-wave ones.

Conclusions

The aim of this thesis was to classify the partial-wave nature of scalar and fermionic operators entering DM annihilation into SM particles, a process that is probed by indirect detection searches. In particular, we have focused on the CMB bound, which is based on the small contribution to the fraction of free electrons produced by DM annihilation after recombination. This bound places constraints on the DM mass m and the thermally-averaged cross-section $\langle \sigma v \rangle$, as shown in Figure 1.11, and, in particular, excludes thermal DM candidates with masses below a few tens of GeV. However, it only applies if DM annihilation occurs in s-wave, which means that $\langle \sigma v \rangle$ does not depend on the relative velocity v of the two incoming DM particles. On the other hand, if DM annihilation proceeds through a p-wave interaction, $\langle \sigma v \rangle \propto v^2$ is no longer constant, so it is strongly suppressed by the time of recombination and the bound is evaded.

To determine the partial-wave nature of each operator, we have worked in the center-of-mass reference frame and in the non-relativistic limit. Since in this regime σv depends on the squared amplitude $|\mathcal{A}|^2_{\rm NR}$, the classification of the operators can be inferred directly by studying the latter. We have first considered complex scalar DM operators, annihilating through $\Phi^\dagger \Phi \to \mathrm{SM}\,\overline{\mathrm{SM}}$, finding that if the process is mediated by a scalar particle, it is purely s-wave, while if it is mediated by a vector particle, it is purely p-wave.

Subsequently, after determining the non-relativistic limit of the spinors u and v entering the general expression of a spinor field $\chi(x)$ in terms of creation and destruction operators, we have studied the partial-wave nature of the fermionic bilinears $\bar{v}^s(q)\Gamma u^r(p)$, relevant for DM annihilation, described by $\chi\bar{\chi} \to \mathrm{SM}\,\overline{\mathrm{SM}}$. The results, summarized in Table 3.1, show that the scalar bilinear is purely p-wave, while the pseudoscalar and the vector bilinears are purely s-wave. In addition, the axial vector, the tensor and the axial tensor bilinears have components of different nature. These results are valid if Dark Matter is a Dirac fermion. On the other hand, if it is described by Majorana fermions, the vector, the tensor and the axial tensor bilinears are not allowed since they are odd under charge conjugation; therefore, the summarizing table reduces to Table 3.2.

We have then considered some additional aspects to complete the picture, such as investigating the role of the mediator in the annihilation process. Indeed, since σv depends on the amplitude and the latter can be expressed as the product of the DM current, the propagator and the SM current, as shown by Equation (3.14), it is generally not sufficient to study only the structure of the DM bilinear to determine the partial-wave nature of the process. However, this is not the case for the scalar, the pseudoscalar and the vector bilinears: in the first two cases, the propagator is just a constant in the center-of-mass frame, so it does not alter the partial-wave structure of the DM bilinear. On the other hand, in the vector case, the term proportional to $k_\mu k_\nu$ in the amplitude vanishes due to the conservation of the vector current, so the partial-wave nature of the process is again determined by the DM bilinear alone. We have therefore focused on the axial vector bilinear, which, as a reminder, has two components of different nature, to determine whether it is possible to switch one of them off. In particular, we have shown that if the amplitude depends on an axial vector DM current and a SM current given by a combination of a vector and an axial vector bilinear, the only way to switch the s-wave contribution off and obtain a purely p-wave annihilation is to set the coupling constant $g^A_{SM} = 0$. On the other hand, if the DM current is coupled to the derivative of the field strength of the mediator, the resulting amplitude only depends on the spatial component of the DM current, regardless of the SM current. As a consequence, the partial-wave nature of the process is always pure: a vector DM current leads to a purely s-wave annihilation, while an axial vector one leads to a purely p-wave annihilation. Finally, we have studied the t-channel annihilation into a pair of mediators, as described by $\chi\bar{\chi} \to AA$, which is relevant when the mediator is much lighter than the DM particles. However, in this case it is not possible to separate the s-wave contributions from the p-wave ones.

To conclude, the approach developed in this thesis for scalar and fermionic DM is general and could be applied to other DM candidates as well. In particular, we could analyze vector spin-1 DM candidates, which would involve a wider class of operators, in order to obtain a more complete picture of which DM annihilation processes can evade the CMB bound.

Appendix

In this appendix we report the detailed derivations of the results presented in Chapter 3, whose physical interpretation is discussed in the main text.

A.1 The scalar fermion bilinear

The result of this section is used in Subsection 3.3.2.

$$
\begin{aligned}
\bar{v}^s(q)u^r(p) &= \begin{pmatrix} -\eta^{s\dagger}\sqrt{\bar{\sigma}\cdot q} & \eta^{s\dagger}\sqrt{\sigma\cdot q}\end{pmatrix}\begin{pmatrix}\sqrt{\sigma\cdot p}\,\xi^r \\ \sqrt{\bar{\sigma}\cdot p}\,\xi^r\end{pmatrix} \\
&\overset{\text{NR}}{\simeq} \frac{1}{4m}\begin{pmatrix} -\eta^{s\dagger}\left(2m+\boldsymbol{\sigma}\cdot\mathbf{q}\right) & \eta^{s\dagger}\left(2m-\boldsymbol{\sigma}\cdot\mathbf{q}\right)\end{pmatrix}\begin{pmatrix}\left(2m-\boldsymbol{\sigma}\cdot\mathbf{p}\right)\xi^r \\ \left(2m+\boldsymbol{\sigma}\cdot\mathbf{p}\right)\xi^r\end{pmatrix} \\
&= \frac{1}{4m}\eta^{s\dagger}\big(-\left(2m+\boldsymbol{\sigma}\cdot\mathbf{q}\right)\left(2m-\boldsymbol{\sigma}\cdot\mathbf{p}\right)+\left(2m-\boldsymbol{\sigma}\cdot\mathbf{q}\right)\left(2m+\boldsymbol{\sigma}\cdot\mathbf{p}\right)\big)\xi^r \\
&= \frac{1}{4m}\eta^{s\dagger}\big(-4m^2+2m\boldsymbol{\sigma}\cdot\mathbf{p}-2m\boldsymbol{\sigma}\cdot\mathbf{q}+(\boldsymbol{\sigma}\cdot\mathbf{q})(\boldsymbol{\sigma}\cdot\mathbf{p}) \\
&\qquad\qquad +4m^2+2m\boldsymbol{\sigma}\cdot\mathbf{p}-2m\boldsymbol{\sigma}\cdot\mathbf{q}-(\boldsymbol{\sigma}\cdot\mathbf{q})(\boldsymbol{\sigma}\cdot\mathbf{p})\big)\xi^r \\
&= \frac{1}{4m}\eta^{s\dagger}\cdot 2\left(2m\boldsymbol{\sigma}\cdot\mathbf{p}-2m\boldsymbol{\sigma}\cdot\mathbf{q}\right)\xi^r \\
&= \frac{1}{4m}\cdot 2\cdot 2m\eta^{s\dagger}\left(\boldsymbol{\sigma}\cdot\mathbf{p}-\boldsymbol{\sigma}\cdot\mathbf{q}\right)\xi^r \\
&= \eta^{s\dagger}\boldsymbol{\sigma}\cdot\left(\mathbf{p}-\mathbf{q}\right)\xi^r\ .
\end{aligned}
\tag{A.1}
$$

A.2 The pseudoscalar fermion bilinear

The result of this section is used in Subsection 3.3.3.

$$
\begin{aligned}
\bar{v}^s(q)\gamma^5 u^r(p) &= \begin{pmatrix} -\eta^{s\dagger}\sqrt{\bar{\sigma}\cdot q} & \eta^{s\dagger}\sqrt{\sigma\cdot q}\end{pmatrix}\begin{pmatrix} -\mathbb{1} & 0 \\ 0 & \mathbb{1}\end{pmatrix}\begin{pmatrix} \sqrt{\sigma\cdot p}\,\xi^r \\ \sqrt{\bar{\sigma}\cdot p}\,\xi^r\end{pmatrix} \\
&= \begin{pmatrix} -\eta^{s\dagger}\sqrt{\bar{\sigma}\cdot q} & \eta^{s\dagger}\sqrt{\sigma\cdot q}\end{pmatrix}\begin{pmatrix} -\sqrt{\sigma\cdot p}\,\xi^r \\ \sqrt{\bar{\sigma}\cdot p}\,\xi^r\end{pmatrix} \\
&\overset{\text{NR}}{\simeq} \frac{1}{4m}\begin{pmatrix} -\eta^{s\dagger}\,(2m+\boldsymbol{\sigma}\cdot\mathbf{q}) & \eta^{s\dagger}\,(2m-\boldsymbol{\sigma}\cdot\mathbf{q})\end{pmatrix}\begin{pmatrix} -\,(2m-\boldsymbol{\sigma}\cdot\mathbf{p})\,\xi^r \\ (2m+\boldsymbol{\sigma}\cdot\mathbf{p})\,\xi^r\end{pmatrix} \\
&= \frac{1}{4m}\eta^{s\dagger}\big(\,(2m+\boldsymbol{\sigma}\cdot\mathbf{q})\,(2m-\boldsymbol{\sigma}\cdot\mathbf{p})+(2m-\boldsymbol{\sigma}\cdot\mathbf{q})\,(2m+\boldsymbol{\sigma}\cdot\mathbf{p})\,\big)\xi^r \\
&= \frac{1}{4m}\eta^{s\dagger}(4m^2-2m\boldsymbol{\sigma}\cdot\mathbf{p}+2m\boldsymbol{\sigma}\cdot\mathbf{q}-(\boldsymbol{\sigma}\cdot\mathbf{q})(\boldsymbol{\sigma}\cdot\mathbf{p}) \\
&\qquad +4m^2+2m\boldsymbol{\sigma}\cdot\mathbf{p}-2m\boldsymbol{\sigma}\cdot\mathbf{q}-(\boldsymbol{\sigma}\cdot\mathbf{q})(\boldsymbol{\sigma}\cdot\mathbf{p}))\xi^r \\
&= \frac{1}{4m}\eta^{s\dagger}\cdot 2\left(4m^2-(\boldsymbol{\sigma}\cdot\mathbf{q})(\boldsymbol{\sigma}\cdot\mathbf{p})\right)\xi^r \\
&\simeq \frac{1}{4m}\cdot 2\cdot 4m^2\eta^{s\dagger}\xi^r \\
&= 2m\eta^{s\dagger}\xi^r\ .
\end{aligned}
\tag{A.2}
$$

A.3 The vector fermion bilinear

The results of this section are used in Subsection 3.3.4.

$$\begin{aligned}
\bar{v}^s(q)\gamma^\mu u^r(p) &= \begin{pmatrix} -\eta^{s\dagger}\sqrt{\bar{\sigma}\cdot q} & \eta^{s\dagger}\sqrt{\sigma\cdot q}\end{pmatrix}\begin{pmatrix} 0 & \sigma^\mu \\ \bar{\sigma}^\mu & 0\end{pmatrix}\begin{pmatrix} \sqrt{\sigma\cdot p}\,\xi^r \\ \sqrt{\bar{\sigma}\cdot p}\,\xi^r\end{pmatrix} \\
&= \begin{pmatrix} -\eta^{s\dagger}\sqrt{\bar{\sigma}\cdot q} & \eta^{s\dagger}\sqrt{\sigma\cdot q}\end{pmatrix}\begin{pmatrix} \sigma^\mu\sqrt{\bar{\sigma}\cdot p}\,\xi^r \\ \bar{\sigma}^\mu\sqrt{\sigma\cdot p}\,\xi^r\end{pmatrix} \\
&\overset{\text{NR}}{\simeq} \frac{1}{4m}\begin{pmatrix} -\eta^{s\dagger}\,(2m+\boldsymbol{\sigma}\cdot\mathbf{q}) & \eta^{s\dagger}\,(2m-\boldsymbol{\sigma}\cdot\mathbf{q})\end{pmatrix}\begin{pmatrix} \sigma^\mu\,(2m+\boldsymbol{\sigma}\cdot\mathbf{p})\,\xi^r \\ \bar{\sigma}^\mu\,(2m-\boldsymbol{\sigma}\cdot\mathbf{p})\,\xi^r\end{pmatrix} \\
&= \frac{1}{4m}\eta^{s\dagger}\big(-(2m+\boldsymbol{\sigma}\cdot\mathbf{q})\,\sigma^\mu\,(2m+\boldsymbol{\sigma}\cdot\mathbf{p}) \\
&\qquad\qquad +(2m-\boldsymbol{\sigma}\cdot\mathbf{q})\,\bar{\sigma}^\mu\,(2m-\boldsymbol{\sigma}\cdot\mathbf{p})\big)\xi^r\ .
\end{aligned} \tag{A.3}$$

Temporal component

$$\begin{aligned}
\bar{v}^s(q)\gamma^0 u^r(p) &\simeq \frac{1}{4m}\eta^{s\dagger}\big(-(2m+\boldsymbol{\sigma}\cdot\mathbf{q})\,(2m+\boldsymbol{\sigma}\cdot\mathbf{p})+(2m-\boldsymbol{\sigma}\cdot\mathbf{q})\,(2m-\boldsymbol{\sigma}\cdot\mathbf{p})\big)\xi^r \\
&= \frac{1}{4m}\eta^{s\dagger}\big(-4m^2-2m\boldsymbol{\sigma}\cdot\mathbf{p}-2m\boldsymbol{\sigma}\cdot\mathbf{q}-(\boldsymbol{\sigma}\cdot\mathbf{q})(\boldsymbol{\sigma}\cdot\mathbf{p}) \\
&\qquad\qquad +4m^2-2m\boldsymbol{\sigma}\cdot\mathbf{p}-2m\boldsymbol{\sigma}\cdot\mathbf{q}+(\boldsymbol{\sigma}\cdot\mathbf{q})(\boldsymbol{\sigma}\cdot\mathbf{p})\big)\xi^r \\
&= \frac{1}{4m}\eta^{s\dagger}\cdot 2\,(-2m\boldsymbol{\sigma}\cdot\mathbf{p}-2m\boldsymbol{\sigma}\cdot\mathbf{q})\,\xi^r \\
&= -\frac{1}{4m}\cdot 2\cdot 2m\eta^{s\dagger}\,(\boldsymbol{\sigma}\cdot\mathbf{p}+\boldsymbol{\sigma}\cdot\mathbf{q})\,\xi^r \\
&= -\eta^{s\dagger}\boldsymbol{\sigma}\cdot(\mathbf{p}+\mathbf{q})\,\xi^r\ .
\end{aligned} \tag{A.4}$$

Spatial component

$$\begin{aligned}
\bar{v}^s(q)\gamma^i u^r(p) &\simeq \frac{1}{4m}\eta^{s\dagger}\big(-(2m+\boldsymbol{\sigma}\cdot\mathbf{q})\,\sigma^i\,(2m+\boldsymbol{\sigma}\cdot\mathbf{p}) \\
&\qquad\qquad -(2m-\boldsymbol{\sigma}\cdot\mathbf{q})\,\sigma^i\,(2m-\boldsymbol{\sigma}\cdot\mathbf{p})\big)\xi^r \\
&= \frac{1}{4m}\eta^{s\dagger}\big(-4m^2\sigma^i-2m\sigma^i\,(\boldsymbol{\sigma}\cdot\mathbf{p})-2m\,(\boldsymbol{\sigma}\cdot\mathbf{q})\,\sigma^i-(\boldsymbol{\sigma}\cdot\mathbf{q})\sigma^i(\boldsymbol{\sigma}\cdot\mathbf{p}) \\
&\qquad\qquad -4m^2\sigma^i+2m\sigma^i\,(\boldsymbol{\sigma}\cdot\mathbf{p})+2m\,(\boldsymbol{\sigma}\cdot\mathbf{q})\,\sigma^i-(\boldsymbol{\sigma}\cdot\mathbf{q})\sigma^i(\boldsymbol{\sigma}\cdot\mathbf{p})\big)\xi^r \\
&= \frac{1}{4m}\eta^{s\dagger}\cdot 2\left(-4m^2\sigma^i-(\boldsymbol{\sigma}\cdot\mathbf{q})\sigma^i(\boldsymbol{\sigma}\cdot\mathbf{p})\right)\xi^r \\
&\simeq -\frac{1}{4m}\cdot 2\cdot 4m^2\eta^{s\dagger}\sigma^i\xi^r \\
&= -2m\eta^{s\dagger}\sigma^i\xi^r\ .
\end{aligned} \tag{A.5}$$

A.4 The axial vector fermion bilinear

The results of this section are used in Subsection 3.3.5.

$$
\begin{aligned}
\bar{v}^s(q)\gamma^\mu\gamma^5 u^r(p) &= \begin{pmatrix} -\eta^{s\dagger}\sqrt{\bar{\sigma}\cdot q} & \eta^{s\dagger}\sqrt{\sigma\cdot q}\end{pmatrix}\begin{pmatrix} 0 & \sigma^\mu \\ \bar{\sigma}^\mu & 0\end{pmatrix}\begin{pmatrix} -\mathbb{1} & 0 \\ 0 & \mathbb{1}\end{pmatrix}\begin{pmatrix} \sqrt{\sigma\cdot p}\,\xi^r \\ \sqrt{\bar{\sigma}\cdot p}\,\xi^r\end{pmatrix} \\
&= \begin{pmatrix} -\eta^{s\dagger}\sqrt{\bar{\sigma}\cdot q} & \eta^{s\dagger}\sqrt{\sigma\cdot q}\end{pmatrix}\begin{pmatrix} 0 & \sigma^\mu \\ \bar{\sigma}^\mu & 0\end{pmatrix}\begin{pmatrix} -\sqrt{\sigma\cdot p}\,\xi^r \\ \sqrt{\bar{\sigma}\cdot p}\,\xi^r\end{pmatrix} \\
&= \begin{pmatrix} -\eta^{s\dagger}\sqrt{\bar{\sigma}\cdot q} & \eta^{s\dagger}\sqrt{\sigma\cdot q}\end{pmatrix}\begin{pmatrix} \sigma^\mu\sqrt{\bar{\sigma}\cdot p}\,\xi^r \\ -\bar{\sigma}^\mu\sqrt{\sigma\cdot p}\,\xi^r\end{pmatrix} \\
&\overset{\text{NR}}{\simeq} \frac{1}{4m}\begin{pmatrix} -\eta^{s\dagger}\,(2m+\boldsymbol{\sigma}\cdot\mathbf{q}) & \eta^{s\dagger}\,(2m-\boldsymbol{\sigma}\cdot\mathbf{q})\end{pmatrix}\begin{pmatrix} \sigma^\mu\,(2m+\boldsymbol{\sigma}\cdot\mathbf{p})\,\xi^r \\ -\bar{\sigma}^\mu\,(2m-\boldsymbol{\sigma}\cdot\mathbf{p})\,\xi^r\end{pmatrix} \\
&= -\frac{1}{4m}\eta^{s\dagger}\big(\,(2m+\boldsymbol{\sigma}\cdot\mathbf{q})\,\sigma^\mu\,(2m+\boldsymbol{\sigma}\cdot\mathbf{p}) \\
&\qquad\qquad +\,(2m-\boldsymbol{\sigma}\cdot\mathbf{q})\,\bar{\sigma}^\mu\,(2m-\boldsymbol{\sigma}\cdot\mathbf{p})\,\big)\xi^r\ .
\end{aligned}
\tag{A.6}
$$

Temporal component

$$
\begin{aligned}
\bar{v}^s(q)\gamma^0\gamma^5 u^r(p) &\simeq -\frac{1}{4m}\eta^{s\dagger}\big(\,(2m+\boldsymbol{\sigma}\cdot\mathbf{q})\,(2m+\boldsymbol{\sigma}\cdot\mathbf{p}) + (2m-\boldsymbol{\sigma}\cdot\mathbf{q})\,(2m-\boldsymbol{\sigma}\cdot\mathbf{p})\,\big)\xi^r \\
&= -\frac{1}{4m}\eta^{s\dagger}\big(4m^2 + 2m\boldsymbol{\sigma}\cdot\mathbf{p} + 2m\boldsymbol{\sigma}\cdot\mathbf{q} + (\boldsymbol{\sigma}\cdot\mathbf{q})(\boldsymbol{\sigma}\cdot\mathbf{p}) \\
&\qquad\qquad + 4m^2 - 2m\boldsymbol{\sigma}\cdot\mathbf{p} - 2m\boldsymbol{\sigma}\cdot\mathbf{q} + (\boldsymbol{\sigma}\cdot\mathbf{q})(\boldsymbol{\sigma}\cdot\mathbf{p})\big)\xi^r \\
&= -\frac{1}{4m}\eta^{s\dagger}\cdot 2\left(4m^2 + (\boldsymbol{\sigma}\cdot\mathbf{q})\,(\boldsymbol{\sigma}\cdot\mathbf{p})\right)\xi^r \\
&\simeq -\frac{1}{4m}\cdot 2\cdot 4m^2\eta^{s\dagger}\xi^r \\
&= -2m\eta^{s\dagger}\xi^r\ .
\end{aligned}
\tag{A.7}
$$

Spatial component

$$
\begin{aligned}
\bar{v}^s(q)\gamma^i\gamma^5 u^r(p) &\simeq -\frac{1}{4m}\eta^{s\dagger}\big(\,(2m+\boldsymbol{\sigma}\cdot\mathbf{q})\,\sigma^i\,(2m+\boldsymbol{\sigma}\cdot\mathbf{p}) \\
&\qquad\qquad -\,(2m-\boldsymbol{\sigma}\cdot\mathbf{q})\,\sigma^i\,(2m-\boldsymbol{\sigma}\cdot\mathbf{p})\,\big)\xi^r \\
&= -\frac{1}{4m}\eta^{s\dagger}\big(4m^2\sigma^i + 2m\sigma^i\,(\boldsymbol{\sigma}\cdot\mathbf{p}) + 2m\,(\boldsymbol{\sigma}\cdot\mathbf{q})\,\sigma^i + (\boldsymbol{\sigma}\cdot\mathbf{q})\sigma^i(\boldsymbol{\sigma}\cdot\mathbf{p}) \\
&\qquad\qquad - 4m^2\sigma^i + 2m\sigma^i\,(\boldsymbol{\sigma}\cdot\mathbf{p}) + 2m\,(\boldsymbol{\sigma}\cdot\mathbf{q})\,\sigma^i - (\boldsymbol{\sigma}\cdot\mathbf{q})\sigma^i(\boldsymbol{\sigma}\cdot\mathbf{p})\big)\xi^r \\
&= -\frac{1}{4m}\eta^{s\dagger}\cdot 2\left(2m\sigma^i\,(\boldsymbol{\sigma}\cdot\mathbf{p}) + 2m\,(\boldsymbol{\sigma}\cdot\mathbf{q})\,\sigma^i\right)\xi^r \\
&= -\frac{1}{4m}\cdot 2\cdot 2m\eta^{s\dagger}\left(\sigma^i\,(\boldsymbol{\sigma}\cdot\mathbf{p}) + (\boldsymbol{\sigma}\cdot\mathbf{q})\,\sigma^i\right)\xi^r \\
&= -\eta^{s\dagger}\left(\sigma^i\,(\boldsymbol{\sigma}\cdot\mathbf{p}) + (\boldsymbol{\sigma}\cdot\mathbf{q})\,\sigma^i\right)\xi^r\ .
\end{aligned}
\tag{A.8}
$$

A.5 The tensor fermion bilinear

The results of this section are used in Subsection 3.3.6.

$$
\begin{aligned}
\bar{v}^s(q)\gamma^\mu\gamma^\nu u^r(p) &= \begin{pmatrix} -\eta^{s\dagger}\sqrt{\bar{\sigma}\cdot q} & \eta^{s\dagger}\sqrt{\sigma\cdot q}\end{pmatrix}\begin{pmatrix} 0 & \sigma^\mu \\ \bar{\sigma}^\mu & 0\end{pmatrix}\begin{pmatrix} 0 & \sigma^\nu \\ \bar{\sigma}^\nu & 0\end{pmatrix}\begin{pmatrix} \sqrt{\sigma\cdot p}\,\xi^r \\ \sqrt{\bar{\sigma}\cdot p}\,\xi^r\end{pmatrix} \\
&= \begin{pmatrix} -\eta^{s\dagger}\sqrt{\bar{\sigma}\cdot q} & \eta^{s\dagger}\sqrt{\sigma\cdot q}\end{pmatrix}\begin{pmatrix} 0 & \sigma^\mu \\ \bar{\sigma}^\mu & 0\end{pmatrix}\begin{pmatrix} \sigma^\nu\sqrt{\bar{\sigma}\cdot p}\,\xi^r \\ \bar{\sigma}^\nu\sqrt{\sigma\cdot p}\,\xi^r\end{pmatrix} \\
&= \begin{pmatrix} -\eta^{s\dagger}\sqrt{\bar{\sigma}\cdot q} & \eta^{s\dagger}\sqrt{\sigma\cdot q}\end{pmatrix}\begin{pmatrix} \sigma^\mu\bar{\sigma}^\nu\sqrt{\sigma\cdot p}\,\xi^r \\ \bar{\sigma}^\mu\sigma^\nu\sqrt{\bar{\sigma}\cdot p}\,\xi^r\end{pmatrix} \\
&\overset{\text{NR}}{\simeq} \frac{1}{4m}\begin{pmatrix} -\eta^{s\dagger}\,(2m+\boldsymbol{\sigma}\cdot\mathbf{q}) & \eta^{s\dagger}\,(2m-\boldsymbol{\sigma}\cdot\mathbf{q})\end{pmatrix}\begin{pmatrix} \sigma^\mu\bar{\sigma}^\nu\,(2m-\boldsymbol{\sigma}\cdot\mathbf{p})\,\xi^r \\ \bar{\sigma}^\mu\sigma^\nu\,(2m+\boldsymbol{\sigma}\cdot\mathbf{p})\,\xi^r\end{pmatrix} \\
&= \frac{1}{4m}\eta^{s\dagger}\big(-(2m+\boldsymbol{\sigma}\cdot\mathbf{q})\,\sigma^\mu\bar{\sigma}^\nu\,(2m-\boldsymbol{\sigma}\cdot\mathbf{p}) \\
&\qquad\qquad +(2m-\boldsymbol{\sigma}\cdot\mathbf{q})\,\bar{\sigma}^\mu\sigma^\nu\,(2m+\boldsymbol{\sigma}\cdot\mathbf{p})\big)\xi^r\ .
\end{aligned}
\tag{A.9}
$$

Component with $\mu = 0$ and $\nu = 0$

$$
\begin{aligned}
\bar{v}^s(q)\gamma^0\gamma^0 u^r(p) &\simeq \frac{1}{4m}\eta^{s\dagger}\big(-(2m+\boldsymbol{\sigma}\cdot\mathbf{q})\,(2m-\boldsymbol{\sigma}\cdot\mathbf{p})+(2m-\boldsymbol{\sigma}\cdot\mathbf{q})\,(2m+\boldsymbol{\sigma}\cdot\mathbf{p})\big)\xi^r \\
&= \frac{1}{4m}\eta^{s\dagger}\big(-4m^2+2m\boldsymbol{\sigma}\cdot\mathbf{p}-2m\boldsymbol{\sigma}\cdot\mathbf{q}+(\boldsymbol{\sigma}\cdot\mathbf{q})(\boldsymbol{\sigma}\cdot\mathbf{p}) \\
&\qquad\qquad +4m^2+2m\boldsymbol{\sigma}\cdot\mathbf{p}-2m\boldsymbol{\sigma}\cdot\mathbf{q}-(\boldsymbol{\sigma}\cdot\mathbf{q})(\boldsymbol{\sigma}\cdot\mathbf{p})\big)\xi^r \\
&= \frac{1}{4m}\eta^{s\dagger}\cdot 2\,(2m\boldsymbol{\sigma}\cdot\mathbf{p}-2m\boldsymbol{\sigma}\cdot\mathbf{q})\,\xi^r \\
&= \frac{1}{4m}\cdot 2\cdot 2m\eta^{s\dagger}\,(\boldsymbol{\sigma}\cdot\mathbf{p}-\boldsymbol{\sigma}\cdot\mathbf{q})\,\xi^r \\
&= \eta^{s\dagger}\boldsymbol{\sigma}\cdot(\mathbf{p}-\mathbf{q})\,\xi^r\ .
\end{aligned}
\tag{A.10}
$$

Component with $\mu = 0$ and $\nu = j$

$$\begin{aligned}
\bar{v}^s(q)\gamma^0\gamma^j u^r(p) &\simeq \frac{1}{4m}\eta^{s\dagger}\big(\,(2m+\boldsymbol{\sigma}\cdot\mathbf{q})\,\sigma^j\,(2m-\boldsymbol{\sigma}\cdot\mathbf{p}) \\
&\qquad + (2m-\boldsymbol{\sigma}\cdot\mathbf{q})\,\sigma^j\,(2m+\boldsymbol{\sigma}\cdot\mathbf{p})\,\big)\xi^r \\
&= \frac{1}{4m}\eta^{s\dagger}(4m^2\sigma^j - 2m\sigma^j\,(\boldsymbol{\sigma}\cdot\mathbf{p}) + 2m\,(\boldsymbol{\sigma}\cdot\mathbf{q})\,\sigma^j - (\boldsymbol{\sigma}\cdot\mathbf{q})\sigma^j(\boldsymbol{\sigma}\cdot\mathbf{p}) \\
&\qquad + 4m^2\sigma^j + 2m\sigma^j\,(\boldsymbol{\sigma}\cdot\mathbf{p}) - 2m\,(\boldsymbol{\sigma}\cdot\mathbf{q})\,\sigma^j - (\boldsymbol{\sigma}\cdot\mathbf{q})\sigma^j(\boldsymbol{\sigma}\cdot\mathbf{p}))\xi^r \qquad \text{(A.11)} \\
&= \frac{1}{4m}\eta^{s\dagger}\cdot 2\left(4m^2\sigma^j - (\boldsymbol{\sigma}\cdot\mathbf{q})\sigma^j(\boldsymbol{\sigma}\cdot\mathbf{p})\right)\xi^r \\
&\simeq \frac{1}{4m}\cdot 2\cdot 4m^2\eta^{s\dagger}\sigma^j\xi^r \\
&= 2m\eta^{s\dagger}\sigma^j\xi^r\ .
\end{aligned}$$

Component with $\mu = i$ and $\nu = 0$

$$\begin{aligned}
\bar{v}^s(q)\gamma^i\gamma^0 u^r(p) &\simeq \frac{1}{4m}\eta^{s\dagger}\big(-(2m+\boldsymbol{\sigma}\cdot\mathbf{q})\,\sigma^i\,(2m-\boldsymbol{\sigma}\cdot\mathbf{p}) \\
&\qquad - (2m-\boldsymbol{\sigma}\cdot\mathbf{q})\,\sigma^i\,(2m+\boldsymbol{\sigma}\cdot\mathbf{p})\,\big)\xi^r \\
&= \frac{1}{4m}\eta^{s\dagger}\big(-4m^2\sigma^i + 2m\sigma^i\,(\boldsymbol{\sigma}\cdot\mathbf{p}) - 2m\,(\boldsymbol{\sigma}\cdot\mathbf{q})\,\sigma^i + (\boldsymbol{\sigma}\cdot\mathbf{q})\sigma^i(\boldsymbol{\sigma}\cdot\mathbf{p}) \\
&\qquad - 4m^2\sigma^i - 2m\sigma^i\,(\boldsymbol{\sigma}\cdot\mathbf{p}) + 2m\,(\boldsymbol{\sigma}\cdot\mathbf{q})\,\sigma^i + (\boldsymbol{\sigma}\cdot\mathbf{q})\sigma^i(\boldsymbol{\sigma}\cdot\mathbf{p}))\xi^r \qquad \text{(A.12)} \\
&= \frac{1}{4m}\eta^{s\dagger}\cdot 2\left(-4m^2\sigma^i + (\boldsymbol{\sigma}\cdot\mathbf{q})\sigma^i(\boldsymbol{\sigma}\cdot\mathbf{p})\right)\xi^r \\
&\simeq -\frac{1}{4m}\cdot 2\cdot 4m^2\eta^{s\dagger}\sigma^i\xi^r \\
&= -2m\eta^{s\dagger}\sigma^i\xi^r\ .
\end{aligned}$$

Component with $\mu = i$ and $\nu = j$

$$\begin{aligned}
\bar{v}^s(q)\gamma^i\gamma^j u^r(p) &\simeq \frac{1}{4m}\eta^{s\dagger}\big(\,(2m+\boldsymbol{\sigma}\cdot\mathbf{q})\,\sigma^i\sigma^j\,(2m-\boldsymbol{\sigma}\cdot\mathbf{p}) \\
&\qquad - (2m-\boldsymbol{\sigma}\cdot\mathbf{q})\,\sigma^i\sigma^j\,(2m+\boldsymbol{\sigma}\cdot\mathbf{p})\,\big)\xi^r \\
&= \frac{1}{4m}\eta^{s\dagger}(4m^2\sigma^i\sigma^j - 2m\sigma^i\sigma^j(\boldsymbol{\sigma}\cdot\mathbf{p}) + 2m(\boldsymbol{\sigma}\cdot\mathbf{q})\sigma^i\sigma^j - (\boldsymbol{\sigma}\cdot\mathbf{q})\sigma^i\sigma^j(\boldsymbol{\sigma}\cdot\mathbf{p}) \\
&\qquad - 4m^2\sigma^i\sigma^j - 2m\sigma^i\sigma^j(\boldsymbol{\sigma}\cdot\mathbf{p}) + 2m(\boldsymbol{\sigma}\cdot\mathbf{q})\sigma^i\sigma^j + (\boldsymbol{\sigma}\cdot\mathbf{q})\sigma^i\sigma^j(\boldsymbol{\sigma}\cdot\mathbf{p}))\xi^r \qquad \text{(A.13)} \\
&= \frac{1}{4m}\eta^{s\dagger}\cdot 2\left(2m(\boldsymbol{\sigma}\cdot\mathbf{q})\sigma^i\sigma^j - 2m\sigma^i\sigma^j(\boldsymbol{\sigma}\cdot\mathbf{p})\right)\xi^r \\
&= \frac{1}{4m}\cdot 2\cdot 2m\eta^{s\dagger}\left((\boldsymbol{\sigma}\cdot\mathbf{q})\sigma^i\sigma^j - \sigma^i\sigma^j(\boldsymbol{\sigma}\cdot\mathbf{p})\right)\xi^r \\
&= \eta^{s\dagger}\left((\boldsymbol{\sigma}\cdot\mathbf{q})\sigma^i\sigma^j - \sigma^i\sigma^j(\boldsymbol{\sigma}\cdot\mathbf{p})\right)\xi^r\ .
\end{aligned}$$

A.6 The axial tensor fermion bilinear

The results of this section are used in Subsection 3.3.7.

$$
\begin{aligned}
\bar{v}^s(q)\gamma^\mu\gamma^\nu\gamma^5 u^r(p) &= \begin{pmatrix} -\eta^{s\dagger}\sqrt{\bar{\sigma}\cdot q} & \eta^{s\dagger}\sqrt{\sigma\cdot q}\end{pmatrix}\begin{pmatrix} 0 & \sigma^\mu \\ \bar{\sigma}^\mu & 0\end{pmatrix}\begin{pmatrix} 0 & \sigma^\nu \\ \bar{\sigma}^\nu & 0\end{pmatrix}\begin{pmatrix} -\mathbb{1} & 0 \\ 0 & \mathbb{1}\end{pmatrix}\begin{pmatrix} \sqrt{\sigma\cdot p}\,\xi^r \\ \sqrt{\bar{\sigma}\cdot p}\,\xi^r\end{pmatrix} \\
&= \begin{pmatrix} -\eta^{s\dagger}\sqrt{\bar{\sigma}\cdot q} & \eta^{s\dagger}\sqrt{\sigma\cdot q}\end{pmatrix}\begin{pmatrix} 0 & \sigma^\mu \\ \bar{\sigma}^\mu & 0\end{pmatrix}\begin{pmatrix} 0 & \sigma^\nu \\ \bar{\sigma}^\nu & 0\end{pmatrix}\begin{pmatrix} -\sqrt{\sigma\cdot p}\,\xi^r \\ \sqrt{\bar{\sigma}\cdot p}\,\xi^r\end{pmatrix} \\
&= \begin{pmatrix} -\eta^{s\dagger}\sqrt{\bar{\sigma}\cdot q} & \eta^{s\dagger}\sqrt{\sigma\cdot q}\end{pmatrix}\begin{pmatrix} 0 & \sigma^\mu \\ \bar{\sigma}^\mu & 0\end{pmatrix}\begin{pmatrix} \sigma^\nu\sqrt{\bar{\sigma}\cdot p}\,\xi^r \\ -\bar{\sigma}^\nu\sqrt{\sigma\cdot p}\,\xi^r\end{pmatrix} \\
&= \begin{pmatrix} -\eta^{s\dagger}\sqrt{\bar{\sigma}\cdot q} & \eta^{s\dagger}\sqrt{\sigma\cdot q}\end{pmatrix}\begin{pmatrix} -\sigma^\mu\bar{\sigma}^\nu\sqrt{\sigma\cdot p}\,\xi^r \\ \bar{\sigma}^\mu\sigma^\nu\sqrt{\bar{\sigma}\cdot p}\,\xi^r\end{pmatrix} \\
&\overset{\text{NR}}{\simeq} \frac{1}{4m}\begin{pmatrix} \eta^{s\dagger}\,(2m+\boldsymbol{\sigma}\cdot\mathbf{q}) & \eta^{s\dagger}\,(2m-\boldsymbol{\sigma}\cdot\mathbf{q})\end{pmatrix}\begin{pmatrix} \sigma^\mu\bar{\sigma}^\nu\,(2m-\boldsymbol{\sigma}\cdot\mathbf{p})\,\xi^r \\ \bar{\sigma}^\mu\sigma^\nu\,(2m+\boldsymbol{\sigma}\cdot\mathbf{p})\,\xi^r\end{pmatrix} \\
&= \frac{1}{4m}\eta^{s\dagger}\big(\,(2m+\boldsymbol{\sigma}\cdot\mathbf{q})\,\sigma^\mu\bar{\sigma}^\nu\,(2m-\boldsymbol{\sigma}\cdot\mathbf{p}) \\
&\qquad + (2m-\boldsymbol{\sigma}\cdot\mathbf{q})\,\bar{\sigma}^\mu\sigma^\nu\,(2m+\boldsymbol{\sigma}\cdot\mathbf{p})\,\big)\xi^r\ .
\end{aligned}
\tag{A.14}
$$

Component with $\mu = 0$ and $\nu = 0$

$$
\begin{aligned}
\bar{v}^s(q)\gamma^0\gamma^0\gamma^5 u^r(p) &\simeq \frac{1}{4m}\eta^{s\dagger}\big(\,(2m+\boldsymbol{\sigma}\cdot\mathbf{q})\,(2m-\boldsymbol{\sigma}\cdot\mathbf{p}) + (2m-\boldsymbol{\sigma}\cdot\mathbf{q})\,(2m+\boldsymbol{\sigma}\cdot\mathbf{p})\,\big)\xi^r \\
&= \frac{1}{4m}\eta^{s\dagger}\big(4m^2 - 2m\boldsymbol{\sigma}\cdot\mathbf{p} + 2m\boldsymbol{\sigma}\cdot\mathbf{q} - (\boldsymbol{\sigma}\cdot\mathbf{q})(\boldsymbol{\sigma}\cdot\mathbf{p}) \\
&\qquad + 4m^2 + 2m\boldsymbol{\sigma}\cdot\mathbf{p} - 2m\boldsymbol{\sigma}\cdot\mathbf{q} - (\boldsymbol{\sigma}\cdot\mathbf{q})(\boldsymbol{\sigma}\cdot\mathbf{p})\big)\xi^r \\
&= \frac{1}{4m}\eta^{s\dagger}\cdot 2\left(4m^2 - (\boldsymbol{\sigma}\cdot\mathbf{q})(\boldsymbol{\sigma}\cdot\mathbf{p})\right)\xi^r \\
&\simeq \frac{1}{4m}\cdot 2\cdot 4m^2\eta^{s\dagger}\xi^r \\
&= 2m\eta^{s\dagger}\xi^r\ .
\end{aligned}
\tag{A.15}
$$

Component with $\mu = 0$ and $\nu = j$

$$\begin{aligned}
\bar{v}^s(q)\gamma^0\gamma^j\gamma^5 u^r(p) &\simeq \frac{1}{4m}\eta^{s\dagger}\big(-(2m+\boldsymbol{\sigma}\cdot\mathbf{q})\,\sigma^j\,(2m-\boldsymbol{\sigma}\cdot\mathbf{p}) \\
&\qquad +(2m-\boldsymbol{\sigma}\cdot\mathbf{q})\,\sigma^j\,(2m+\boldsymbol{\sigma}\cdot\mathbf{p})\,\big)\xi^r \\
&= \frac{1}{4m}\eta^{s\dagger}\big(-4m^2\sigma^j + 2m\sigma^j\,(\boldsymbol{\sigma}\cdot\mathbf{p}) - 2m\,(\boldsymbol{\sigma}\cdot\mathbf{q})\,\sigma^j + (\boldsymbol{\sigma}\cdot\mathbf{q})\sigma^j(\boldsymbol{\sigma}\cdot\mathbf{p}) \\
&\qquad +4m^2\sigma^j + 2m\sigma^j\,(\boldsymbol{\sigma}\cdot\mathbf{p}) - 2m\,(\boldsymbol{\sigma}\cdot\mathbf{q})\,\sigma^j - (\boldsymbol{\sigma}\cdot\mathbf{q})\sigma^j(\boldsymbol{\sigma}\cdot\mathbf{p})\big)\xi^r \qquad \text{(A.16)} \\
&= \frac{1}{4m}\eta^{s\dagger}\cdot 2\left(2m\sigma^j\,(\boldsymbol{\sigma}\cdot\mathbf{p}) - 2m\,(\boldsymbol{\sigma}\cdot\mathbf{q})\,\sigma^j\right)\xi^r \\
&= \frac{1}{4m}\cdot 2\cdot 2m\eta^{s\dagger}\left(\sigma^j\,(\boldsymbol{\sigma}\cdot\mathbf{p}) - (\boldsymbol{\sigma}\cdot\mathbf{q})\,\sigma^j\right)\xi^r \\
&= \eta^{s\dagger}\left(\sigma^j\,(\boldsymbol{\sigma}\cdot\mathbf{p}) - (\boldsymbol{\sigma}\cdot\mathbf{q})\,\sigma^j\right)\xi^r\ .
\end{aligned}$$

Component with $\mu = i$ and $\nu = 0$

$$\begin{aligned}
\bar{v}^s(q)\gamma^i\gamma^0\gamma^5 u^r(p) &\simeq \frac{1}{4m}\eta^{s\dagger}\big((2m+\boldsymbol{\sigma}\cdot\mathbf{q})\,\sigma^i\,(2m-\boldsymbol{\sigma}\cdot\mathbf{p}) \\
&\qquad -(2m-\boldsymbol{\sigma}\cdot\mathbf{q})\,\sigma^i\,(2m+\boldsymbol{\sigma}\cdot\mathbf{p})\,\big)\xi^r \\
&= \frac{1}{4m}\eta^{s\dagger}\big(4m^2\sigma^i - 2m\sigma^i\,(\boldsymbol{\sigma}\cdot\mathbf{p}) + 2m\,(\boldsymbol{\sigma}\cdot\mathbf{q})\,\sigma^i - (\boldsymbol{\sigma}\cdot\mathbf{q})\sigma^i(\boldsymbol{\sigma}\cdot\mathbf{p}) \\
&\qquad -4m^2\sigma^i - 2m\sigma^i\,(\boldsymbol{\sigma}\cdot\mathbf{p}) + 2m\,(\boldsymbol{\sigma}\cdot\mathbf{q})\,\sigma^i + (\boldsymbol{\sigma}\cdot\mathbf{q})\sigma^i(\boldsymbol{\sigma}\cdot\mathbf{p})\big)\xi^r \qquad \text{(A.17)} \\
&= \frac{1}{4m}\eta^{s\dagger}\cdot 2\left(-2m\sigma^i\,(\boldsymbol{\sigma}\cdot\mathbf{p}) + 2m\,(\boldsymbol{\sigma}\cdot\mathbf{q})\,\sigma^i\right)\xi^r \\
&= -\frac{1}{4m}\cdot 2\cdot 2m\eta^{s\dagger}\left(\sigma^i\,(\boldsymbol{\sigma}\cdot\mathbf{p}) - (\boldsymbol{\sigma}\cdot\mathbf{q})\,\sigma^i\right)\xi^r \\
&= -\eta^{s\dagger}\left(\sigma^i\,(\boldsymbol{\sigma}\cdot\mathbf{p}) - (\boldsymbol{\sigma}\cdot\mathbf{q})\,\sigma^i\right)\xi^r\ .
\end{aligned}$$

Component with $\mu = i$ and $\nu = j$

$$\begin{aligned}
\bar{v}^s(q)\gamma^i\gamma^j\gamma^5 u^r(p) &\simeq \frac{1}{4m}\eta^{s\dagger}\big(-(2m+\boldsymbol{\sigma}\cdot\mathbf{q})\,\sigma^i\sigma^j\,(2m-\boldsymbol{\sigma}\cdot\mathbf{p}) \\
&\qquad -(2m-\boldsymbol{\sigma}\cdot\mathbf{q})\,\sigma^i\sigma^j\,(2m+\boldsymbol{\sigma}\cdot\mathbf{p})\,\big)\xi^r \\
&= -\frac{1}{4m}\eta^{s\dagger}\big(4m^2\sigma^i\sigma^j - 2m\sigma^i\sigma^j(\boldsymbol{\sigma}\cdot\mathbf{p}) + 2m(\boldsymbol{\sigma}\cdot\mathbf{q})\sigma^i\sigma^j - (\boldsymbol{\sigma}\cdot\mathbf{q})\sigma^i\sigma^j(\boldsymbol{\sigma}\cdot\mathbf{p}) \\
&\qquad +4m^2\sigma^i\sigma^j + 2m\sigma^i\sigma^j(\boldsymbol{\sigma}\cdot\mathbf{p}) - 2m(\boldsymbol{\sigma}\cdot\mathbf{q})\sigma^i\sigma^j - (\boldsymbol{\sigma}\cdot\mathbf{q})\sigma^i\sigma^j(\boldsymbol{\sigma}\cdot\mathbf{p})\big)\xi^r \qquad \text{(A.18)} \\
&= -\frac{1}{4m}\eta^{s\dagger}\cdot 2\left(4m^2\sigma^i\sigma^j - (\boldsymbol{\sigma}\cdot\mathbf{q})\sigma^i\sigma^j(\boldsymbol{\sigma}\cdot\mathbf{p})\right)\xi^r \\
&\simeq -\frac{1}{4m}\cdot 2\cdot 4m^2\eta^{s\dagger}\sigma^i\sigma^j\xi^r \\
&= -2m\eta^{s\dagger}\sigma^i\sigma^j\xi^r\ .
\end{aligned}$$

Bibliography

[1]D. Baumann, *Cosmology* (Cambridge University Press, Cambridge, UK, 2022).

[2]J. Pinochet, «Illuminating dark matter I: A guide for physics teachers», Phys. Educ. **59**, 055018 (2024).

[3]European Space Agency, *The Bullet Cluster*, ESA Multimedia, (July 2007) `https://www.esa.int/ESA_Multimedia/Images/2007/07/The_Bullet_Cluster2`.

[4]S. L. Dubovsky, D. S. Gorbunov, and G. I. Rubtsov, «Narrowing the window for millicharged particles by CMB anisotropy», JETP Lett. **79**, 1–5 (2004).

[5]V. Poulin, P. D. Serpico, and J. Lesgourgues, «A fresh look at linear cosmological constraints on a decaying dark matter component», J. Cosmol. Astropart. Phys. **2016**, 036 (2016).

[6]V. De Luca, A. Mitridate, M. Redi, J. Smirnov, and A. Strumia, «Colored Dark Matter», Phys. Rev. D **97**, 115024 (2018).

[7]N. Bernal, M. Heikinheimo, T. Tenkanen, K. Tuominen, and V. Vaskonen, «The Dawn of FIMP Dark Matter: A Review of Models and Constraints», Int. J. Mod. Phys. A **32**, 1730023 (2017).

[8]T.-T. Yu, «2024 TASI Lectures: A Dark Matter Primer», arXiv preprint (2025).

[9]N. Bernal, F. Elahi, C. Maldonado, and J. Unwin, «Ultraviolet Freeze-in and Non-Standard Cosmologies», J. Cosmol. Astropart. Phys. **2019**, 026 (2019).

[10]C. A. J. O'Hare, «Cosmology of axion dark matter», PoS **COSMICWISPers**, 040 (2024).

[11]C. Armand et al. (Fermi-LAT, HAWC, H.E.S.S., MAGIC, VERITAS), «Combined dark matter searches towards dwarf spheroidal galaxies with Fermi-LAT, HAWC, H.E.S.S., MAGIC, and VERITAS», in 37th International Cosmic Ray Conference (ICRC 2021), Vol. ICRC2021 (2021), p. 527.

[12]N. Aghanim et al., «Planck 2018 results. VI. Cosmological parameters», Astron. Astrophys. **641**, A6 (2020).

[13]M. Schumann, «Direct Detection of WIMP Dark Matter: Concepts and Status», J. Phys. G **46**, 103003 (2019).

[14]B. Penning, «The Pursuit of Dark Matter at Colliders – An Overview», J. Phys. G **45**, 063001 (2018).

[15]A. A. Penzias and R. W. Wilson, «A measurement of excess antenna temperature at 4080 Mc/s», Astrophys. J. **142**, 419–421 (1965).

[16]European Space Agency, *Planck CMB*, ESA Multimedia, (Mar. 2013) https://www.esa.int/ESA_Multimedia/Images/2013/03/Planck_CMB.

[17]D. Baumann and H. V. Peiris, «Cosmological Inflation: Theory and Observations», Adv. Sci. Lett. **2**, 105–120 (2009).

[18]ICTP High Energy, Cosmology and Astroparticle Physics, *Lecture 3 / Physics of the Early Universe*, Online Video, YouTube: https://youtu.be/4NDa_yFqums, HECAP Postgraduate Diploma Programme Lecture., 2017.

[19]D. Green, P. D. Meerburg, and J. Meyers, «Aspects of Dark Matter Annihilation in Cosmology», J. Cosmol. Astropart. Phys. **2019**, 025 (2019).

[20]A. A. Kaurov, D. Hooper, and N. Y. Gnedin, «The Effects of Dark Matter Annihilation on Cosmic Reionization», Astrophys. J. **833**, 162 (2016).

[21]C. Dvorkin, K. Blum, and M. Zaldarriaga, «Perturbed Recombination from Dark Matter Annihilation», Phys. Rev. D **87**, 103522 (2013).

[22]L. Zhang, X. Chen, Y.-A. Lei, and Z.-g. Si, «The impacts of dark matter particle annihilation on recombination and the anisotropies of the cosmic microwave background», Phys. Rev. D **74**, 103519 (2006).

[23]M. E. Peskin and D. V. Schroeder, *An Introduction to Quantum Field Theory* (Addison-Wesley, Reading, USA, 1995).

[24]M. Srednicki, *Quantum Field Theory* (Cambridge University Press, Cambridge, UK, 2007).

[25]E. Bertuzzo, «Quantum Field Theory», Lecture notes, Università degli Studi di Modena e Reggio Emilia, Academic Year 2025–2026, 2025.

[26]M. Cirelli, E. Del Nobile, and P. Panci, «Tools for model-independent bounds in direct dark matter searches», J. Cosmol. Astropart. Phys. **2013**, 019 (2013).